

Deltares

Enabling Delta Life



Morphological effects of mega-nourishments



Morphological effects of mega-nourishments

Using the MOHOLK model for understanding effects of mega-nourishments in the areas around North Holland and Marsdiep

C.M. van der Hout, P.K. Tonnon, J.G. de Ronde

Title
Morphological effects of mega-nourishments

Client	Project	Pages
MT	1200659-000	98

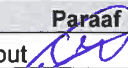
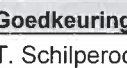
Trefwoorden
Mega-nourishment, Texel, North Holland, Delft3D, morphology

Samenvatting

This report describes the development of the Moholk model, an advanced large-scale morphological model for the Holland Coast and the Western Wadden Sea, and the application of the model on modelling the morphological effects of various mega-nourishment scenarios and locations. The Moholk model is developed with the former HCZ model (Roelvink et al., 2001b) as starting point. The main adjustments are the Delft3D version, the hydrodynamic boundary conditions, the morphological updating scheme, the sediment transport formula and some parameter settings. The outdated RAM approach has been replaced by the advanced parallel online method (Roelvink, 2006) and the recently developed transport formula TR2004 has been applied.

The predicted hydrodynamics and sediment transports along the Holland Coast and in the Texel Inlet compare quite well with reference studies (Van de Rest, 2004 and Elias, 2006). The morphological development is somewhat overestimated, but the general pattern around the Texel Inlet compares well with vaklodgingen measurements.

Four locations on the North Holland coast and the Texel Inlet have been examined with mega nourishments of 5 Million m³/year for 10 years and two locations have been examined for 10 years after an ultra nourishment of 50 Million m³. In general the nourishments do not disappear, but diffuse in 10 years up to two kilometres, due to their influence on the local hydrodynamics. It is concluded that a mega-nourishment does not trigger the system to change the import of sediment into the Marsdiep tidal basin, but that nourishment of the Noorderhaaks shoal or the Texelstroom tidal channel do have advantages on future development of the Marsdiep Delta.

Versie	Datum	Auteur	Paraaf	Review	Paraaf	Goedkeuring	Paraaf
1.2	2009-10-22	C.M. van der Hout		L. van Rijn		T. Schilperoort	
		P.K. Tonnon					
		J.G. de Ronde					

State
Final

Content

1	Introduction	1
2	Physical principles of Mega nourishments	3
3	Mega nourishments	11
3.1	Scenario description	11
3.2	Ultra nourishment scenarios, Callantsoog Long (A1) and Callantsoog Cross (A2)	12
3.3	Scenario A3 Noorderhaaks	20
3.4	Scenario A4 Channel nourishment in Wadden Sea	21
3.5	Scenario A5 Callantsoog	23
3.6	Discussion	25
4	Conclusions and recommendations	27
4.1	Conclusions	27
4.1.1	Effects of Mega nourishments	27
4.1.2	Model development	28
4.1.3	Model validation	28
4.2	Recommendations	29
4.2.1	Delft3D	29
4.2.2	Validation	29
5	Literature	31
	Bijlage(n)	
A	Setup of the model	33
A.1	Model development	33
A.2	Model schematization of Moholk model	34
A.2.1	Delft3D Version	34
A.2.2	Flow model	34
A.2.3	Wave model	36
A.2.4	Sediment transport	39
A.2.5	Morphology	39
A.2.6	Tidal schematisation	40
A.2.7	Validation and sensitivity analyses	40
B	Validation of the model	B-1
B.1	Tidal schematisation	B-1
B.1.1	Tidal schematization method	B-1
B.1.2	Comparison water levels and depth-averaged long shore velocities	B-1
B.2	Risidual currents	B-4
B.2.1	Residual tidal current	B-4
B.2.2	Marsdiep Inlet	B-5
B.3	Sediment transport	B-8
B.3.1	Longshore transports	B-8
B.3.2	Cross-shore transports	B-11

B.4	Sensitivity of transport formula and bed roughness	B-12
B.4.1	Nearshore longshore transport	B-12
B.4.2	Deep water longshore transport	B-13
B.5	Morphodynamics	B-15
B.5.1	Surf zone	B-15
B.5.2	Marsdiep delta	B-16
B.6	Synthesis	B-23
C	Validation of longshore currents, comparison with former studies	C-25
C.1	Comparison with Van Rijn, 1995, Van Rijn e.a, 1995 and Van Rijn, 1997	C-25
C.2	Comparison of TR2004 and TR1993 within Delft3D	C-29
C.3	Comparison of MOHOLK results with the measurements of the “ Dammetje van Wiersma”	C-32
C.4	Final comparison	C-33
D	Wave climate, contribution different conditions	D-34
E	Sensitivity of tidal forcing	E-37
E.1	Description of tidal schematizations	E-37
E.2	Time averaged residual longshore transports	E-37
E.2.1	Nearshore	E-37
E.2.2	Offshore	E-38
E.2.3	Marsdiep	E-39
E.3	Neumann boundaries	E-41
E.3.1	Formulae for deriving Neumann boundaries	E-41
E.3.2	Computer program INTCOM	E-41
E.3.3	HVM – model	E-42
E.3.4	Mathematical derivation	E-42
E.3.5	Conclusion on methods	E-43
E.3.6	Lateral boundary in Wadden Sea	E-43
F	Update van Rijn 2004	F-45
G	Sensitivity of proposed parameters	G-48
G.1	General sensitivity analysis	G-48
G.2	Wave-current interaction	G-51
G.2.1	Bucket model	G-51
G.2.2	Moholk Model time series	G-53
G.2.3	Conclusion	G-56
H	Wind influence on residual current	H-57

1 Introduction

At present, the BKL (Basis Kustlijn, Basic Coast Line) and coastal foundation of The Netherlands is maintained by nourishing 12 Million m³ per year. In the near future it has been advised that this should be increased to about 20 Million m³ per year (De Ronde, 2008). This increase from 12 to 20 Million m³ per year is necessary due to:

- Compensation of the dredging and dumping strategy of Rotterdam harbour, whereby material is dredged in the coastal foundation area and dumped seaward of this area.
- Compensation of the maintenance of the shipping lanes and other activities, whereby sand taken out of the coastal foundation is sold on the market.
- Compensation for the closure of the Zuiderzee
- Compensation for lowering of the surface due to gas mining.

The report of the delta-committee (Delta-committee, 2008) is giving a coastal perspective with a significant broadening of about 1 km and a nourishment of 85 Million m³ per year. In the concept "Ontwerp National Waterplan", of the Ministry of Transport, Public Works and Water Management' it is mentioned that further research is necessary on required nourishment volumes in the future for coastline management and on the effects of larger nourishment volumes on morphology, ecology, fishery and recreation.

Goals for these mega nourishments are;

- Maintaining safety and position of the coastline.
- Preventing further erosion of the outer delta of the Marsdiep. At this moment the outer delta is diminishing with an amount of 4 to 6 Million m³ per year.
- Maintaining or increasing the inter tidal areas in the Wadden sea area of the Marsdiep system.

Mega nourishments of 5 Million m³ or even more were unthinkable until a few years ago. Normal nourishment volumes in Holland vary between 0.5 and 2 Million m³. However, knowledge and techniques have developed rapidly and during the last two years two nourishments of nearly 8 Million m³ have been completed in the northern part of the Holland Coast near Den Helder.

At this moment, the experience with large nourishments is still small. The 8 Million m³ nourishments near Den Helder are under evaluation, but also require a longer observation time for gaining knowledge on the behaviour. There is a need for more knowledge on the behaviour of large nourishments; how will they develop and what will be their effects on the surrounding environment.

From the above the following research question has been derived: What are the morphological effects of mega nourishments? This report describes the morphological research on mega nourishments and ultra nourishments on the coast between Petten and Den Helder and in the area of the Marsdiep Inlet. The above mentioned goals are evaluated and several nourishment locations and nourishment schemes are compared to each other.

Before the discussion of the results in chapter 2 the main physics concerning mega or ultra nourishments are presented, together with their expected impacts. In Chapter 3 several designs of ultra nourishments of 50 Mm³ are discussed together with their developments in time . Finally conclusions and recommendations are given in chapter 4.

In the appendices the development of the model and the final settings are described and special attention is given to the verification of the longshore transports along the coast and the sensitivity of the model to different formulations and parameter settings.

2 Physical principles of Mega nourishments

Before the model results of the development of 5 Mega nourishments are presented in the next chapter first the physical principles concerning (mega) nourishments will be discussed. This is done to make it possible to make a rough first estimation of what can be expected on the development of the nourishments as an basis for the further discussion of the model results given further on in this report.

Mega nourishments can be implemented as beach nourishments or as shoreface nourishments. In the latter case the nourishment is placed as a submerged structure at the edge of the surf zone, usually on the seaward flank of the outer breaker bar of the coastal zone.

At most locations the Dutch coastal zone is characterized by a system of one or more shore-parallel breaker bars and troughs. The bars move in onshore or offshore direction depending on the wave conditions. During stormy conditions the larger waves break near the crest of the bars and a three-dimensional current pattern consisting of a longshore current and a cross-shore undertow is generated, as shown in figure 2.1.

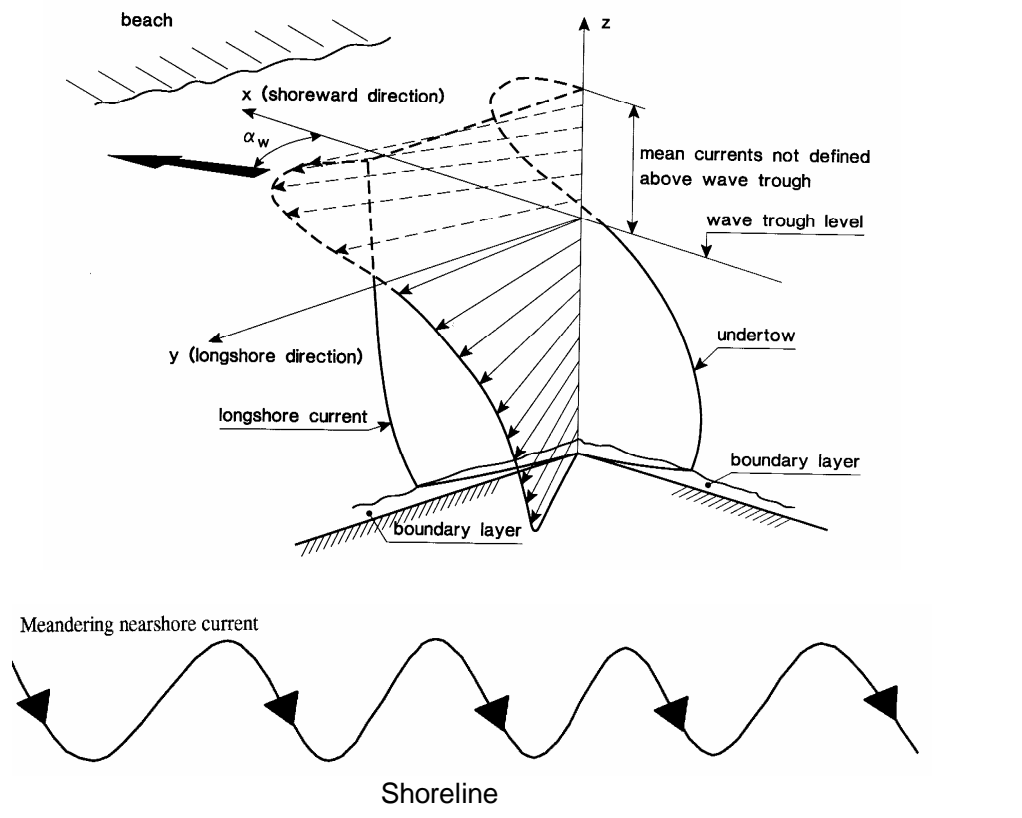


Figure 2.1 Typical features of hydrodynamics in surf zone
 Top: Flow structure in surf zone (3D view)
 Bottom: Meandering longshore current (plan view)

Longshore currents with velocities between 1 and 2 m/s are only generated when the breaking waves have an oblique orientation to the crest of the bars. The longshore current

shows low-frequency oscillations on the time scale of minutes (infragravity time scale), expressing a meandering type of behaviour (see figure 2.1) which is also known as shear waves. The variation of the velocity oscillations is about 25% of the magnitude of the longshore current velocity.

The cross-shore return velocities in the lower part of the water depth are strongly related to the onshore mass flux between the crest and the trough of the waves, which are propagating into shallow water, increasing in height during the shoaling and breaking process and resulting in the piling up of water (wave set-up) in the inner surf zone. This drives a cross-shore return flow (undertow) compensating the onshore mass flux. The seaward-directed undertow is maximum at the crest of the bars with values between 0.5 and 1 m/s. Wind-induced set-up intensifies the wave-induced undertow.

Longshore variability of the breaker bar system may result in the generation of localized seaward-going currents, known as rip currents, which are fed by the longshore currents, see figure 2.2. These rip currents spreading out in the deeper surf zone in combination with adjacent landward-going surface currents (mass flux velocities) can be interpreted as horizontal circulation cells, moving gradually along the coast.

Low-frequency wave motions are manifest in the inner surf zone where bound long waves are released (into free waves) due to the breaking process. Furthermore, the horizontal variation of the breaking position of irregular waves generates variations of set-up and hence low-frequency oscillations (surf beat).

Tidal currents generally are weak in the surf zone due to the strong effect of bottom friction in shallow depth. More important are wind-induced currents, which respond rapidly to the wind stresses near the surface and tend to be aligned with the wind direction and have longshore values of the order of 1 m/s intensifying the wave-induced longshore current.

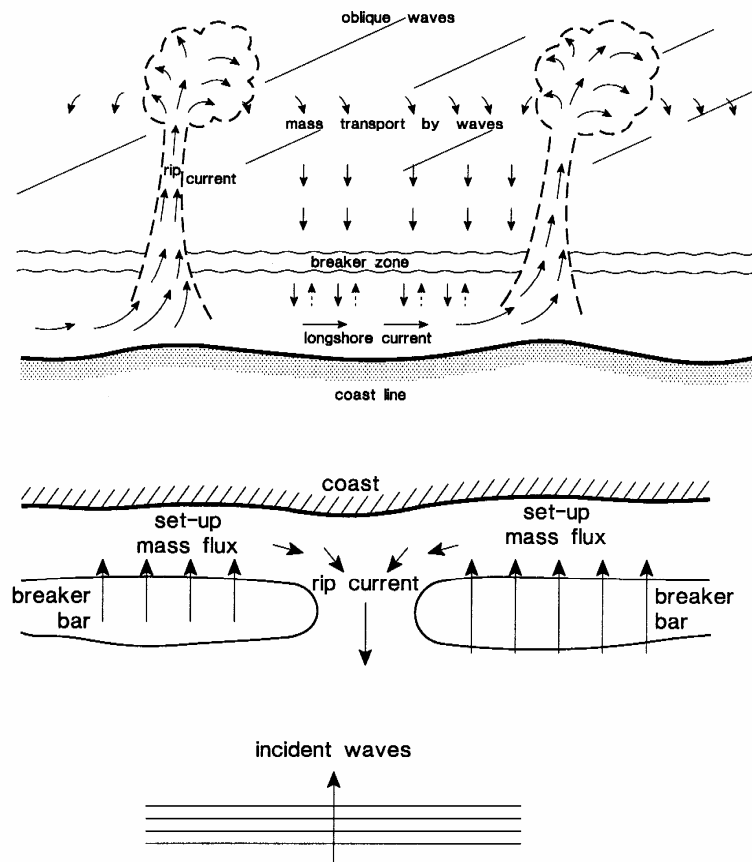


Figure 2.2 Rip channel and rip current

The longshore current can carry an enormous amount of sand along the shore. During storm conditions with a surf zone width (b) of 300 m, a depth (h) of 3 m, a longshore velocity (v) of 1 m/s and a depth-averaged sand concentration (c) of 0.1 to 0.5 kg/m³, the longshore transport ($Q_s = bhvc$) is in the range of 5000 to 25000 m³ per day. The annual net longshore transport strongly depends on the wave climate (wave height and wave direction) and is in the range of 100, 000 to 300,000 m³/year to the North for the Dutch coastal zone between Den Helder and Hoek van Holland.

During mild weather conditions the smaller waves do not break at the bars, but shoal over the bar crests resulting in the transformation of the wave profile from a sinusoidal wave profile into a forward leaning wave profile with a relatively large onshore peak velocity. This process strongly promotes the onshore transport of sand over the bars into the troughs. As the net transport rates involved are rather small (in the range of 10 to 100 m³/year), the onshore migration of the bars (with a volume of order 500 m³) is only noticeable on the time scale of seasons. Offshore migration of the bars generally prevails during storm events.

A shoreface nourishment (underwater nourishment) can be seen as a submerged structure such as a soft reef or a submerged breakwater, see figure 2.3. A basic effect is the reduction of wave height (wave filtering effect) and the associated longshore current in the lee of the structure, leading to a reduction of the longshore transport capacity. Another important hydrodynamic effect is the generation of set-up currents due to the increased water level in

the lee zone as a result of water transport over the structure generated by wave breaking. This surplus water trapped inshore drives currents, which flow along paths of least resistance toward both distal ends of the submerged structure.

The smaller waves do not break, but only shoal over the nourishment area becoming more asymmetric forward leaning waves resulting in the increase of onshore transport processes. Both cross-shore and longshore effects result in the trapping of sand behind the shoreface nourishment area. Basically, a shoreface nourishment behaves in the same way as a low-crested, submerged breakwater showing deposition in the lee of the structure, shoreline accretion on the updrift side and shoreline erosion on the downdrift side, see figure 2.3.

Analysis of several shoreface nourishments along the Dutch coast show that about 20% to 40% of the nourished sediment moves onshore (Deltares, 2009). After 3 to 5 years the zone landward of the nourishment area shows a volume increase of about 20% to 40% of the original nourishment volume. After about 10 years the dune zone shows a similar volume increase (Arens, 2008). At most locations the beach zone does not benefit much from the nourishment, it merely acts as a bypassing zone. Most of the nourished sediments move in longshore direction.

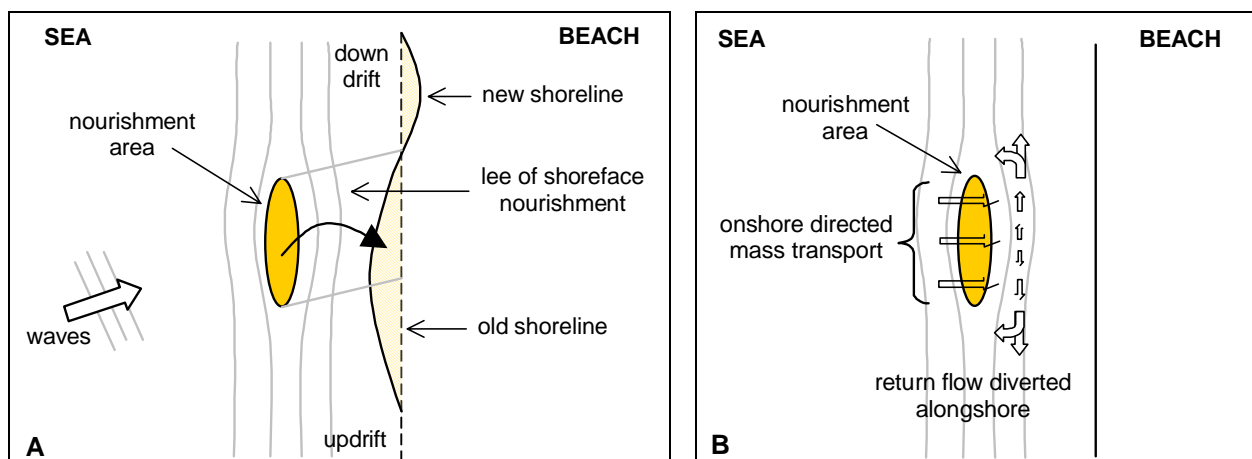


Figure 2.3 Effects of a shoreface nourishment

Summarizing, the hydrodynamic and morphodynamic effects of a shoreface nourishment are:

- Dissipation of wave energy by breaking processes (wave filter) and reduction of wave-driven longshore currents in the lee area during stormy conditions.
- Generation of shoaling waves.
- Generation of set-up currents at end sections.
- Generation of low-frequency waves in lee area.
- Trapping of sand in the lee area and updrift of the structure due to partial blocking of the wave-driven longshore current; downdrift erosion may occur.

To assess the effect of a shoreface nourishment (as shown in figure 2.4) on the longshore sediment transport, some exploring computations for the coastal profile of Egmond have been made using a cross-shore process model. The sand particle size is $d_{50} = 0.2$ mm. Wave heights in the range of 2 to 3 m (present during 10% to 20% of the time) are considered as these waves are most effective for growth and onshore migration of sand. The wave incidence angle is constant at 30° for all model runs.

The effect of the nourishment on the integrated longshore sand transport (LST) is, as follows:

- Nourishment section up to bar crest: increase of LST of about 20%.
- Landward flank of nourishment section: decrease of LST of about 50%.
- Inner surf zone from trough up to beach: decrease of LST of 20%.

The reduction of the longshore transport (LST) increases with increasing crest level of the nourishment area (bar formation and growth, see figure 2.4).

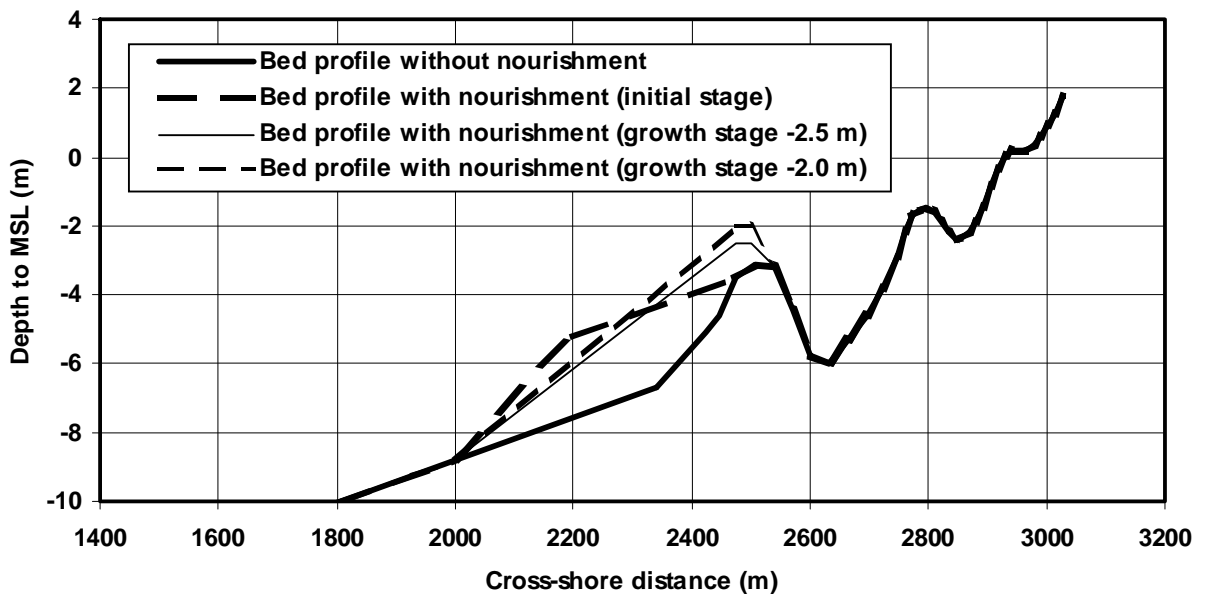


Figure 2.4 Shoreface nourishment; initial stage and two schematized growth stages

Figure 2.5 shows the morphological changes of a shoreface nourishment due to shoaling waves ($H_{s,0}=1.5$ m) over 100 days. The migration distance varies between 10 and 40 m over 100 days which corresponds to onshore sand transport in the range of 20 to 100 m^3/m over 100 days. The nourishment profile shows a slight tendency to grow due to the shoaling waves of 1.5 m as observed in nature. As the beach zone (-3/+3 m) is situated at about 200 m shorewards from the shoreface nourishment, it will take at least 5 years of low wave conditions (which occur during about 75% of the time; $H_{s,0}<1.5$ m) before the nourishment can migrate to the beach zone (-3 to +3 m). Hence, it is rather difficult for the sediments to pass the deep trough landward of the nourishment area.

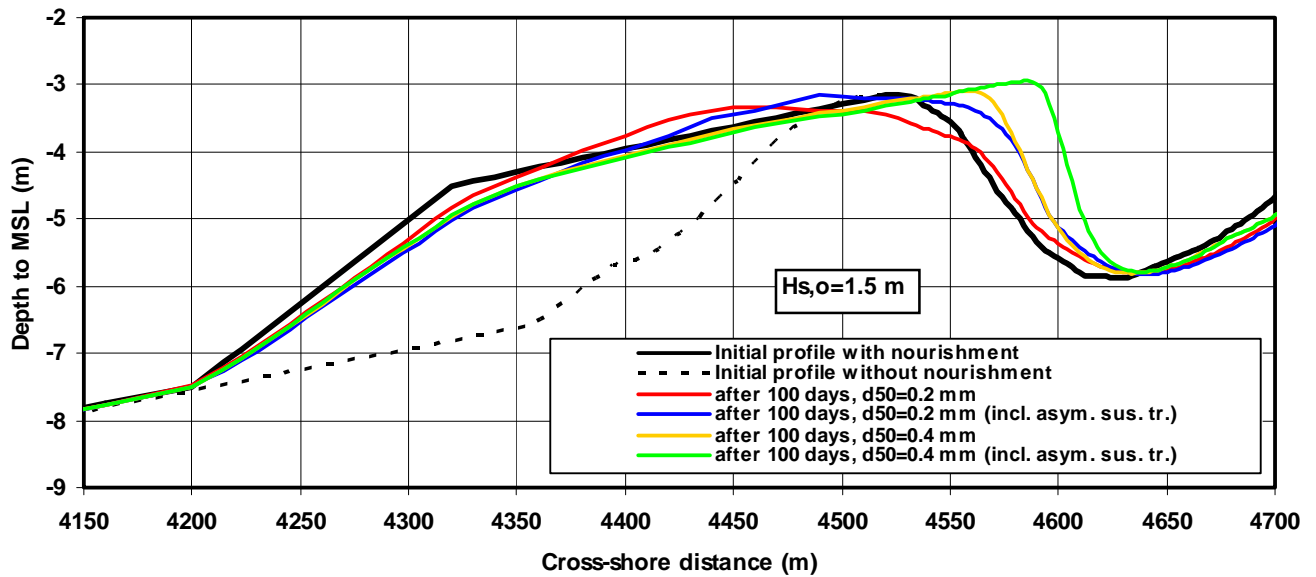


Figure 2.5 Onshore migration of shoreface nourishment; $H_{s,o}=1.5$ m

Figure 2.6 shows the morphological changes (offshore migration) of the shoreface nourishment for storm events with $H_{s,o}$ in the range of 2.25 to 5 m (which occur during about 20% of the time or less). As can be observed, these conditions result in the formation of new bars and offshore-directed migration of the nourishment. The sediment (in the range of 50 to 100 m^3/m) is eroded from the crest region and deposited at the seaward flank over a period of 5 to 50 days.

On the seasonal time scale with low and high waves, the shoreface nourishment will be gradually spread out in both onshore and offshore direction. The annual transport from the crest region to both flanks (seaward and landward) of the bar is of the order of 50 to 100 $m^3/m/year$ yielding a lifetime of the order of 5 years given an initial volume of about 400 m^3/m . The lifetime increases for larger volumes (mega nourishments).

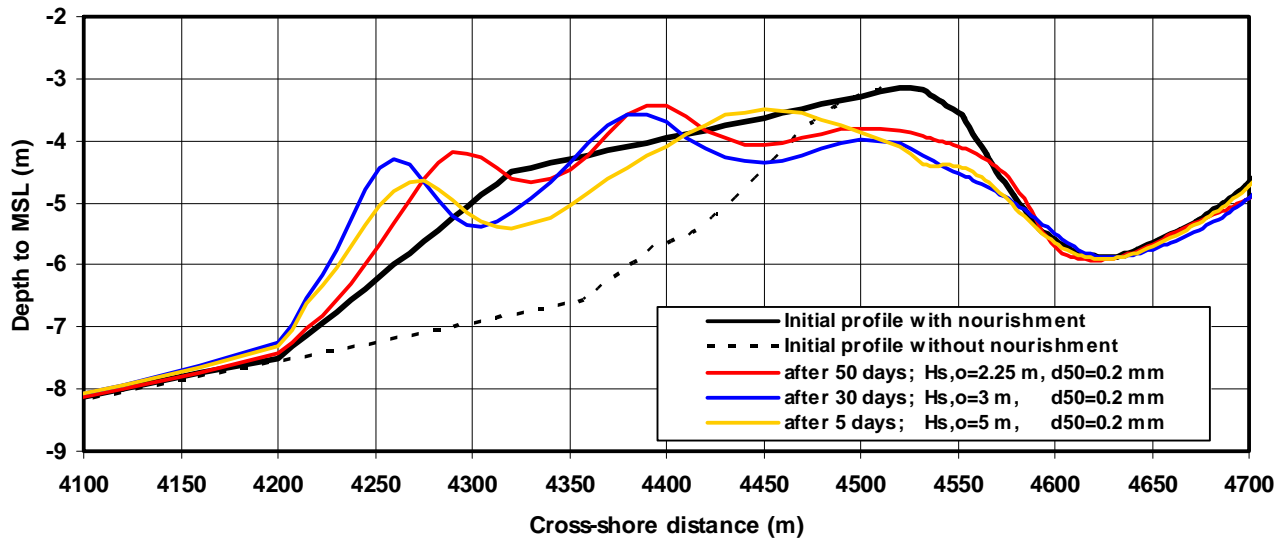


Figure 2.6 Offshore migration of shoreface nourishment; $H_{s,o}=2.25$ to 5 m

Conclusions:

Overall, the nourishment area will move as a large-scale sand wave along the shore due to the gradients of the longshore transport, while at the same time it will be dispersed at its sides due to longshore and cross-shore transport gradients. About 30% of the nourished sediment gradually moves onshore and will ultimately contribute to the growth of the dune zone (with a time lag of the order of 10 years).

Assuming a net longshore transport gradient (on the length scale of the nourishment) of $Q_{sl} = 100,000 \text{ m}^3/\text{year}$, a sand wave height of $H_{sw} = 5 \text{ m}$ and a width of $B_{sw} = 500 \text{ m}$, the migration speed of the sand wave will be of the order of 100 m per year or 1 km per decade ($C_{sw} = Q_{sl}/0.5 B_{sw} H_{sw}$).

Given a net cross-shore transport rate of about $Q_{sc} = 50 \text{ m}^3/\text{m}/\text{year}$, it will be dispersed over a time period of about 50 years ($T_L = B_{sw} H_{sw}/Q_{sc}$).

These order of magnitude estimates apply to the straight coastal zone far away from tidal inlets. Close to these inlets the tide-induced and wind-induced velocities are dominant and the wave-induced longshore velocities gradually fade away (smaller waves and deeper water and thus less breaking). The total tide-induced sediment transport through the inlets is an order of magnitude larger than the wave-induced longshore transport which has an episodic character (storm effects).

The MOHOLK model which is a two-dimensional depth-averaged model on a relatively large grid to cover the complete Dutch coastal zone, is capable of simulating the longshore transport processes due to waves and tides correctly both along the straight coast and near tidal inlets, but it cannot represent the coastal cross-shore processes with sufficient accuracy, because the grid resolution in cross-shore is too crude. A fully three-dimensional approach on a small grid is required to represent the vertical structure of the hydrodynamics involved.

3 Mega nourishments

A need is foreseen in the future for larger nourishment volumes to be applied to the coastal system to maintain the coastal fundament. In the last years individual nourishment volumes were usually between 0.5 and 3 Mm³. In the future, mega nourishments of 10 Mm³ or even much bigger are foreseen and the question then rises what is the effect of such a large nourishment volume. Studies indicate that the sand demand of the Wadden Sea takes place at the cost of the sand volume in the adjacent coast of North-Holland and Texel. Mega nourishments might interfere with the current sediment transport and provide more sediment to be imported into the Marsdiep basin. The Moholk-model will help to predict the behaviour of mega nourishments and to evaluate, which locations might function better over others.

3.1 Scenario description

To get a better understanding of the development of the nourished volume and to get a better retrieval of the pathways of the nourished sand an exaggeration of the volume of nourished sand was chosen. Ultra nourishments with a total volume of about 50 Mm³ are evaluated over a period of 10 years. The nourishment locations are chosen on the North-Holland coast, on the outer delta and inside the delta basin. Along the North-Holland coast two nourishment locations are considered for nourishing 50 Mm³ at the start of the 10 years evaluation. The development of the nourishment is then followed for 10 years. Three nourishment locations are considered for the nourishment of 5 Mm³ per year for 10 years (in total also 50 Mm³). In the model the yearly volume is nourished in the first two months of the year. Table 3.1 provides the nourishment alternatives for the nourishment locations indicated in figure 3.1.

Besides protection of the coast, the nourishments are intended to increase the sediment transport into the Wadden Sea, through the Marsdiep inlet. Therefore the evaluation of the nourishment scenarios is also focused on the sedimentation and erosion of the Texel Tidal inlet, to indicate the relative effect of the nourishment procedure and nourishment location.

Scenario	Nourishment volume	Nourishment area
A1	50 Mm ³	Long / Callantsoog
A2	50 Mm ³	Cross / Callantsoog
A3	5 Mm ³ /year for 10 years	Noorderhaaks
A4	5 Mm ³ /year for 10 years	Texelstroom
A5	5 Mm ³ /year for 10 years	Short and broad / Callantsoog

Table 3.1 Characteristics of the nourishment scenarios

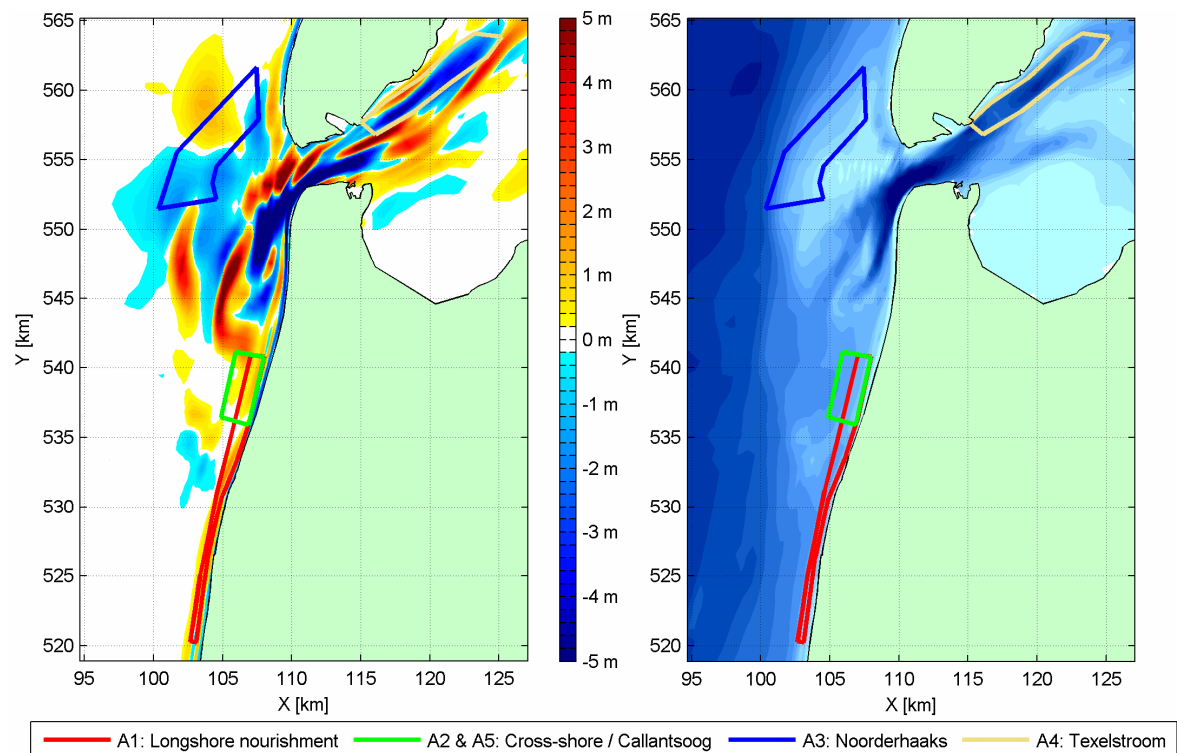


Figure 3.1 The positions of the nourishment locations on the North Holland coast and the Marsdiep Delta on the cumulative sedimentation and erosion map of the autonomous development (left) and on the bathymetry map (right)

3.2 Ultra nourishment scenarios, Callantsoog Long (A1) and Callantsoog Cross (A2)

The scenarios consider an ultra nourishment of 50 Mm^3 at the start of the calculation. The Callantsoog Long nourishment is spread out along the coastline with a length of 20 km longshore and a width varying between 0.5 km and 1 km cross-shore. The Callantsoog Cross nourishment has a length of 5 km longshore and a width of 2 km offshore (Figure 3.2). The nourishments are placed seaward of the outer breaker bar with a maximum bed level up to -5 m NAP, thereby enlarging the outer breaker bank with 0.5 km up to 2 km. The Callantsoog Long nourishment is placed outward up to a water depth of 10 m and the Callantsoog Cross nourishment up to a water depth of 11 m.

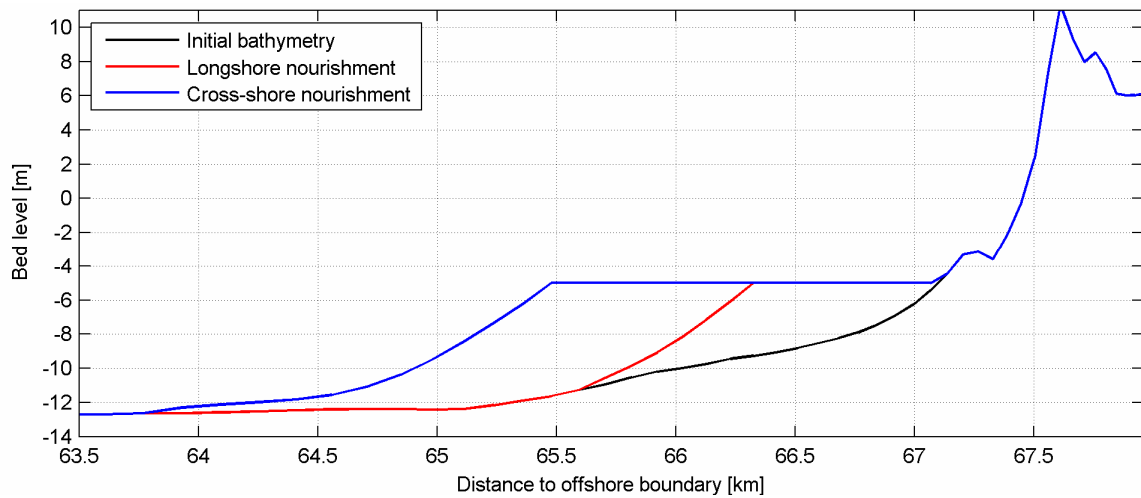


Figure 3.2 Cross-section of nourishments A1 and A2 at 15 km from Den Helder

A nourishment volume of 50 Mm^3 has an impact on the local hydrodynamics, such as the residual tidal current (figure 3.3, first panel), but also on the size of the surf zone as large waves break further from the coast on the nourished area (figure 3.3, lower panel). The plot shows a higher flow velocity at the location of the Callantsoog nourishment areas and a lower flow velocity just shoreward of the location of the Callantsoog nourishment areas. This leads to a lee effect, where more sedimentation between the nourishment and the beach will occur due to the decrease in flow velocity. This effect is larger and on a smaller scale for scenario A2 than for scenario A1.

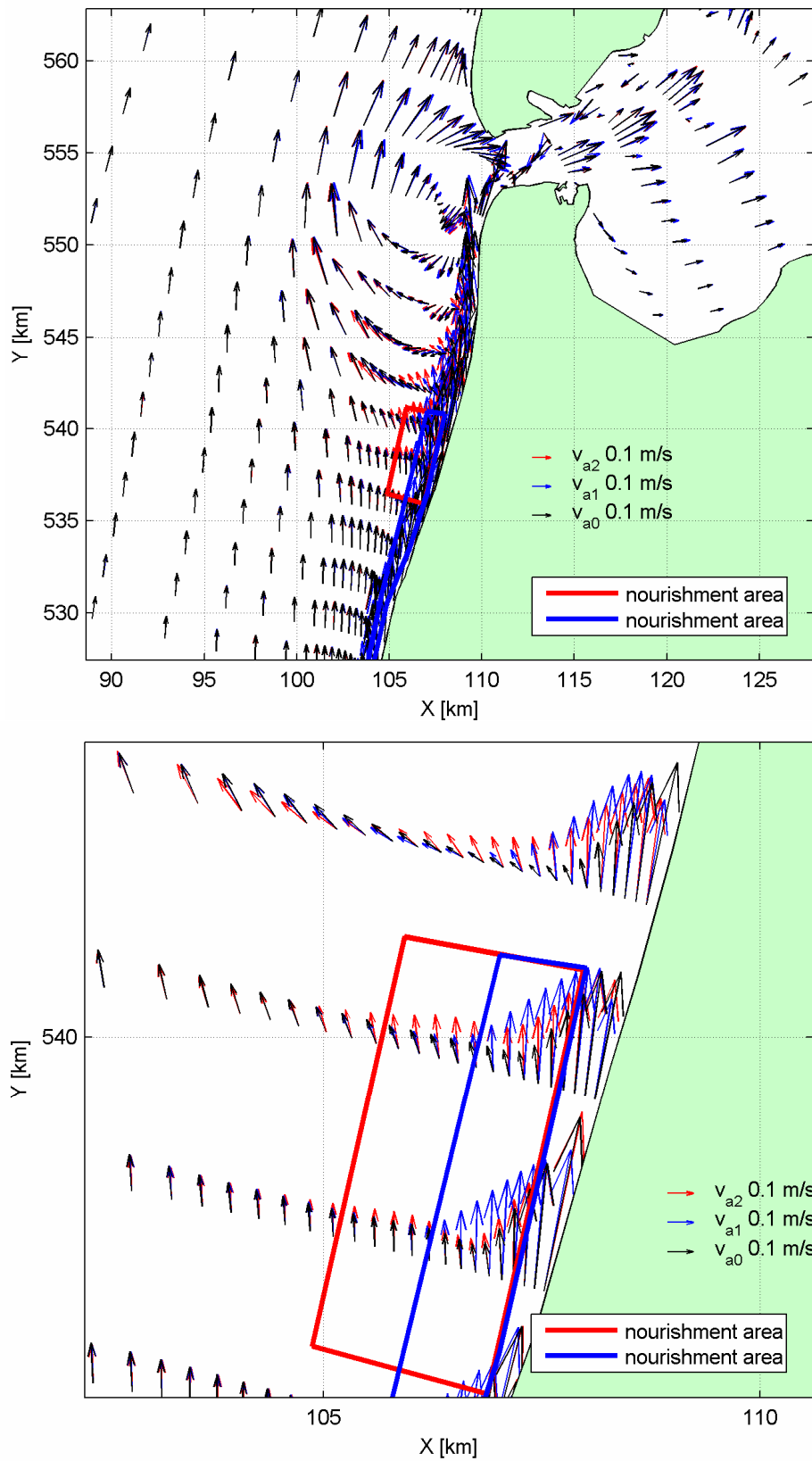


Figure 3.3 Residual current due to tide and waves ($H_s=2.9$ m, dir 240 deg) without (black vectors) and with nourishment A1 (blue vectors) and nourishment A2 (red vectors)

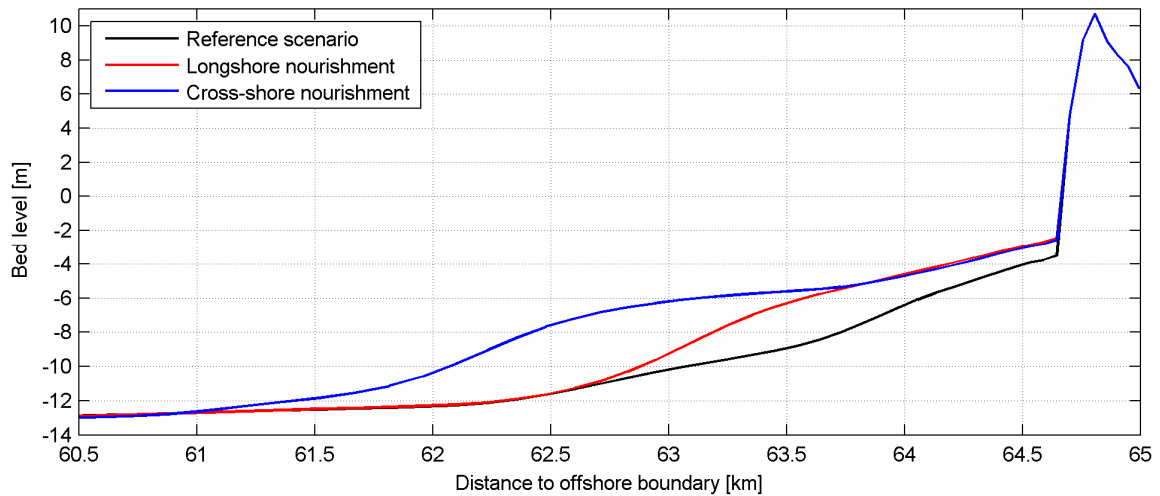


Figure 3.4 Cross-section of developed bed level for nourishments A1 and A2 with reference to the autonomous development at 15 km from Den Helder. The initial profiles are shown in figure 3.2

The area between the nourishment and the beach accretes more than in the autonomous development for both scenarios (figure 3.4) due to the lee effect and at the sides more erosion or less accretion occurs. This phenomenon was also seen in the study for the Egmond nourishment case (Van Duin et al, 2004). Due to the difference in cross-shore size, the two scenarios behave differently.

If the bed level development for the two nourishments is compared to the bed level development in the autonomous situation, then the relative effect of the nourishments can be determined. The relative effect is determined within three polygons; the nourishment area (0 kilometre), within a 2 kilometre zone around the nourishment area and within a 5 kilometre zone around the nourishment area. The results are shown in table 3.2. The relative erosion with respect to the autonomous development is 17% for scenario A1 (Callantsoog Long) and 15% for scenario A2 (Callantsoog Cross). Although the differences are small, it seems that the Callantsoog Long nourishment is moving more than the Callantsoog Cross nourishment. This is contrary to the expectations, where it was supposed that a more seaward protruding nourishment would trigger more nourished sediment to be redistributed after 10 years. The lee-effect, as mentioned above, is the driving factor for this contradictory outcome.

Scenario	A1			A2		
	0km	2km	5km	0km	2km	5km
Initial volume [Mm ³]	50.0	50.0	50.0	50.0	50.0	50.0
5 yr relative [Mm ³]	45.0	48.5	48.4	45.4	48.3	49.3
Erosion 5 yr	10%	3%	4%	9%	3%	1%
10 yr relative [Mm ³]	41.6	47.0	47.2	42.7	46.9	48.9
Erosion 10 yr	17%	6%	6%	15%	6%	2%

Table 3.2 Sediment volume change in nourishment area per scenario with respect to the autonomous development (scenario A0)

The nourishment mainly remains in the nourishment area, which is remarkable as nourishments usually lose their initial shape and merge into the surrounding area within 5 years. However, this case considers a very large nourishment (15 times larger than usual), thus in percentage the development is small, but in absolute numbers the erosion of nearly 1

Million m³ per year is almost four times the volume decrease of 470,000 m³ in 2 years in the Egmond case (van Duin et.al., 2004). Van Rijn and Walstra, 2004 state that it is known that from monitored nourishments about 70% of the supplied sand was still present after four years.

On a larger scale the effect of the nourishments is not significant. In figure 3.3, the currents are affected on the southwestern side of the outer delta and in the Nieuwe Schulpengat but no further than that. Together with the fact that the nourishments remained for more than 90% in the nourishment area, the effects on the outer delta and basin are almost zero. On the sedimentation and erosion maps (figure 3.5) more erosion of the gullies Schulpengat and Nieuwe Schulpengat occurs and larger ebb-shield deposition at the ends of these channels. Also in the Helsdeur less erosion occurs and less sedimentation of the Molengat along the Texel coast. The effect of the Callantsoog Cross nourishment is somewhat larger than for the Callantsoog Long nourishment. In the sediment balance the same sediment volume is imported into the Marsdiep basin as occurs for the autonomous situation (figure 3.6A and B). Only between the sections North Holland and outer delta a difference in the sediment balance is seen for the two scenarios compared to the autonomous situation, which has mostly to do with the nourishment locations overlapping the border between the two sections.

One has to bear in mind that a 2D model setting has been used, causing the cross-shore transports to be underestimated.

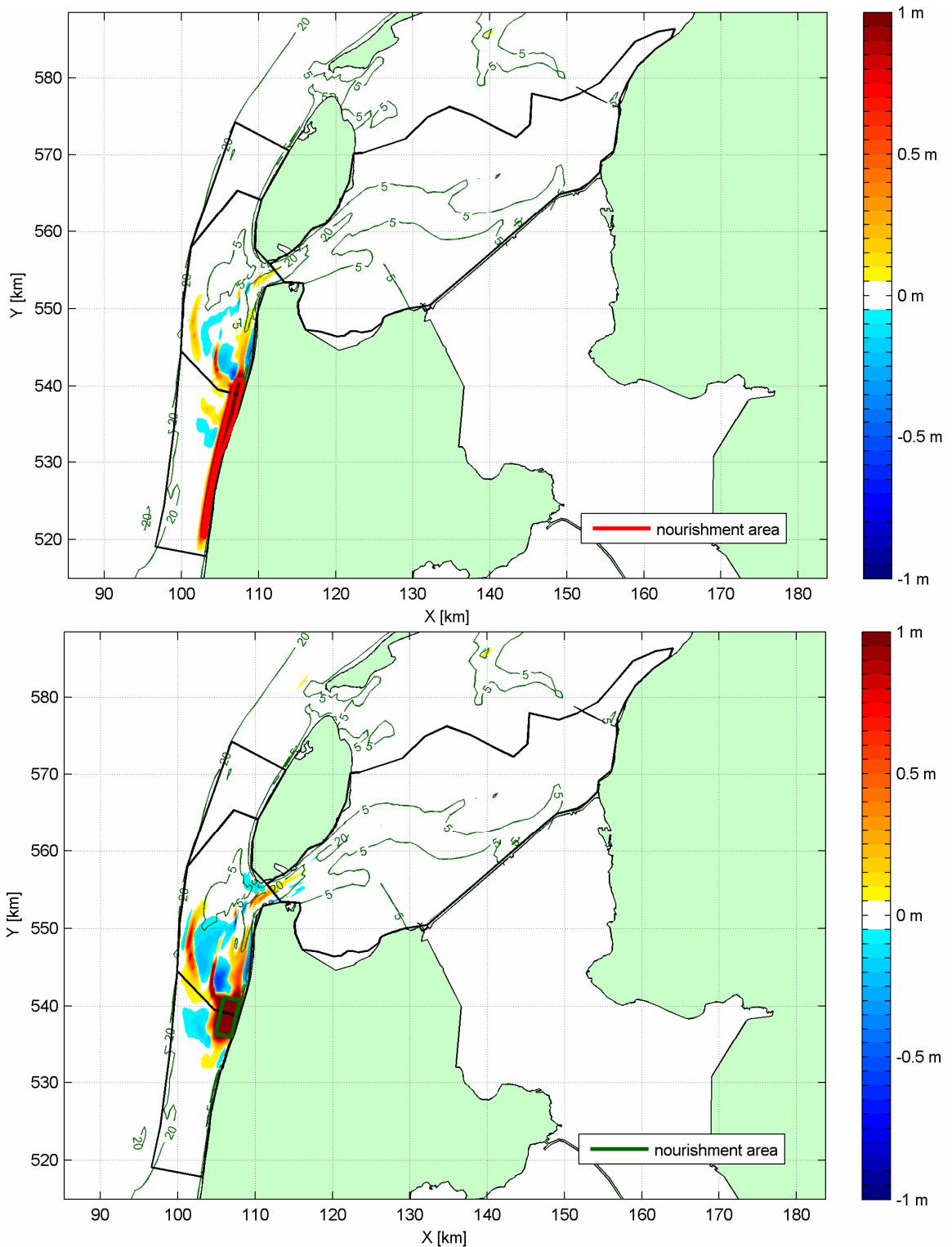


Figure 3.5 Cumulative sedimentation and erosion values in the Marsdiep delta with respect to the autonomous development. Upper panel: Scenario A1; Longshore nourishment, lower panel: Scenario A2; cross-shore nourishment

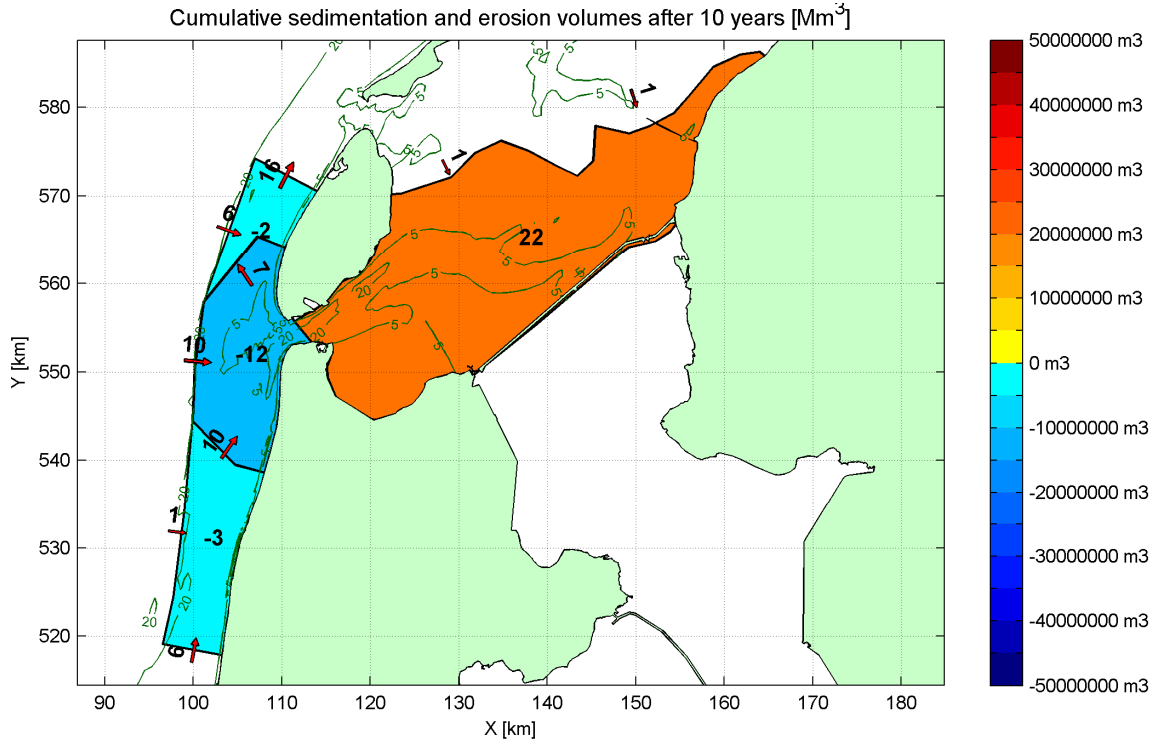


Figure 3.6A Scenario A0 Autonomous situation. Sedimentation and erosion in 10 years of morphological simulation in sections; 1) Marsdiep delta 2) Marsdiep basin 3) Texel coast and 4) North-Holland coast, including sediment exchange ($Mm^3/10yr$) in between sections and with the surrounding environment

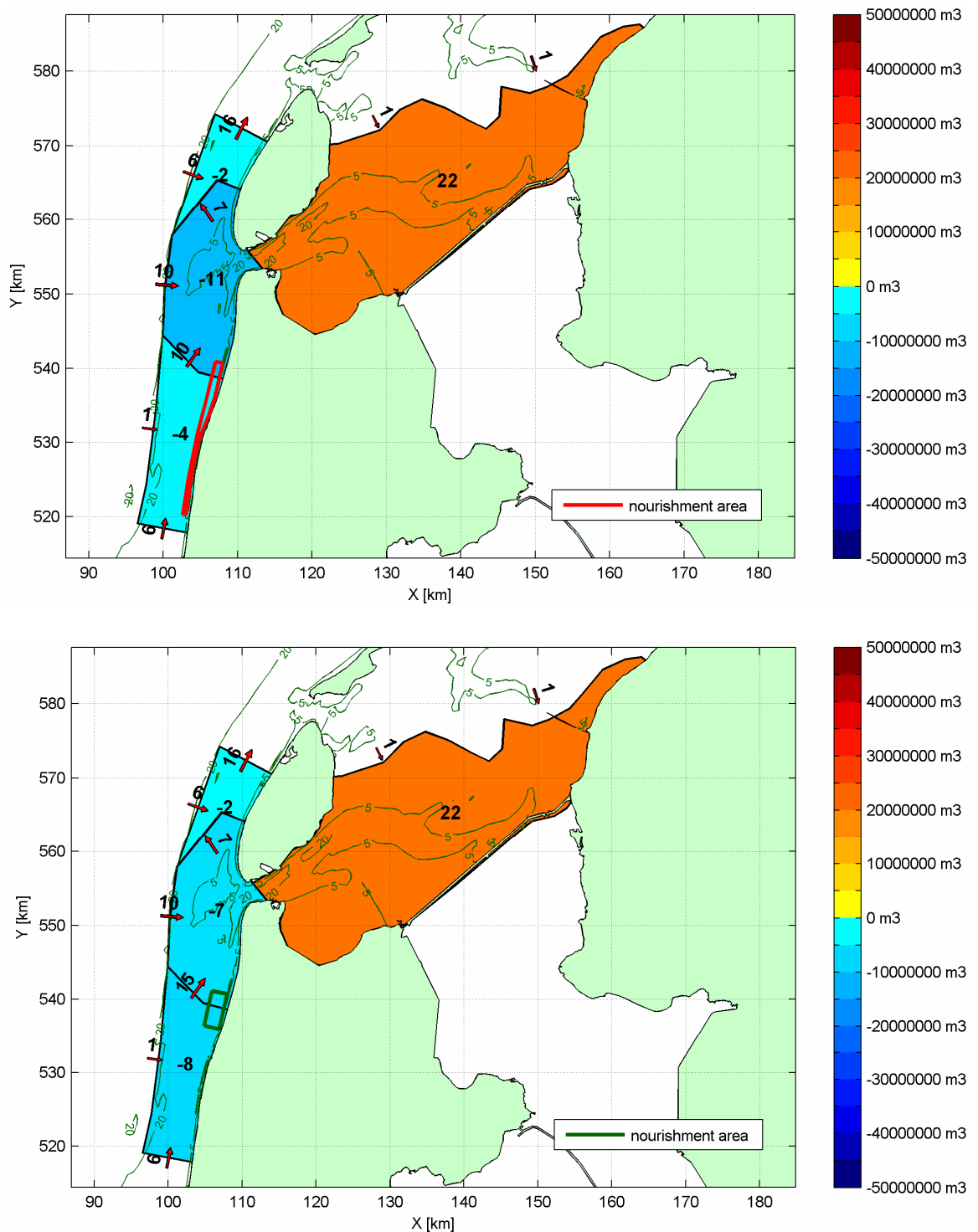


Figure 3.6B Cumulative sedimentation and erosion volumes in sections with import and export of sediment for scenario A1 (top panel) and scenario A2 (bottom panel). Volumes in Mm^3 per 10 years

3.3 Scenario A3 Noorderhaaks

In scenario A0 (autonomous situation) as well as in nature (measurements) a degradation is seen of the volume of the shoal Noorderhaaks, at the cost of infilling of the Wadden Sea. By nourishing this shoal, the degradation will be mitigated and the sediment is supplied with the large sediment circulation cell of the outer delta. This will mitigate the degradation of the Noorderhaaks and might enlarge the sediment transport towards the Marsdiep basin and increase the sediment import. The nourishment is designed with a maximum height up to NAP -5 m and up to 10 m from the northern side of the shoal, where in the autonomous development erosion takes place (figure 3.1; left). The nourishment location is at the seaward side of the shoal, where dumping is easily done by large dredgers. A volume of total 50 million m³ sand is nourished with a yearly volume of 5 Mm³. The yearly volume is nourished in the first two months of the year.

The cumulative sedimentation and erosion map in figure 3.7 shows a large bed level increase in the nourishment area with respect to the autonomous development. In 10 years the average bed level increase within the nourishment area is 1.07 m with respect to an average decrease of 0.37 m without the nourishment (a relative increase of 1.44 m). The Noorderhaaks shoal is shifting less in landward direction, as the eastern tip is accreting less (blue in figure 3.7) than in the autonomous situation and the western side is eroding less (yellow and red areas in figure 3.7). A small part of the nourished sand is used for a larger development of the ebb shields of Schulpengat and Nieuwe Schulpengat and a small part is transported to the Marsdiep and Texelstroom. On a larger scale (figure 3.8) the import and export of sediment of the Marsdiep delta and of the sections remains the same with or without the nourishment. Less than one million m³ is transported more from the outer delta section into the Texel coast section, the remaining nourished sand remains inside the outer delta section.

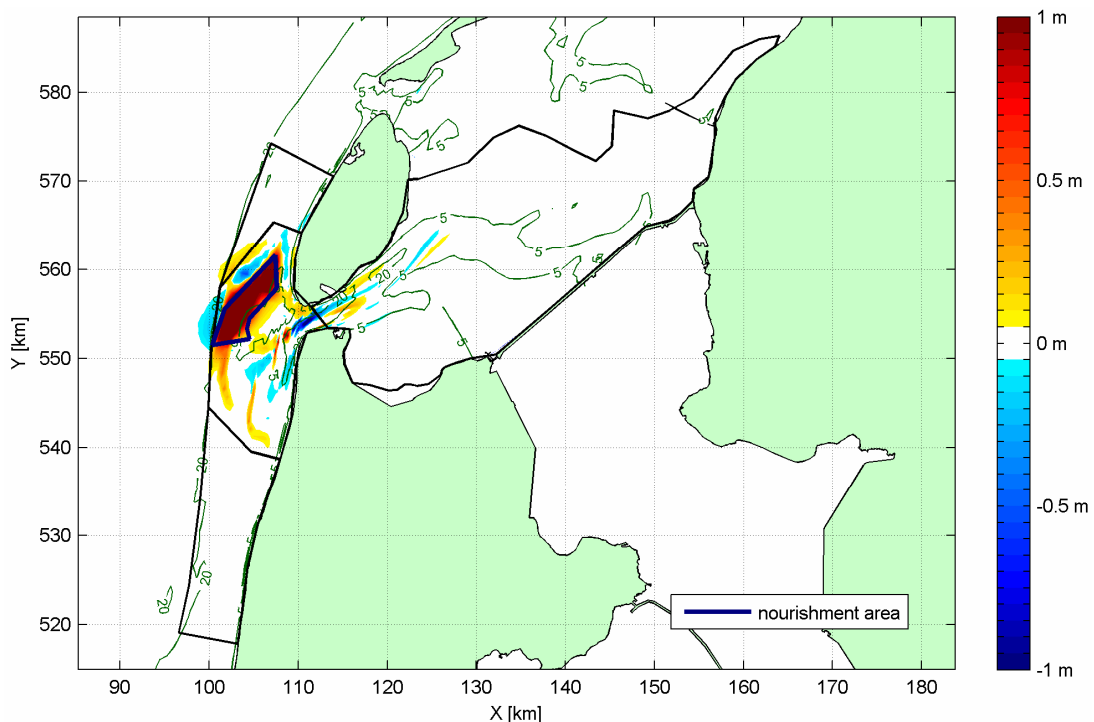


Figure 3.7 Cumulative sedimentation and erosion values in the Marsdiep delta relative to the autonomous development for scenario A3 Noorderhaaks

volume of 5 Mm³/year over a period of 10 years. The yearly volume is nourished in the first two months of the year.

As expected, not much of the nourished sediment remained in the nourishment area. After five years 3.5 Mm³ of the 25 Mm³ was recovered and after 10 years the nourishment area has even eroded more than the nourishment volume. However, relative to the autonomous development, with intensive erosion, it is seen that the nourishment mostly benefits the nourishment area itself. The diffusion and propagation of the nourishment is larger for this scenario than for the other scenarios. Relatively, 36% of the nourishment remains within the nourishment polygon. Of the eroded sediment more sediment has been transported outside the 2 kilometre polygon (5.3 Mm³), than in case of the other nourishment alternatives (1.8 and 1.3 Mm³; table 3.3).

The relative sedimentation and erosion map in figure 3.9 shows that this larger area of influence extends to the Helsdeur channel and that even the channels Nieuwe Schulpengat and Schulpengat are affected. These two channels erode less and the adjacent ebb shields are accreting less. The nourishment in the Texelstroom channels seems to affect the tidal current in the tidal delta, as the development of the two channels is ebb-dominated (as is the development in the Texelstroom), the Malzwin channel (southern gully in the Wadden Sea) is eroded up to half a meter more and the Molengat is accreting more than in the autonomous development.

On the large scale sediment balance the effect of the nourishment is not noticeable (compare figure 3.10 with figure 3.6A). Compared to the autonomous situation 2 million m³ sediment is imported less from the outer delta to the Marsdiep basin.

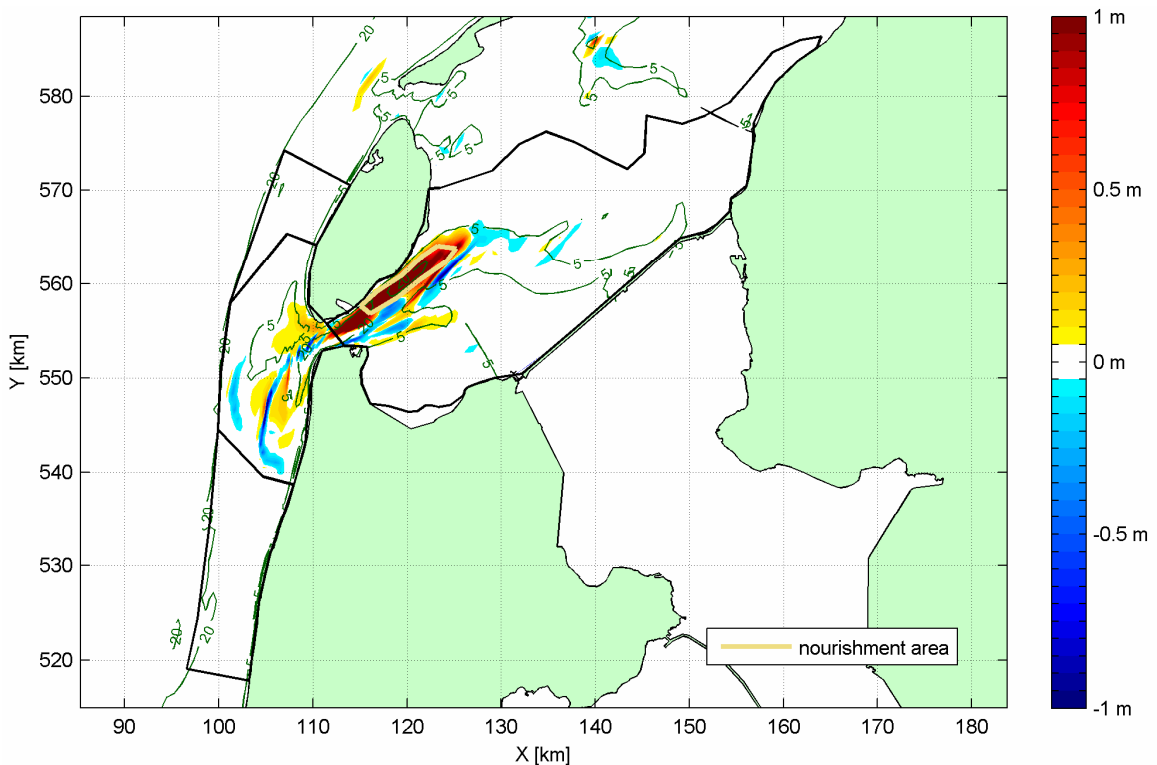


Figure 3.9 Cumulative sedimentation and erosion values in the Marsdiep delta with respect to the autonomous development for scenario A4 Texelstroom

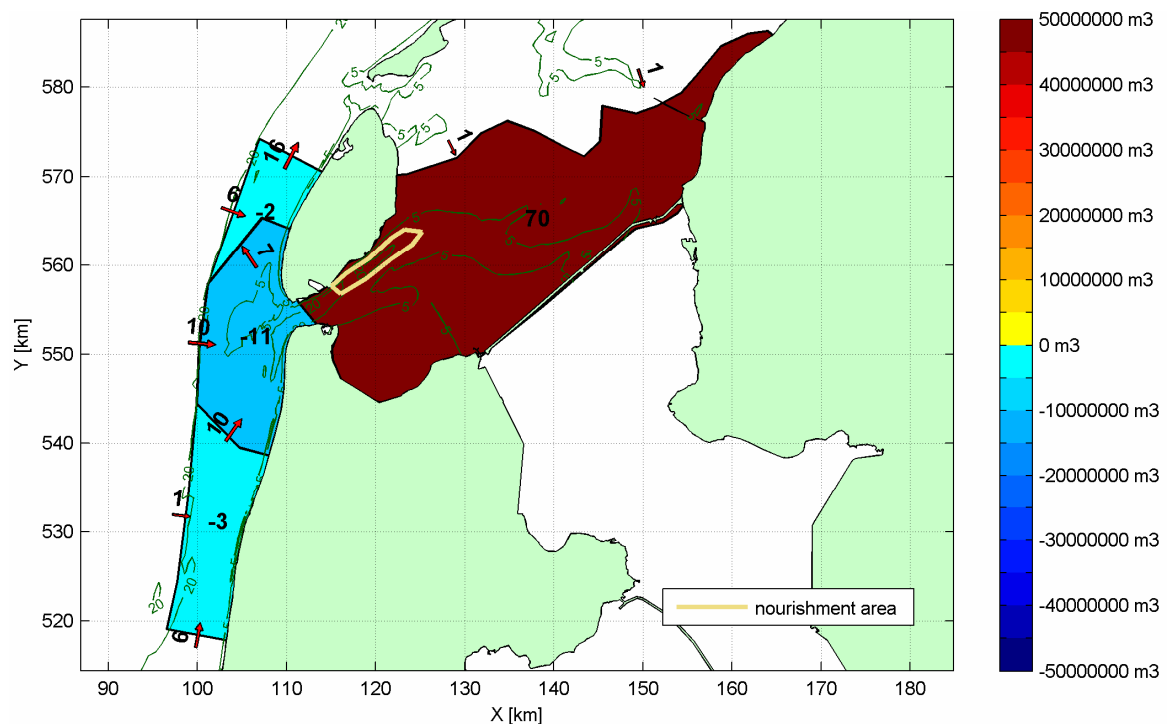


Figure 3.10 Cumulative sedimentation and erosion volumes in sections with import and export of sediment for scenario A4 Texelstroom. Volumes in Mm^3 per 10 years

3.5 Scenario A5 Callantssoog

In order to investigate the sensitivity of an “instantaneous” nourishment to a more gradual yearly nourishment the Callantssoog Cross scenario (A2) is recalculated with a yearly nourishment of 5 Mm^3 for 10 years.

From the relative cumulative sedimentation and erosion map in figure 3.11 it can be seen that the influence of the nourished sand remains close to the nourishment area on the southern part of the outer delta. At this nourishment location 77% of the nourishment remains in the nourishment area after 10 years (table 3.3), thereby only changing the bathymetry locally. This affects the tidal currents and wave driven currents on a local scale. Although the sediment is not much redistributed, it does have an affect on the currents through the Schulpengat and Nieuwe Schulpengat channels. The channels erode less and the ebb-shields are formed further southward. Comparing the large-scale sediment balance in figure 3.12 with the sediment balance of the autonomous development (figure 3.6A), the nourishment does not create a net extra sediment transport to the Marsdiep basin or other areas in the ebb-tidal delta region.

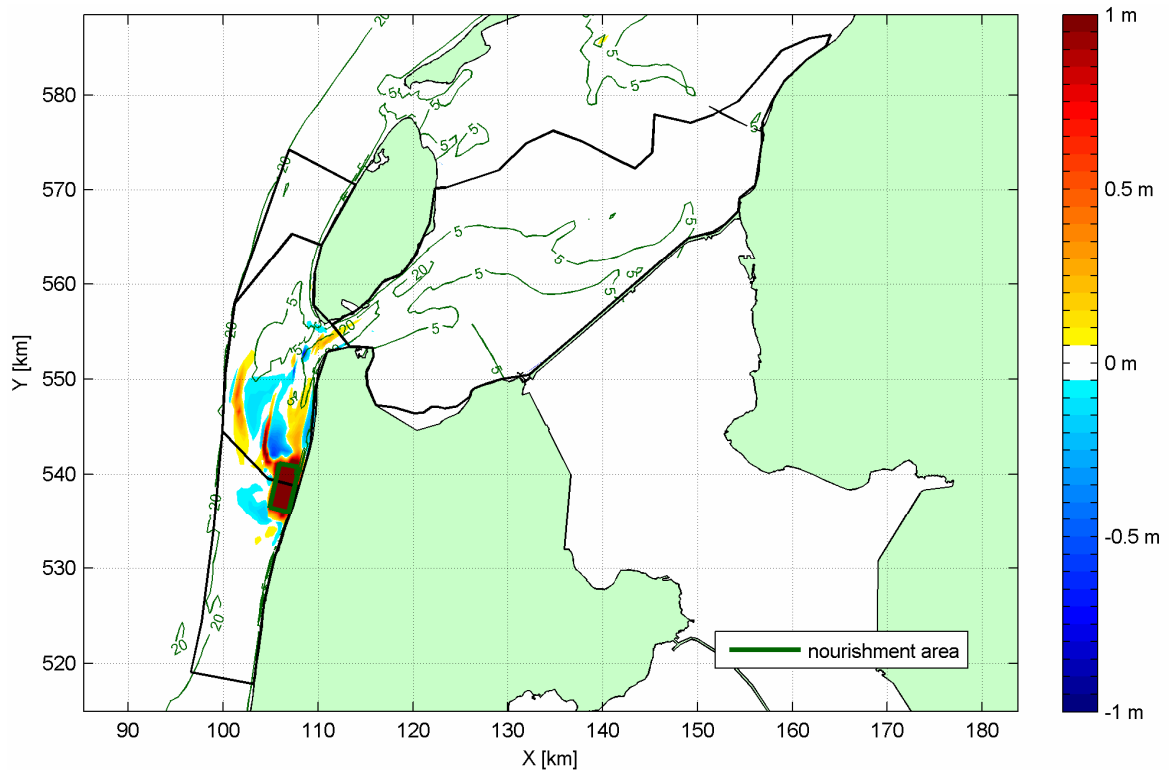


Figure 3.11 Cumulative sedimentation and erosion values in the Marsdiep delta with respect to the autonomous development for scenario A5 Callantssoog

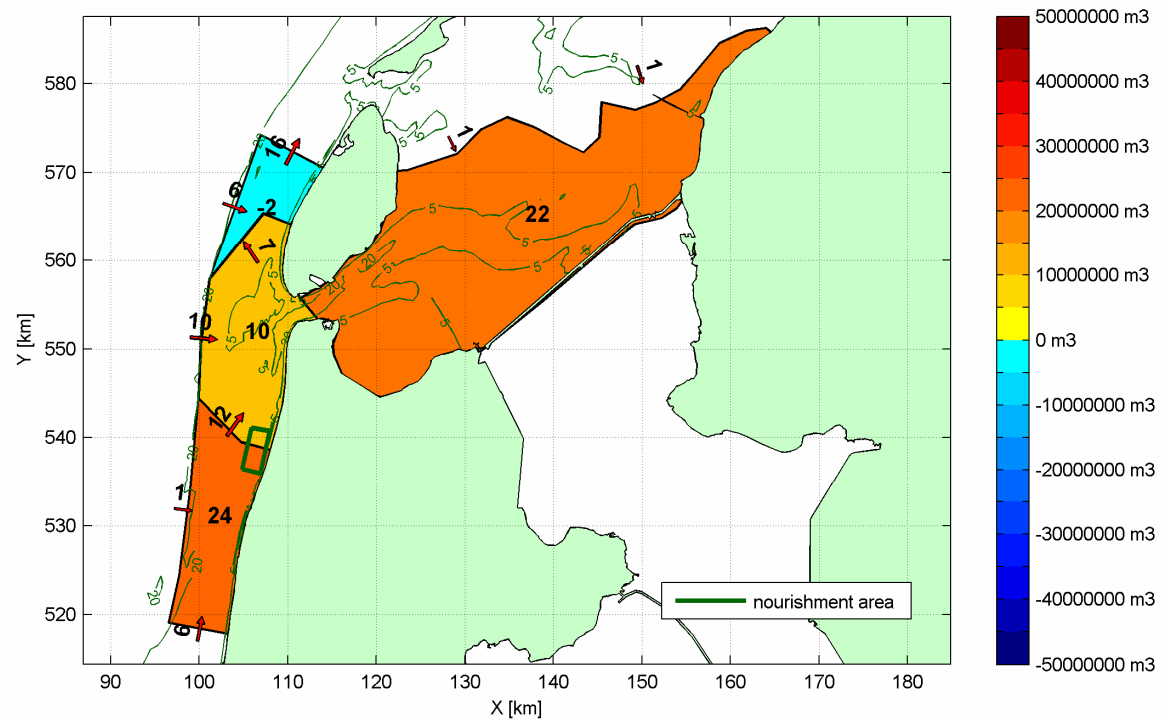


Figure 3.12 Cumulative sedimentation and erosion volumes in sections with import and export of sediment for scenario A5 Callantssoog. Volumes in Mm^3 per 10 years

3.6 Discussion

In previous studies (Van Duin et al., 2004, Grunnet et al., 2004) on the effects of nourishments with Delft3D, the model did represent the volume changes very well but the small-scale sedimentation and erosion locations were not correctly modelled. In the appendixes, the predicting capacity of the coarse Moholk-model is validated for the large-scale hydrodynamics and morphodynamics. Small-scale problems occurred mostly due to the excessive deepening of the tidal channels. Therefore, the results of the various scenarios need to be compared with each other in relative perspective with the autonomous development; scenario A0.

Independent of the nourishment strategy (all in once or spread over the years), ultra nourishments of 50 Mm^3 in the coastal zone or on shoals remain mostly in place. The erosion of the nourishment varied between 1,7% per year or $0,85 \text{ Mm}^3$ per year for the Callantssoog and Noorderhaaks nourishments and 3,6 % per year or $1,8 \text{ Mm}^3$ per year for the Marsdiep nourishment. Most of this material remained in the vicinity of the nourishment. Taking an extended area, with boundaries 5 km outside the nourishment, the erosion was only 0,6% per year or $0,3 \text{ Mm}^3$ per year for the Callantssoog and Noorderhaaks nourishments and 0,2 % or $0,1 \text{ Mm}^3$ per year for the Marsdiep nourishment.

The two scenarios A2 and A5 shared the same nourishment location with a different nourishment scheme, respectively single nourishment of 50 Mm^3 and yearly nourishment of 5 Mm^3 . The differences between these two scenarios are small. Figures 3.5B and 3.11 (relative sedimentation and erosion patterns for respectively scenario A2 and A5) show the same erosion and sedimentation patterns, but the values are somewhat larger for scenario A2, the single nourishment. After 10 years the relative erosion is higher for the yearly nourishment (23%) than for the single nourishment (15%). This difference is limited to the area up to two kilometres from the nourishment location, where for both locations the relative erosion is equally quite low being 6% (single) and 4% (yearly). These numbers indicate a larger diffusion or propagation of the sand volume for the yearly nourished volume, but still limited in spatial scale. The instantaneous nourishment has a larger effect on the tidal currents and wave induced currents due to the longer presence, which results in magnitude difference between figures 3.5 and 3.11.

When nourishing a tidal gully, in this case in the deepest part of a strongly ebb-dominated gully, the sediment will be distributed more within the tidal delta until deposited on shoals or ebb shields. Nourishing a gully is more effective in adding sediment to the sediment circulation system. The natural circulation system will deposit the sediments where necessary for the long term development.

All nourishment scenarios have an effect on the outer delta development with respect to the autonomous development (figures 3.5, 3.7, 3.9 and 3.11). In all cases the affected areas are:

- The gullies and ebb-shields of Schulpengat and Nieuwe Schulpengat on the southern part of the outer delta.
- The steep slope at the eastern side of Noorderhaaks bordering the deep gullies Helsdeur and Breewijd.
- Molengat sedimentation rate.

These three areas are the most dynamic parts of the area. Measurements indicate that indeed these areas are developing rapidly, as is also the case for the shoal Noorderhaaks. All nourishments, except for the Texelstroom nourishment, show more erosion of the gullies Schulpengat and Nieuwe Schulpengat in combination with more deposition on the ebb-shields, with the cross-shore nourishment scenario being most effective. This indicates that these nourishments enlarge the tidal currents through the gullies relative to the autonomous development, while the gully nourishment decreases these currents.

Concluding, a nourishment does not give rise to more erosion or more sedimentation in the system, it just provides more sediment to the bottom which eventually on the very long term (> 50 years) might be needed on an erosion spot. An ultra nourishment of 50 Mm³ on the North-Holland coast did hardly affect the large-scale system, it was only effective within 2 km from the nourishment on both the hydrodynamics and the morphodynamics. Therefore, a mega nourishment will not directly enhance the sediment import of the Wadden Sea if the large scale currents and bathymetry are not adjusted for larger sediment import. The net sediment import seems to be more dependent on the tidal forcing and basin geometry, and on the availability of sediment on the outer delta. At the moment the availability of sediment seems to be sufficient and the system may be importing at maximum speed.

On the long term, it will be effective to supply the shoal Noorderhaaks to decelerate the landward movement and to increase the sediment volume of the outer delta. Then, the import of sediment to the Wadden Sea will at least not be limited by the availability of sediment.

4 Conclusions and recommendations

4.1 Conclusions

In order to evaluate the effects of mega-nourishments on the North-Holland coast in a time span of more than 10 years the Moholk was developed and used. The model proved to be a useful and at the same time efficient in calculating large-scale sediment transports along the Dutch coast.

4.1.1 Effects of Mega nourishments

Independent of the nourishment strategy (all in once or spread over the years), Mega nourishments of 50 Mm³ in the coastal zone or on shoals remain mostly in place. The erosion of the nourishment varied between 1,7% per year or 0,85 Mm³ per year for the Callantsoog and Noorderhaaks nourishments and 3,6 % per year or 1,8 Mm³ per year for the Marsdiep nourishment. Most of this material remained in the vicinity of the nourishment. Taking an extended area, with boundaries 5 km outside the nourishment, the erosion was only 0,6% per year or 0,3 Mm³ per year for the Callantsoog and Noorderhaaks nourishments and 0,2 % or 0,1 Mm³ per year for the Marsdiep nourishment.

Scenarios A3 Noorderhaaks and scenario A4 Texelstroom seem the most promising scenarios of the five investigated, when interaction with and feeding of the surrounding area is required. For the mega-nourishment to be most effective, direct interaction within the dynamic system is necessary. The Texelstroom nourishment has a positive effect on the ebb-tidal current, which is the driving factor for the erosion in the Nieuwe Schulpengat channel. The Noorderhaaks nourishment is, besides supplying a sediment reserve to the outer delta, effective in decreasing the landward movement of the shoal and thus decreases scouring of the channel Helsdeur.

The difference between an ultra nourishment of 50 Mm³ and a yearly nourishment of 5 Mm³ is not significant. The yearly nourishment scheme diffuses more, but after 10 years this is still limited to 2 kilometres.

All five nourishment scenarios at the North Holland coast and Marsdiep tidal area (see figure 3.1 for locations) primarily affect the erosion and sedimentation development on the Marsdiep outer delta. In all cases the affected areas are:

- The gullies and ebb-shields of Schulpengat and Nieuwe Schulpengat on the southern part of the outer delta.
- The eastern side of Noorderhaaks bordering the deep gullies Helsdeur and Breewijd.
- Molengat.

These three areas are the most dynamic parts of the model, affected by large ebb and flood tidal currents to and from the Marsdiep tidal basin. All nourishments, one more than another, thus affect ebb and flood currents through the channels. Of the five nourishment alternatives that have been modelled with the Moholk model, there is not one alternative that increases

the sediment import significantly into the Marsdiep basin. The nourishments mainly remain stable in the nourishment area, diffusion occurs up to 2 kilometres.

4.1.2 Model development

In chapter 2 the development of the newly developed Moholk model is described. This model is based on the former HCZ model (Roelvink, 2001) that uses the outdated RAM approach and a fixed beach profile for long-term morphodynamic simulation. The Moholk model uses the advanced morphological updating method 'parallel online', which is more time efficient, and a dynamic development of the beach profile. It is a relative coarse coastal model (highest resolution in the nearshore of 22 m by 260 m) containing the most important driving factors; tidal currents, wave driven currents, sediment transport and accelerated bed updating. The model covers almost the entire coastline, only parts of the southern delta and the eastern Dutch Wadden Sea are not included.

4.1.3 Model validation

With the coarse Moholk model the primary currents in the surf zone, the offshore and in the Wadden Sea tidal inlets are accurately modelled. This involves tidal ebb and flood currents, a residual northward current along the coastline due to tide, wind and waves, circulation patterns and ebb and flood dominated channels in the tidal inlets. The large size of the model does not allow to include secondary effects such as salinity and 3D circulation to be involved, while at the same time have a relatively fast model. The exclusion has minor effects on the closed Holland Coast and some larger effects on the complex hydrodynamics in the tidal inlets. The residual current in the Marsdiep Inlet is more exporting than the NIOZ ferry measurements indicate (Elias et al, 2006b, Buijsman and Ridderinkhof, 2008b).

For the closed coastal system, from Hoek van Holland up to the Hondsbossche Sea Wall, the residual longshore transport shows good agreement with the literature study by Van de Rest, 2004. In the nearshore, defined from the dune foot (+3 m NAP) up to a water depth of 8 m NAP, the average longshore transport is in the order of 100,000 m³/year. Up to a water depth of 20 meters the average longshore transport is 450,000 m³/year and from the beach to 60 km offshore the longshore transport is modelled in the order of 2 million m³. The average sediment import through the Marsdiep Inlet after morphological spin-up is circa 0.5 Mm³. This sediment import is rather low compared to the most recent sand balance study of the Western Wadden Sea (Elias, 2006) with volume import estimate of 5 – 6 Mm³/year. The erosion and deposition areas identified in the Moholk-model compare very well with those defined in the sand transport model by Elias, 2006, as well as are the sediment circulation on the outer delta. The westward movement of the shoal Noorderhaaks is also modelled in the Moholk model, which is an important driving process for the changing discharge volumes in the ebb and flood channels.

When comparing the model results of the mega nourishments on a general level with the predictions made in Chapter 2 the conclusion is that these compare well. When mega nourishments are placed in coastal areas away from intense tidal forces (e.g. tidal gullies with high current velocities) the erosion rate will be less than 1 Mm³ per year. The main forces (longshore en cross shore) play only a role in a relatively small area (several km) around the nourishment. Taking these distances into account the erosion is less than 0,3 Mm³ per year.

4.2 Recommendations

Although reasonable and promising results have been achieved within this research, there are still some improvements needed to achieve a more accurate and stable model. These recommendations consider mostly model settings and boundary conditions, but also validation measures.

4.2.1 Delft3D

- Apply Neumann boundary conditions on the lateral boundaries to limit the effect of inconsistent combination of prescribed water levels with different wind and wave fields. Gerben de Boer has built a routine within nesthd1 and nesthd2 to derive Neumann boundary conditions from a larger model, with multiple sections on the lateral boundaries.
- A smoother bathymetry, for example after one morphological year, to avoid that spin-up effects influence the results. Small-scale sand banks, for example on top of Noorderhaaks, are not beneficial for this large-scale model and are best eliminated from the initial bathymetry for better interpretation of the results.
- By combination of enlarging the initial sediment layer and including multiple sand fractions the channels will not erode too much and horizontal movement is allowed. Dastgheib et al, 2009, have made some promising results on this subject for the western Wadden Sea.
- Validating the parameters alfaBn (slope factor), SusW and BedW (factor for onshore/offshore sediment transport), ThetSD (factor for erosion of adjacent dry cells) on the cross-shore transport and the steep beach slope and channel slopes.
- Develop a beach module in which the smooth slope of the beach and the nearby foreshore remains stable.
- Shift the eastern Wadden Sea boundary one tidal divide further to the east. The Amelander tidal divide functions more as a tidal divide than the Terschelling tidal divide. Besides, the model boundary will not interact in the connected basins of the Marsdiep and the Vlie.
- Derive a new wave climate, which is representative for the Holland Coast and the Western Wadden Sea. The present morphological wave climate is derived for the Haringvliet.
- Investigate the effect of the horizontal eddy diffusivity on the nourishment development. This parameter is in the present model set at 10, but it is recommended by Dano Roelvink to lower this value to 0.1 for models including morphology.

4.2.2 Validation

- The sediment transport along the Holland Coast needs further validation if used as an area of interest. This validation should consider the coastal development near harbour breakwaters and groins.
- Use the results of the recently performed mega-nourishments of 7 Mm³ each at Julianadorp to calibrate the nourishment development.
- Sediment transport through the Marsdiep Inlet is not only dependent on the tide and waves, but also on three-dimensional processes as Coriolis, channel curvature and density differences which generate secondary currents. In Delft3D these effects can only be introduced by calculating in 3D, instead of in 2D depth

averaged mode. However, it is not clear if the import and export of sediment will be correctly modelled if included, as the general knowledge on this system is still not sufficient. In the present model, none of these effects is accounted for. It is recommended to develop more knowledge on this subject with a combination of numerical modelling and data analysis.

5 Literature

- Arens, B., 2008. Effecten van suppleties op duinontwikkeling (RAP2009.02)
- Buijsman, M.C., H. Ridderinkhof, 2008a. Variability of secondary currents in a weakly stratified tidal inlet with low curvature. *Continental Shelf Research* 28 (2008) 1711-1723.
- Buijsman, M.C., H. Ridderinkhof, 2008b. Long-term evolution of sand waves in the Marsdiep inlet. II: Relation to hydrodynamics. *Continental Shelf Research* 28 (2008) 1202-1215
- Dastgheib, A., J.A. Roelvink, M. van der Wegen, 2009. Effect of different sediment mixtures on the long-term morphological simulation of tidal basins. NCK-days 2009, Texel.
- Dastgheib, A., J.A. Roelvink, Z.B. Wang, 2008. Long-term process-based morphological modeling of the Marsdiep Tidal Basin. *Marine Geology* 256 (2008) 90-100
- Delta-committee, 2008. Samen werken met Water, Rapport Deltacommissie.
- Deltares, 2009. Evaluatie kustlijnzorg 2008
- De Ronde, J.G. 2008 Toekomstige langjarige suppletiebehoefte. Deltares Rapport Z4582.24
- Elias, E.P.L. 2006. Morphodynamics of Texel Inlet. PhD Thesis, TU Delft.
- Elias, E.P.L. et al. 2006a. Morfodynamica van het zeegat van Texel. Rapport Technische Universiteit Delft in samenwerking met Rijkswaterstaat RIKZ.
- Elias, E.P.L., J. Cleveringa, M.C. Buijsman, J.A. Roelvink, M.J.F. Stive 2006b. Field and model data analysis of sand transport patterns in Texel Tidal inlet (the Netherlands). *Coastal Engineering* 53 (2006) 505-529
- Elias, E.P.L. and Tonnon, P.K. 2007. Long-term modelling of the Holland coast – setup and validation of a 2dh morphodynamic model. WL | Delft Hydraulics report Z4345.51
- Grunnet, N.M., D.J.R. Walstra, B.G. Ruessink, 2004. *Coastal Engineering* 51 (2004) 581-607.
- Kluyver, M. 2006. Smart nourishment of the Frisian Inlet. MSc Thesis, TU Delft.
- Ontwerp Nationaal Waterplan, 2008. Ministry of Transport, Public Works and Water Management.
- Roelvink, J.A., van Holland., G., Bosboom, J., 1988. Kleinschalig morfologisch onderzoek MV2, Fase1. Validatie Morfologische modellering Haringvlietmonding. WL | Delft Hydraulics report Z2428, June 1988.

Roelvink, J.A., van der Kaaij, T., and Ruessink, B.G. (2001a). Calibration and verification of large-scale 2D/3D flow models, MARE consortium report no. Z3029.11, ONL Coast and Sea studies, June 2001 (final)

Roelvink, J.A., van der Kaaij, T., Ruessink, B.G. and Bos, K.J. (2001b) Reference scenarios and design alternatives, MARE consortium report no. Z3029.12, ONL Coast and Sea studies.

Roelvink, et al. 2001. Calibration and verification of large-scale 2D/3D flow models - Phase 1. WL | Delft Hydraulics report Z3029.10.

Roelvink, J.A. 2006. Coastal morphodynamic evolution techniques. Coastal Engineering 53 (2006) 277-287.

Stam, J.M.T., 1999. Zandverlies op diep water aan de Hollandse kust, Rapport RIKZ-99.006.

Stive, M. J. F., and Eysink, W. D. (1989). Voorspelling ontwikkeling kustlijn 1990-2090. fase3. Deelrapport 3.1: Dynamisch model van het Nederlandse Kuststelsel (in Dutch), Report H825. Waterloopkundig laboratorium, Delft.

Tonnon, P.K., 2005. Morphological modeling of an artificial sand ridge near Hoek van Holland, The Netherlands. Report Z3079.40, WL | Delft Hydraulics, Delft

Van de Rest, P. 2004. Morfodynamica en hydrodynamica van de Hollandse Kust. MSc Thesis, TU Delft.

Van der Valk et al. 2008. Long term morphological development of the Netherlands Coast. VOP Kustlijnverzorging 2007. Deltares. Report Z4345

Van Duin, M.J.P., N.R. Wiersma, D.J.R. Walstra, L.C. van Rijn, M.J.F. Stive, 2004. Nourishing the shoreface: observations and hind casting of the Egmond case, The Netherlands. Coastal Engineering 51 (2004) 813-837

Van Rijn, L. C. 1995. Sand budget and coastline changes of the central coast of Holland between Den Helder and Hoek van Holland period 1964-2040, Report H2129. WL | Delft Hydraulics, Delft.

Van Rijn e.a., 1995, Yearly-averaged sediment transport at the -20 and -8 m NAP depth contours of Jarkus profiles 14,40,76 and 103. Report H1887, project kustgenese, Delft Hydraulics.

Van Rijn L.C., 1997. Sediment transport and budget of the central coastal zone of Holland. Coastal Engineering, 32 (1997) 61-93.

Van Rijn, L.C. and Walstra, D.J.R., 2004. Morphology of mining areas and effect on coast, literature review. Report Z3079, WL | Delft Hydraulics, Delft.

Van Rijn, L.C. et al. 2004. Description of TRANSPOR2004 and implementation in Delft3D-ONLINE. WL | Delft Hydraulics report Z3784.10

Van Rijn, e.a.,2005. Sand transport and morphology of offshore sand mining pits. Final report of the European project SANDPIT.

Setup of the model

This chapter describes the newly developed Moholk model, which is based upon the former HCZ model (Roelvink et al., 2001b) that uses the outdated RAM approach and a fixed beach profile for long-term morphodynamic simulations. Herein the tidal and wave schematization applied in the present Moholk model is elaborated on, as well as several model settings. In this chapter the final model settings of the Moholk model are summarised.

A.1 Model development

The Holland Coastal Zone (HCZ) Model (Roelvink et al., 2001b) was developed within the Flyland project (Investigation North Sea Location – Coast and Sea, parcel 2) to study 2DH hydrodynamics and morphology related to possible locations for airport islands. The boundary conditions for the HCZ model were derived from the Coarse-grid (Zuno-grof) and Fine-grid (Zuno-fijn) models covering the entire North Sea, which were set-up to study the large-scale 2D/3D hydrodynamic impacts of the airport islands (Roelvink, 2001a). These models were based upon the “Zuidelijke Noordzee model (ZNZ)”, supplied by the Dutch Ministry of Public Works.

In 2007, in the framework of VOP II-1 Kustlijnzorg 2007, the feasibility of developing a large-scale morphodynamic model capable of predicting the long-term sediment transport budget of the Dutch Coast was investigated (Elias and Tonnon, 2007). The Holland Coastal Zone (HCZ) model developed within the Flyland project (Roelvink et al., 2001b) was run using the parallel online approach (Roelvink, 2006), which was shown to result in unrealistic low morphological changes that suggested inaccuracies in the coupling of sub-node simulations. It was concluded that further testing and troubleshooting of the HCZ parallel model was needed. Furthermore, initial sediment patterns and weighed transport rates were found to be inaccurate in comparison to the studies of Stive and Eysink (1989), Van Rijn (1995), Steetzel (1999) and Roelvink (2001b) from which it was concluded that validation of the tidal schematization was required as large residual transports were generated in deep water using the representative morphological tide. The results for the nearshore zone suggested that the wave-driven component was reasonably well schematized. It was recommended that future modelling efforts should focus on validation of the parallel-online method, validation of model schematizations and calibration of validated model approach.

In 2008 and 2009 these recommendations have been performed and this has led to the Moholk model, which contains significant improved features. The main differences between the HCZ-model used in the Flyland study and the Moholk model presently used lie in the present use of the parallel-online method of morphological updating instead of the hybrid MOR/RAM approach. Furthermore beach profile extension and reduction on the longshore sediment transport rates along the Delfland coast was applied in the original model to account for the effect of groynes.

Other improvements are:

- The use of 3rd generation instead of 2nd generation wave field calculation in SWAN
- Development of MorMerge
- Spring-neap tidal cycle instead of 1490 minutes morphological cycle
- Testing of parameter settings:
 - dco in flow-module.
 - wave condition w00.
 - wave breaking calculation mode.
 - wave diffraction.
 - transport formula (in this chapter).
 - wave current interaction.

A.2 Model schematization of Moholk model

A.2.1 Delft3D Version

In this study Delft3D version 3.28.00, with FLOW version 3.60.00.5472 and WAVE version 3.01.00.5061 is used.

A.2.2 Flow model

Grid and bathymetry

The bathymetry is derived from measurements done in the late '90s (Roelvink et al, 2001). The width of the model is 60 km and the curved length along the Dutch coast is about 220 km, with water depths varying between 30 meters and dry land (beach and dunes), see figure A.1. The main characteristics of the flow grid are summarized in table A.1. The size of the grid cells in cross-shore direction in the surf zone (up to water depth of 8 m) varies from 100 m to 22 m. This is accurate enough to represent the wave driven sediment transport. The average number of grid cells in the surf zone is varying between 15 at the South-Holland coast and 8 at the North-Holland coast. In longshore direction the grid size in the surf zone varies between 260 m and 1000 m. The grid in the Marsdiep Inlet is rather coarse and is varying in size between 800 m and 1200 m.

	M-direction (cross-shore)	N-direction (longshore)
Grid cells flow-grid	200	233
Grid cells wave-grid	117	249
Maximum grid size (m)	5500	3500
Minimum grid size (m)	22	260

Table A.1 Grid dimensions of flow grid and wave grid

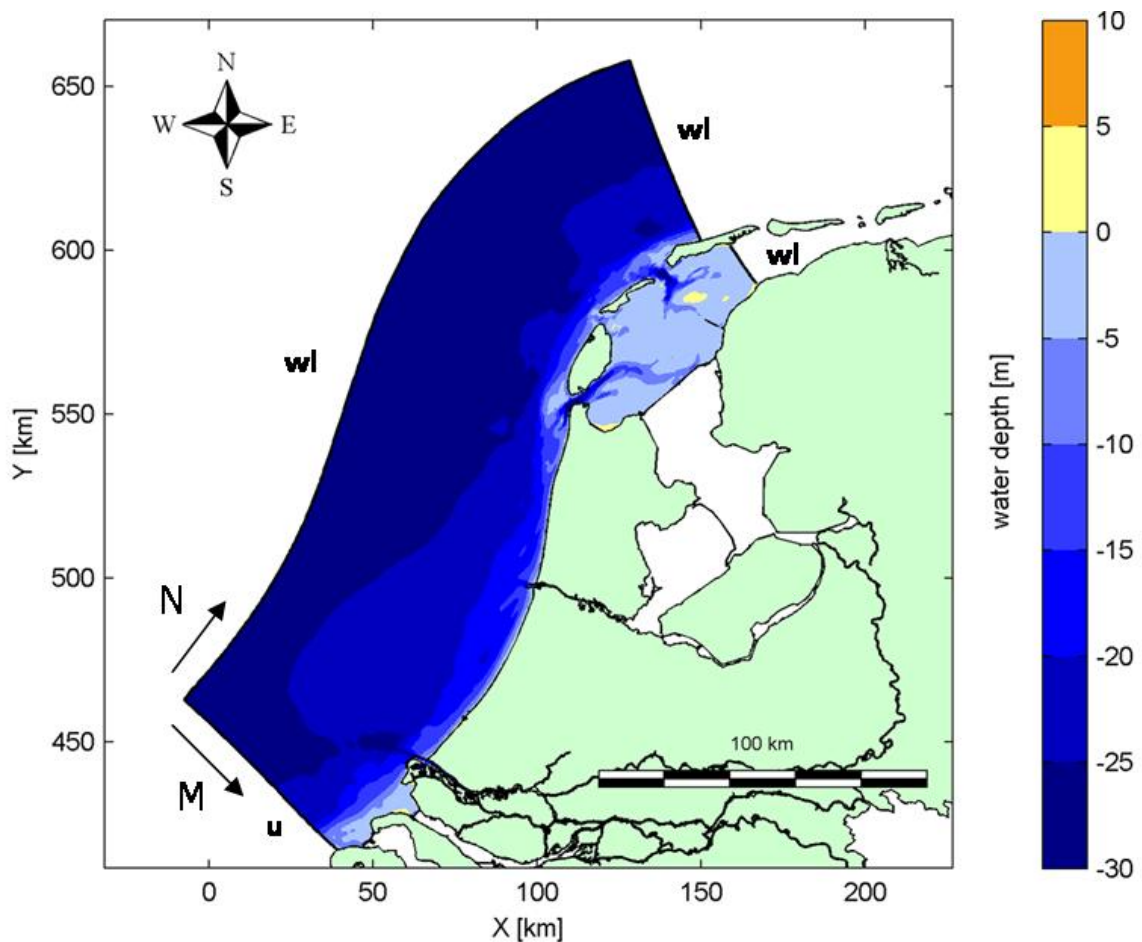


Figure A.1 Model domain of the Moholk model with the boundary condition definitions. The boundary conditions of the four open boundaries are indicated by *wl* (water level) and *u* (velocity)

Boundary conditions

As displayed in figure A.1, four open boundaries are defined. The southern boundary prescribes current velocities and the three other open boundaries prescribe water level variations due to tide. The tidal boundary conditions comprise a 30 days spring neap cycle as the yearly representative tidal forcing. The double neap spring cycle is defined with 39 astronomical components. The time span runs from 23-04-1999 13:00 to 23-05-1999 13:00, which is 43200 min or 30 days. This double spring-neap tide is compared with the formerly used morphological tide in the HCZ model in appendix E. The morphological tide was found not to be representative for the hydrodynamic and morphodynamic behaviour at deep water and near the Texel Inlet. Appendix E also describes the first attempt to convert the lateral boundary conditions for the tide into Neumann boundary conditions. It is recommended to apply Neumann boundaries on the southern and eastern open boundaries when applying varying wave and wind conditions, but due to the large size of the model a simple conversion was not sufficient. A more secure method is to derive new Neumann boundaries with multiple sections on the lateral boundaries. This is recommended to be performed together with a new derivation of a morphological time span, representative for the sediment transport in both shallow and deep water for the entire Dutch coastline.

The boundary conditions include the long term averaged discharge volumes in m³/s through the two sluices at both sides of the Afsluitdijk and through the Nieuwe Waterweg.

The wind in the flow module is set similar to the wind field in the wave module, as given in table A.3.

Parameter settings

Density differences are not accounted for. The sensitivity of the settings for Rouwav (wave-current interaction), wind field in the FLOW module, number of iterations in the WAVE module and the wave force definition on the residual sediment transport has been analyzed. The influence of the wind field, number of iterations and the wave force definition is not significant. The wave current interaction Van Rijn 2004 generates higher sediment transports than the older Fredsoe 1984 definition. These high sediment transports are in agreement with other sediment transport models for the Holland Coast. Details on this sensitivity study can be found in appendix G. The most important settings in the flow module are summarised in table A.2.

Module	Parameter	Value domain	Description
FLOW	thick	2Dh	
	Δt	120 s	flow time step (s)
	ρ_w	1023	water density (kg/m ²)
	K	1	horizontal eddy viscosity
	N	10	horizontal eddy diffusivity
	C	65 m ^{1/2} /s	Chezy coefficient
	Dryflc	0.1 m	threshold depth
	Dco	-999 (default)	Marginal depth
	Wind	Varying	Wind field varies between wave condition
	Rouwav	VR04	Stress formulation due to wave forces
	WaveOL	True	Online wave computation
	Gamax	0.8	Breaker parameter (H_{rms}/d)
	Trttrou	no	bed roughness predictor
	IFORM	-2	Van Rijn 2004 sediment transport formula
	FLPP	30 min	communication interval

Table A.2 Parameter settings of the Moholk model for the FLOW module

A.2.3 Wave model

Grid and bathymetry

The wave grid is several kilometres larger than the flow grid to reduce wave boundary effects. The main characteristics of the wave grid are summarized in table A.1.

Wave climate

The morphologically representative wave conditions were selected by schematization of the wave climate of the YM6 station in directional sectors of 30° and determining low ($H_s < 2\text{m}$) and high ($H_s > 2\text{m}$) morphologically representative wave conditions by weighing the wave heights to the power 2.5 by their probability of occurrence. The wave period, wind speed and direction corresponding with the morphological wave conditions were selected from time series of measured data by computing the average wave period, wind speed and direction for each wave height and direction class. An overview of the morphologically representative wave conditions is given in table A.3. In Appendix D the contribution of each of the wave conditions on the time-averaged longshore transport is discussed.

	Waves			Wind		P (%)
	H_s (m)	T_p (s)	Dir (deg)	U_w (m/s)	Dir (deg)	
W000	0	0	0	0	0	20.95
W01	1.3	5.5	210	7.3	200	9.95
W02	1.2	5.7	240	7.2	225	11.93
W03	1.2	5.8	270	5.9	245	7.46
W04	1.2	6.1	300	4.8	270	7.86
W05	1.2	6.5	330	3.4	315	12.73
W06	1.1	6.3	360	4.2	20	12.06
W08	2.7	7.2	210	13.3	200	3.02
W09	2.9	7.2	240	12.9	230	4.72
W10	3.1	7.8	270	12.6	270	2.74
W11	3.1	8.0	300	11.9	290	2.54
W12	3.1	8.4	330	10.5	325	3.05
W12	2.8	7.8	360	9.1	10	1.04

Table A.3 Morphologic wave and wind conditions (Roelvink et al, 2001)

Coupling with flow

For the wave model 3rd generation SWAN is used within the Delft3D environment. Herein, every 30 minutes a stationary SWAN calculation is performed (for all 11 wave conditions), which restarts at its former result, but with updated water levels, currents and bathymetry. A maximum of 2 iterations is then sufficient to achieve over 96% accuracy of wave height and wave period.

Parameter settings

All settings in the wave module are summarised in table A.4.

Module	Parameter	Value domain	Description
WAVE	Dir space	360°	Directional space
	$\Delta\theta$	10°	Spectral resolution
	freq min	0.05 Hz	Lowest discrete frequency
	freq high	1.00 Hz	Highest discrete frequency
	freq bins	24	Number of frequency bins
	obstacle	dam(4), 1	Type, number obstacles; ratio reflections coeff
	dp min	0.05 m	Threshold depth
	setup	false	wave-related water level setup
	forcing	rad. stress	computation of wave forces
	generation	gradients	generation mode for physics
	mode	3-rd	depth-induced breaking model
	wave breaking	B&J model	coefficient for wave energy dissipation in the B&J model
	alfa1	1	breaker parameter in the B&J model
	gamma2	0.73	breaker parameter in the B&J model
	triads (LTA)	true; 0.1; 2.2	non-linear triad wave-wave interactions; alpha, beta
	bottom friction	JONSWAP;	bottom friction formulation (-); coefficient
	diffraction	0.067	diffraction process
	wind growth	false	formulation for exponential wave growth
	white capping	true	formulation for white capping
	quadruplets	true	quadruplet wave-wave interactions
	ref	true	refraction for waves propagation in spectral space
	fre	true	frequency shift for wave propagation spectral space
	CDD	0.5	diffusion of implicit scheme in directional space
	CSS	0.5	diffusion of implicit scheme in frequency space
	accuracy	98%	accuracy criteria iterative computation
	max iterations	2	maximum number of iterations
	Hs	0.02	fraction relative change w.r.t mean value Hs
	Tm01	0.02	fraction relative change w.r.t mean value Tm01

Table A.4

Parameter settings of the Moholk model for the WAVE module

A.2.4 Sediment transport

The revised sediment transport formula TR2004 is used for the sediment transport calculation. The used Delft3D version contains a revision of the implementation of the TR2004 formulae, which results in different calculated sediment transport volumes than in former Delft3D versions. The differences between these two versions for the Moholk-model are further described in appendix E.

The bed roughness updater is not used, instead a time and space uniform Chezy value of $65 \text{ m}^{1/2}/\text{s}$ is used. The bed roughness updater is a time consuming engine. All settings in the sediment module are summarised in table A.5.

Module	Parameter	Value domain	Description
SED	Cref	Sedtyp	Reference density for hindered settling calculation
	lopsus	0	Suspended sediment size following FacDSS
	Sedtyp	Sand	Type of sediment
	Rhosol	2650 kg/m ³	Density sediment (kg/m ³)
	Seddia	250 µm	d50 median grain diameter sand (µm)
	Cdryb	1600 kg/m ³	Dry bed density d50 median grain diameter sand (kg/m ³)
	Sedthick	5.0 m	Initial sediment layer thickness at bed (m)
	FacDSS	1.0	Factor for initial suspended sediment diameter

Table A.5 Parameter settings of the Moholk model for the sediment module

A.2.5 Morphology

An advanced morphological updating approach, the parallel online method (Roelvink, 2006), is used for a stable and time efficient morphodynamic model. The parallel online method integrates the weighted bed changes of all selected wave conditions at each numerical time step. It has been proven to be a fast method for long term morphodynamic modelling. Per numerical time step the bed change is calculated by combining the different results for the 13 conditions using a weight factor per condition describing the duration of the condition per year. It is a fast method as the different hydrodynamic conditions run simultaneously, or parallel, on the same amount of processors and communicate the calculated bed change to the merging module. With this method, the bed change per wave condition is weighted and merged for all wave conditions at each calculation step. This allows for a shorter calculation time, when the necessary computer network is available. For the application of a higher morphological factor, a shift in the tidal phase between the wave conditions is applied. This generates a smoother bed change per calculation step, as the bed change due to the ebb current in one hydrodynamic condition is counteracted by the bed change due to the flood current in another hydrodynamic condition. With a higher morphological factor, a larger morphological prediction can be made with the same simulation length.

The reference date of the model is April 19th 1999 and the simulation period is 10 years of absolute morphodynamic development, i.e. without the regular human interventions in the

coastal zone, such as the regular maintenance harbour dredging and dumping and the yearly beach and shoreface nourishments. The morfac parameter is set at 120, which results in morphological factors ranging between 1 and 25 for the various wave conditions.

Module	Parameter	Value domain	Description
MOR	<i>Morfac</i>	120	<i>morphological scale factor (-)</i>
	<i>Morupd</i>	true	<i>Update bathymetry during flow run</i>
	<i>Threshd</i>	0.05 m	<i>threshold sediment thickness (m)</i>
	<i>Eqmbc</i>	true	<i>equilibrium sed. concentration profile at open boundaries</i>
	<i>Densin</i>	false	<i>include effect of sediment on water density (-)</i>
	<i>Aksfac</i>	1	<i>Van Rijn's reference height factor</i>
	<i>Rwave</i>	2	<i>estimated ripple height factor (-)</i>
	<i>AlfaBS</i>	1	<i>longitudinal bed gradient factor for bed load transport (-)</i>
	<i>AlfaBN</i>	15	<i>transverse bed gradient factor for bed load transport (-)</i>
	<i>Sus</i>	1.0	<i>current-related reference concentration factor(-)</i>
	<i>Bed</i>	1.0	<i>current-related transport vector magnitude factor (-)</i>
	<i>Susw</i>	0.2	<i>wave-related suspended sediment transport factor (-)</i>
	<i>Bedw</i>	0.2	<i>wave-related bed-load sediment transport factor (-)</i>
	<i>Sedthr</i>	0.25 m	<i>threshold depth for sediment computations (m)</i>
	<i>ThetSD</i>	0.0	<i>Fraction of erosion to assign to adjacent dry cells</i>
	<i>HMaxTH</i>	1.5 m	<i>Max depth for variable THETSD.</i>
	<i>FWFac</i>	1	<i>Tuning parameter for wave streaming</i>
	<i>Multi</i>	true	<i>Parallel computing enabled</i>

Table A.6 Parameter settings of the Moholk model for the morphology module

A.2.6 Tidal schematisation

The tidal boundary conditions comprise a 30 days spring neap cycle as the yearly representative tidal forcing. The double neap spring cycle is defined with 39 astronomical components. The time span runs from 23-04-1999 13:00 to 23-05-1999 13:00, which is 43200 min or 30 days. This double spring-neap tide is compared with the formerly used morphological tide in the HCZ model in appendix E.

A.2.7 Validation and sensitivity analyses

The Moholk model is validated in a thorough way and for several processes in the model a sensitivity analyses has been done. Validation and sensitivity analyses are described in the appendices A to H.

B Validation of the model

B.1 Tidal schematisation

In the model feasibility study carried out in 2007, the representative morphological tide was found to generate large residual transports in deep water from which it was concluded that validation of the tidal schematization was required. The derivation of a new morphological tide however is time-consuming and believed to be unnecessary. The validation of the tidal schematization therefore was carried out more pragmatic by tracing back and assessing the method used to derive the representative morphological tide and by comparing the water levels and depth-averaged velocities at the Noordwijk location with several large-scale models.

B.1.1 Tidal schematization method

The tidal boundary conditions comprise a 30 days spring neap cycle as the yearly representative tidal forcing. The double neap spring cycle is defined with 39 astronomical components. The time span runs from 23-04-1999 13:00 to 23-05-1999 13:00, which is 43200 min or 30 days. This double spring-neap tide is compared with the formerly used morphological tide in the HCZ model in appendix E.

B.1.2 Comparison water levels and depth-averaged long shore velocities

First the Moholk model using astronomical (tidal) components is compared to the CSM and Zuno-fijn large-scale models covering the entire North Sea. The location "Noordwijk meetpunt" was chosen as this output location exists in all three models. Figure B.1 shows water level and depth-averaged long shore velocities for location "Noordwijk meetpunt" over the period 12 June – 12 August 1988 for the CSM (black), Zuno-fijn (blue) and Moholk (red) model. It can be seen that the Moholk model seems to under predict the amplitudes of water level and long shore velocities and that the 'agger' in the water level variation around low water is not modelled correctly in the Moholk model compared to the CSM and Zuno-fijn large-scale North Sea models.

Figure B.2 shows water levels and depth-averaged long shore velocities around the period of the representative morphological ride from August 4 11:35 to August 5 12:25 1988 at "Noordwijk meetpunt" for the CSM (black), Zuno-fijn (blue), Moholk with astronomical tidal components (red) and Moholk with representative morphological tide (green). Although the CSM model is probably defined in another time zone which can be seen from the phase shift of about an hour, the comparison between the model results shows that the Moholk model under predicts the water level amplitudes and that the representative morphological tide does not represent the 'agger' in the water level variation around low water. The peak values of the depth-averaged velocities in the Moholk model are quite similar to the Zuno-fijn model and only a few cm's off in comparison with the CSM model.

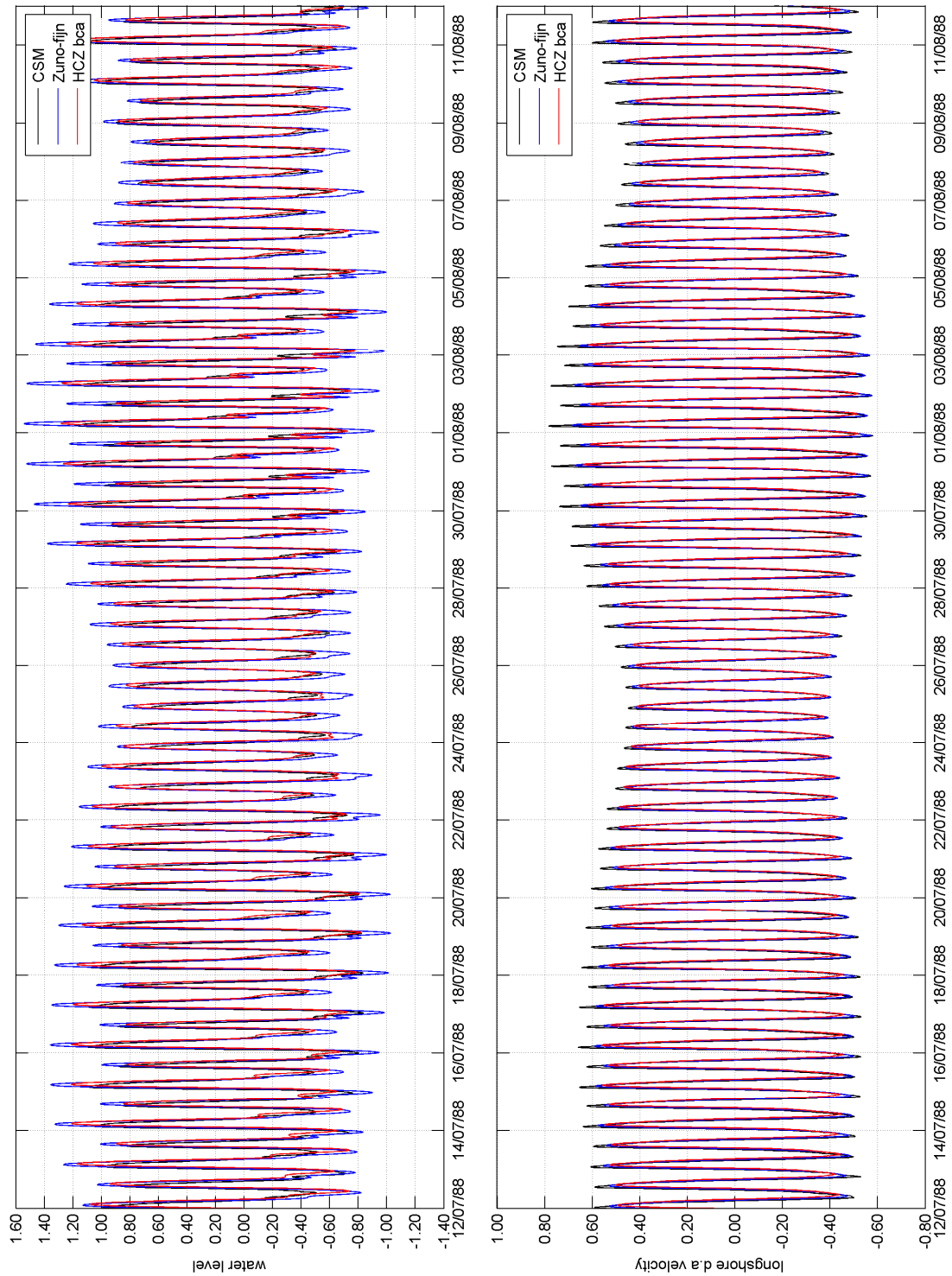


Figure B.1 Water levels and depth-averaged long shore velocities in Noordwijk meetpunt over the period June 12th to August 12th 1988 for CSM (black), Zuno-fijn (blue) and Moholk HCZ (red) model.

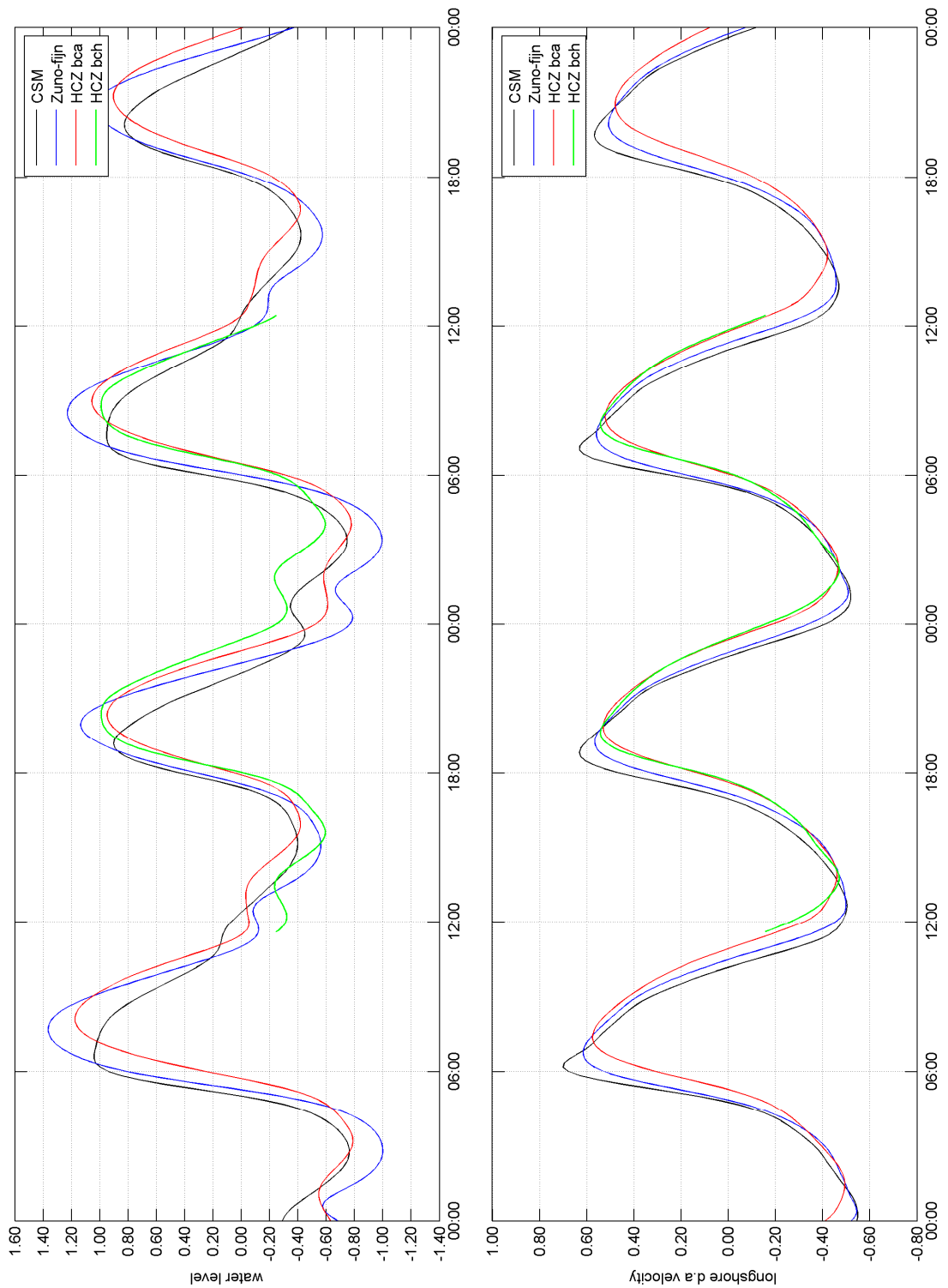


Figure B.2 Water levels and depth-averaged long shore velocities around the period of the representative morphological tide of August 4 11:35 to August 5 12:25 1988 at Noordwijk meetpunt for the CSM (black), Zuno-fijn (blue), Moholk(HCZ) with astronomical tidal components (red) and Moholk (HCZ) with representative morphological tide (green)

It was concluded that the representative morphologic tide under predicts the water level amplitudes, lacks the 'agger' around low water and slightly under predicts the peak velocities. The astronomic (tidal) forcing of the Moholk model represents the water level variation in more detail due to the inclusion of uneven components. As the model is intended for long-term morphodynamic simulations that would require numerous repetitions of the representative morphological tide in order to prevent high morphologic scaling factors is was decided to use the astronomic (tidal) components to drive the model with the advantage of also modelling the effect of the neap-spring tidal variation. Appendix E describes the differences in longshore sediment transport between the morphological tide and the spring neap cycle.

B.2 Residual currents

B.2.1 Residual tidal current

The tidal forcing comprises two spring neap cycles, in total 30 days. The residual tidal current is generated by the higher harmonics in the tide, which create an asymmetrical tide, by the A0 component and by wind driven currents. For the southern North Sea bordering the Dutch coast the asymmetrical tide generates a residual current in northern direction. The long term average wind stress is generated by a wind with a morphological long term average speed of 7 m/s from west southwest. Along the Dutch coast, with average north-south orientation of 25 degrees with respect to the north, this generates a current to the north. The northern residual current due to tide and morphological wind is shown in figure B.3. In the coastal zone, in water depths less than 8 m, the residual current reaches up to 0.1 m/s as generally observed at the Holland Coast (Van Rijn, 1997). In deeper water the residual current approaches 0 m/s. Near the boundaries the influence of the boundaries can be observed, resulting in higher (but unrealistic residual currents). The delta in the south of the model together with the Rotterdam harbour disturb the northern current, and some large eddies are visible. At the outer deltas of the tidal inlets of the Wadden Sea, the northern driven current is influenced by the ebb and flood dominated gullies.

The residual current in figure B.3 is generated by the tidal boundary conditions in combination with the morphological wind. In the Moholk model it is chosen for the flow module to apply the wind belonging to the hydrodynamic condition. This will influence the residual current, and generate more and larger disturbances at the boundaries, see appendix H.

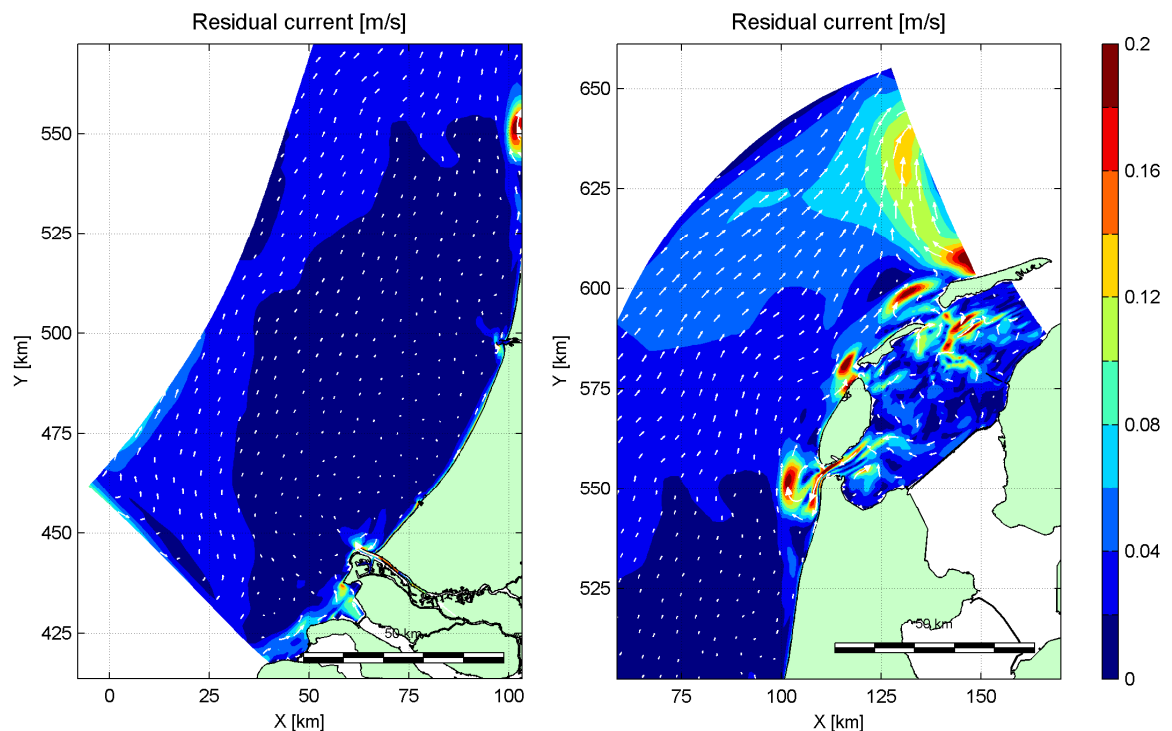


Figure B.3 Residual current due to 30 days tidal forcing, A0-component and wind set-up, without wave forcing. Astronomic boundary conditions covering two neap spring cycles with a morphological wind speed of 7 m/s from 240 degrees north.

B.2.2 Marsdiep Inlet

The current through the Texel inlet is governed by the complex interaction of the alternating tidal current, wind and wave set-up, wave forces and bathymetry of the inlet and basin. The present day bathymetry of the outerdelta with its channels and shoals, figure B.4, has developed as such since the closure of the Zuiderzee and is considered to be in a near equilibrium state since the 70's. The Helderse Zeewering has probably stopped the dynamic movement of the inlet throat and the closure of the Zuiderzee has increased the tidal prism through the inlet. These two factors have contributed to the deepening of the main ebb-tidal channel-system Texelstroom, Helsdeur, Schulpengat and Nieuwe Schulpengat. The Helsdeur and Texelstroom channels are scoured into semi-consolidated layers, which contributes to the stability of the channels (Elias et al, 2006a). During flood, the inflow is more uniform across the inlet, whereas during ebb the outflow is more concentrated in the deeper channel to the north. This inequality causes tidal-mean currents in the flood direction in the southern half and in the ebb direction in the northern half, figures B.6b and B.6c (Buijsman and Ridderinkhof, 2008a).

Secondary currents, also cross-channel or transverse currents, contribute less than 10% to the streamwise currents but are relevant for the mixing and dispersion of momentum and the transport of sediment. These secondary currents arise from three basic mechanisms: (1) transverse density gradients, (2) channel curvature, and (3) Coriolis forcing. It is usually not straightforward to distinguish their individual contributions, however all three are present at the Texel Inlet. (Buijsman and Ridderinkhof, 2008b)

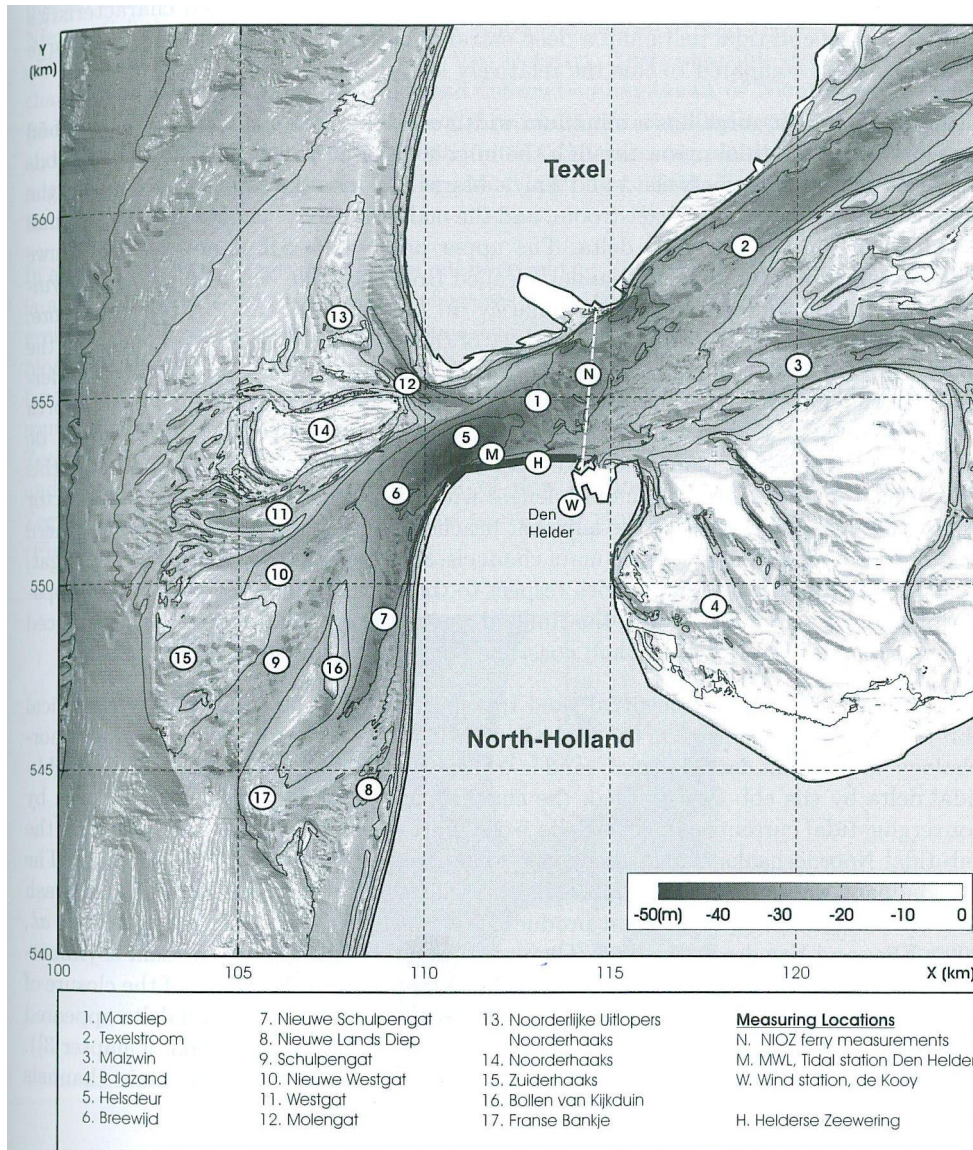


Figure B.4 Overview of Texel Inlet in its present shape with the most important channels and shoals (Elias, 2006)

In the Moholk-model tide, wind and wave effects and long-term averaged discharge volume through the sluices in the Afsluitdijk are modelled through well calibrated boundary conditions, thus a good representation of the longitudinal flow is expected. However, the processes generating the secondary currents are neglected due to the depth-averaged calculation mode. Also density differences are not modelled. This will have its effects on the sediment transport to and from the Marsdiep basin. The objective of this study was however to develop a fast running model for a 10 year morphological forecast with as much functionalities as possible, which means that these effects could not be incorporated.

When looking at the maximum ebb and flood velocities through the Marsdiep delta (figure B.5), it appears that in the throat (Helsedeur) high depth averaged velocities occur of over 1.5 m/s for both the ebb current and the flood current. The ebb-current is higher with velocities at measurement point Den Helder varying between 1.1 and 1.7 m/s and flood current velocities

between 0.8 m/s and 1.2 m/s. Inside the basin the flow is concentrated in the channel Texelstroom near the coast of Texel. On the outer delta the ebb current is concentrated near the coast of North-Holland in the Nieuwe Schulpengat, while the flood current is divided over the channels Nieuwe Schulpengat and Schulpengat in the south and over the Molengat channel in the north of the ebb-tidal delta. Although not many measurements are done on the outer delta, ADCP measurements indicate the same flow pattern in the Texel Inlet (Elias, 2006). Focusing on the Marsdiep, long-term measurements have been done with the ferry. The yearly averaged currents along the cross-section between Den Helder and Texel have been analyzed for 1999 and 2000 (figure B.6b and B.6c). These indicate a flood-dominated residual current in the southern part of the Marsdiep and an ebb-dominated residual current in the northern part. The residual current differs per year along the cross-section, probably due to differences in the meteorological conditions. In the Moholk-model an ebb-dominated current is present both in the northern and southern part, while in the centre a small flood-dominated current is present (figure B.6a). This is not in accordance with the ferry measurements, but it has to be noted that these inaccuracies are a result of the coarseness of the grid. The ebb-dominated current in the southern part indicates the ebb-dominancy of the Malzwin. The magnitude of the ebb dominated current is higher in the northern part, comparing 0.25 m/s in the Moholk-model with 0.15 m/s for the ferry measurements.

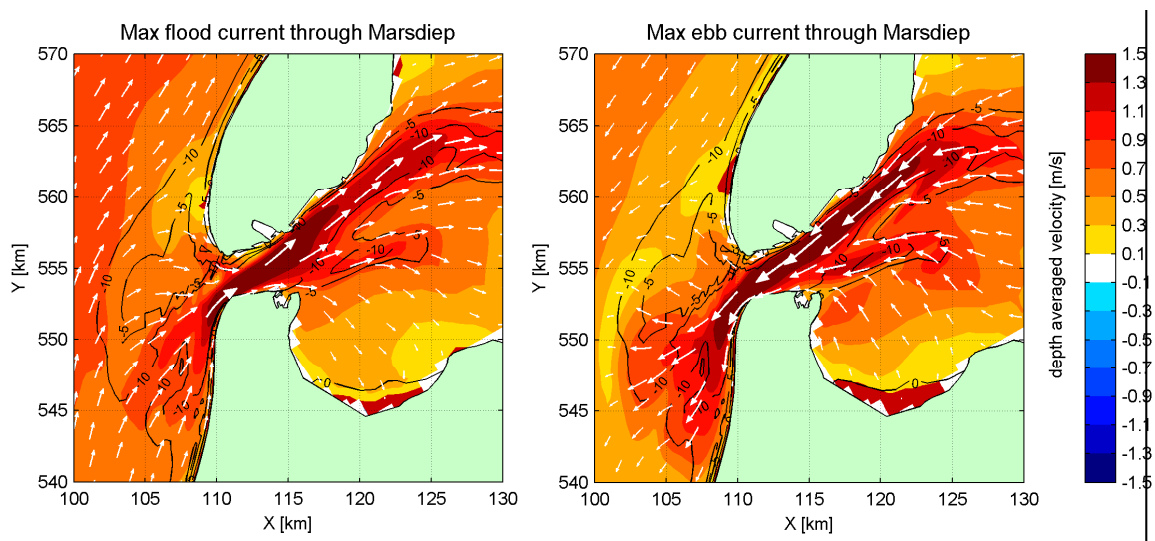


Figure B.5 Max flood current and max ebb current through Marsdiep in Moholk-model

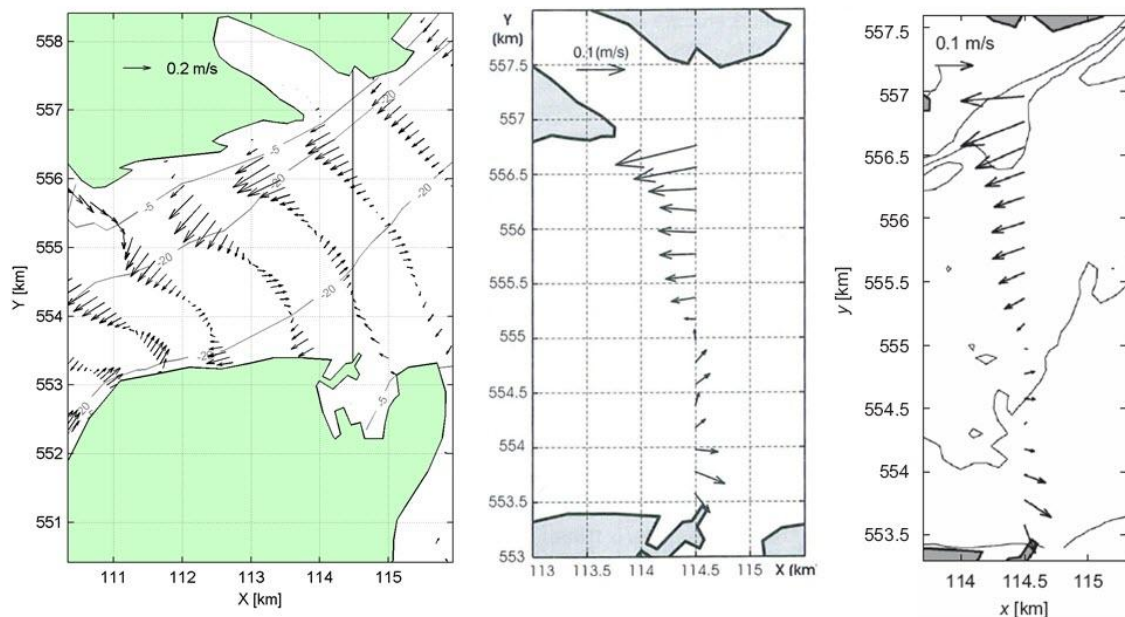


Figure B.6 Residual tidal current through Marsdiep based on the MOHOLK model (left) compared with the ferry measurements for the years 1999 (middle, Elias, 2006) and 2000 (right, Buijsman and Ridderinkhof, 2008a)

B.3 Sediment transport

B.3.1 Longshore transports

Nearshore

The nearshore is defined in this analysis as the area enclosed by the depth lines of -8 m NAP and +3 m NAP, which is dominated by the complex hydrodynamic and sediment transport patterns of the surf zone. This area is dominated by wave action in generating currents and sediment transport, and thus in the residual sediment transport in the longshore direction. The black line in figure B.7 shows the yearly residual longshore sediment transports along the Holland Coast, from Hoek van Holland at km 120 up to Den Helder at km 0, and 20 km along the Texel North Sea coastline.

Just north of the Rotterdam breakwaters, at km 118, the residual transport in the nearshore zone is zero, as the south western waves are blocked by the breakwaters. The transport increases in northward direction until the breakwaters of Scheveningen partially interrupt the sediment transport in this zone at km 100. Northward of Scheveningen, the residual longshore transport is uniform with a rate of about $175 \text{ m}^3/\text{m}/\text{year}$, which is an average value for that coastal stretch (Van de Rest, 2004). In Appendix I figure I.1 it can be seen that although south and north of the Scheveningen harbour the integrated residual total transport over the surf zone is equal, the sediment transport per square meter is higher south of the breakwaters, where north of the breakwaters the surf zone is significant wider. On average, this results in equal residual longshore transports.

North of the IJmuiden breakwaters, the residual longshore transport is lower, due to the rotated coastline towards the dynamic equilibrium angle with respect to waves and tide. The surf zone is much smaller with higher sediment concentrations, due to the steeper coastal profile. From km 30 northward the coastline orientation varies rapidly, the coastal profile

becomes steeper and the transport in northward direction increases. At km 12 the Texel Tidal Inlet is influencing the coastal system largely, with its shoals and deep gullies. North of the Texel Inlet, at the coast of the Texel island (km 0 until -5), there is a small southward transport into the Wadden Sea through the Molengat. Northward of km 5 the Molengat channel widens and the sediment transport in the surf zone is governed by the wave driven currents and is in northward direction again.

Overall, the residual transports calculated with the Moholk model show great resemblance with values from reference studies summarised by Van de Rest, 2004. There are two large differences, being north of the IJmuiden breakwaters and near the tidal delta. North of the IJmuiden breakwaters, close to the breakwater, all other studies calculate a southward directed transport, while in this study only northward transport is seen. Near the Texel Inlet, the longshore transport diminishes in the Moholk-model, while other studies predict a large increase of the longshore transport in the nearshore. This difference has to be sought in the definition of the nearshore in the varying studies, whether the influence of ebb- and flood-dominated gullies is taken into account. In the present study the nearshore is defined by the depth lines of +3 m and -8 m and is very small due to the presence of the Nieuwe Schulpengat.

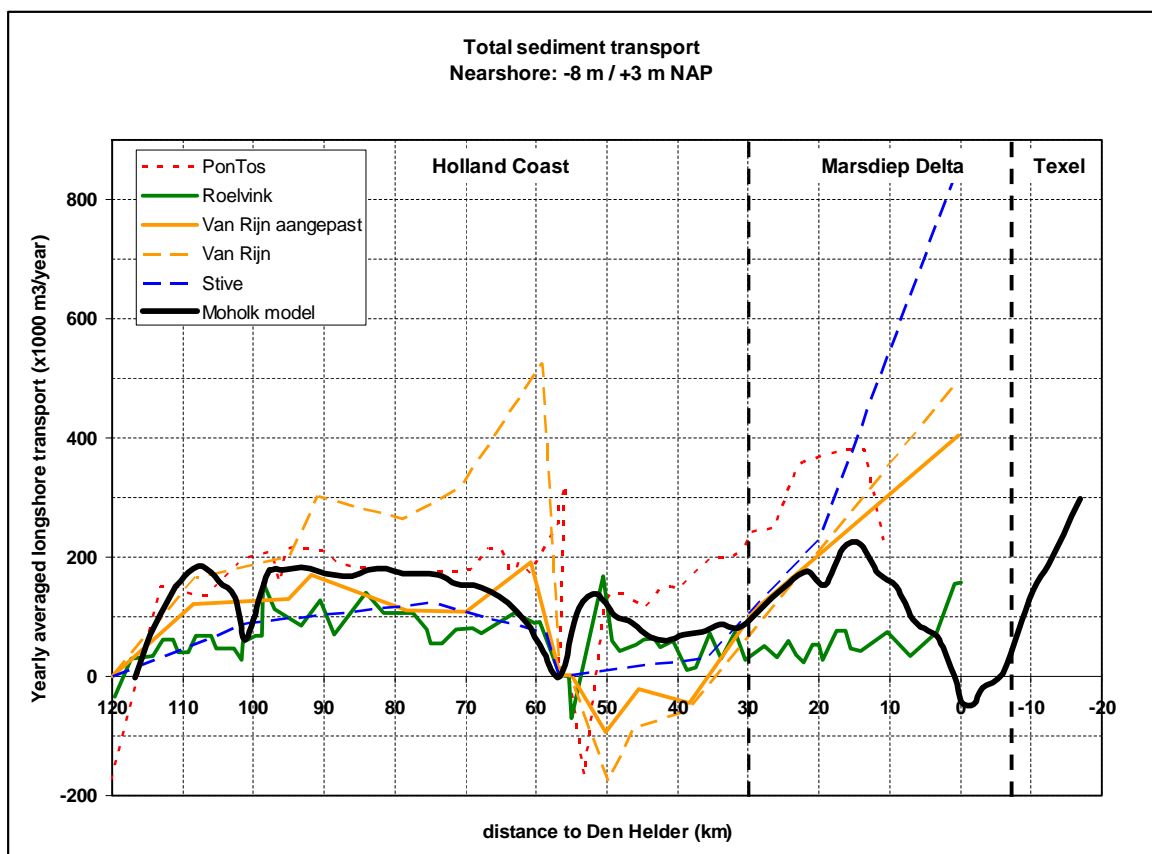


Figure B.7 Comparison of longshore residual transports (excl. pores) in the nearshore, defined between water depths -8 m and +3 m NAP with reference studies from Van de Rest, 2004. The results for the Moholk model are shown up to km -20. Between km 15 en km -10 the Schulpengat is near to the coast and is the zone between -8 m and +3 m NAP very narrow and transport is becoming very small. Between km -15 and km -20 the residual currents along Texel coast become comparable with the residual transports along the Holland coast

Offshore

The offshore is defined in this analysis as the area enclosed by the depth lines of -20 m NAP and -8 m NAP. The water depth line of -20 m is known as the border of the morphologically active zone, or Dutch coastal zone. In this area, the tidal current is the dominant factor in generating currents and the residual sediment transports along the Dutch coastline.

The black line in figure B.8 shows the residual longshore transport offshore (black line) along the Holland Coast between Den Helder and Hoek van Holland, while the blue line is the sum of the nearshore and the offshore transports. The residual transports in the offshore zone (between 8 and 20m waterdepth) are a factor 3 to 4 higher than in the nearshore zone (between dunefoot and 3m waterdepth). However, the transport per unit width of 1meter (normal to the coast) is lower (between 0 and 50 m³/m/year) compared to longshore transports in the surf zone of up to 500 m³/m/year (Appendix I figure I.1 and figure B.9). The width of the offshore zone is much larger than the width of the onshore zone thus the integrated transport is larger. The transport is northward directed, due to the residual tidal and wind current in northward direction. Near the breakwaters of Hoek van Holland and IJmuiden, the northward transport increases due to contracted flows around the breakwaters. Sediment is then transported from the surf zone in offshore direction. At the coast of Zuid-Holland, the sediment transport increases in northward direction, mostly due to enlargement of the cross-shore section in northward direction. At the coast of Noord-Holland, the longshore transport diminishes in northward direction, mostly due to the change in length of the cross-sections (Appendix I figure I.1). Already at the 30 km distance line to Den Helder the influence of the tidal inlet is noticed. A large contracting flow around the delta is generating larger northward transports as seen at km 20. From km 20 to Den Helder a southward transport is plotted, as the ebb-dominated channel Nieuwe Schulpengat is enclosed in the -8m till -20m depth lines.

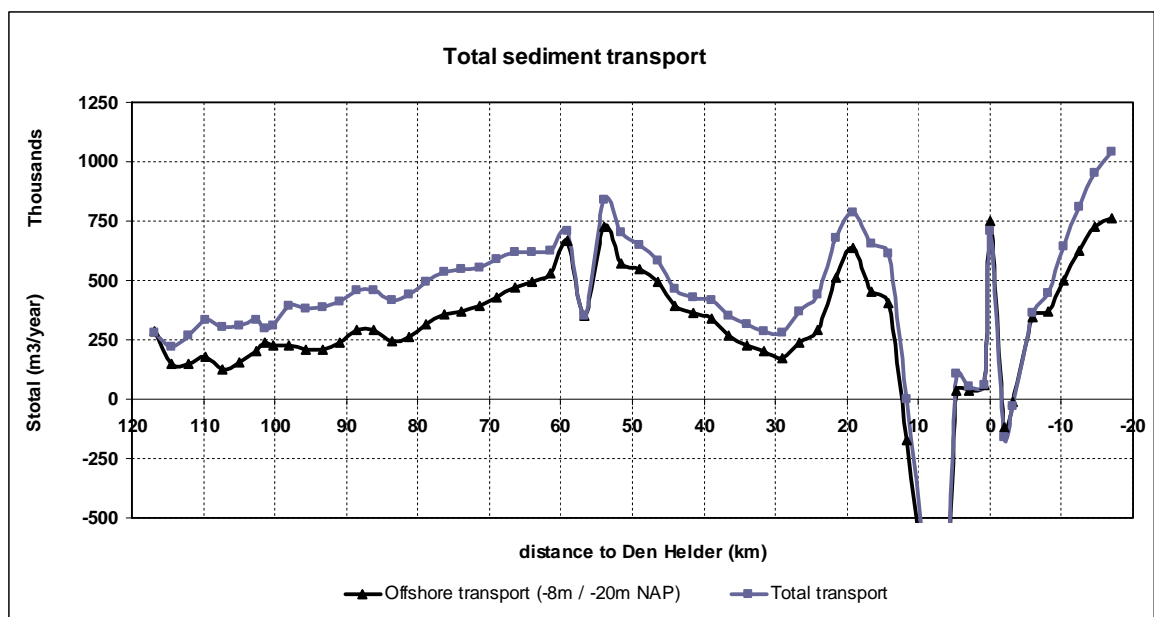


Figure B.8 Longshore residual yearly transports, offshore (defined between water depths -20 m and -8 m NAP) and total (nearshore + offshore, waterdepths between -20 m and +3 m). Between km -10 and km -15 the Schulpengat is making the zone between -20m and -8m very narrow and residual transports are becoming negative (in southern direction). Between km -15 and km -20 the Texel coast is showing northward residual transports again

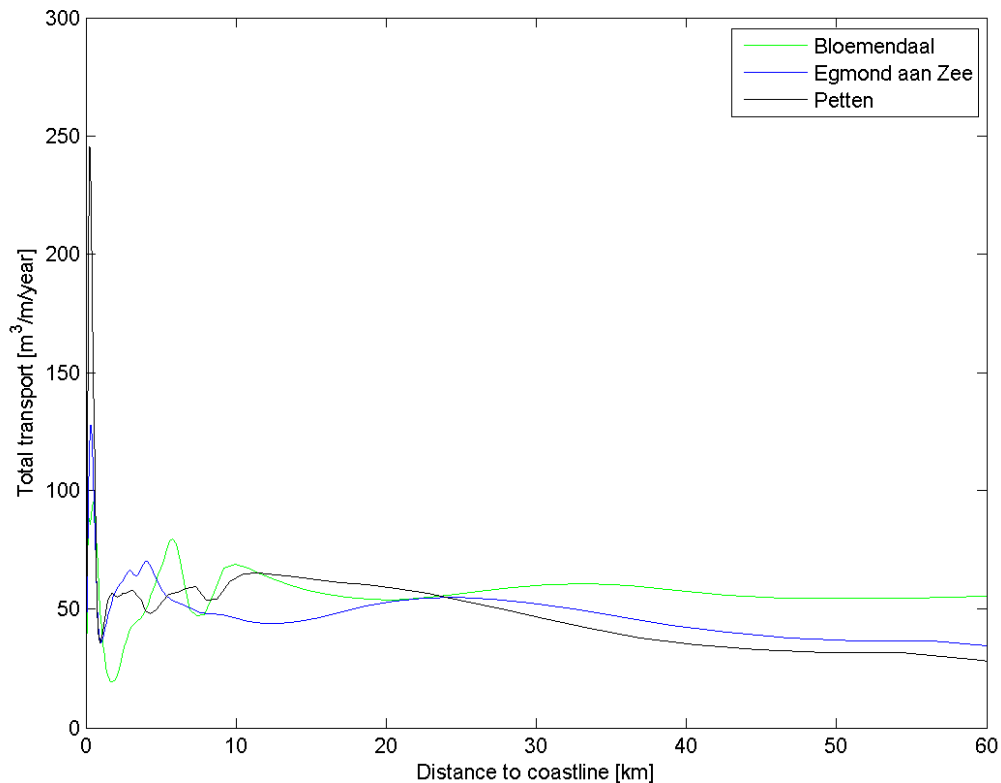


Figure B.9 Total longshore transport ($m^3/m/year$) along three transects on the Holland Coast

Summary longshore transports along closed coast

At all locations the residual transport is in northward direction. In the nearshore, transports are on average $100,000 m^3/year$, in the offshore, transports are on average $350,000 m^3/year$ and from water depth of 20 m up to 35 m the longshore transport is on average $1,6$ million $m^3/year$.

B.3.2 Cross-shore transports

The transport in Appendix I figure I.2 also show the cross-shore transport over the 8m depth line, around the 20 meter depth line, chosen at a distance of 10 km from the shoreline, and three more distances from the coast, being 20 km, 40 km and 60 km. At the 8 m depth line, a large offshore transport is seen of $1-5 m^3/m/year$ for Zuid-Holland and $5-15 m^3/m/year$ for Noord-Holland. Integrated along the coastline of the Holland Coast this means a loss of sand of $1 Mm^3$ per year. In 2DH-mode, the cross-shore transport due to waves is regulated by the SusW and BedW parameters. In this case, the onshore transport due to waves is underestimated by these parameter settings.

The Moholk model covers a larger area than the afore mentioned nearshore and offshore zones. It covers a part of the continental shelf and southern North Sea. The width of the model is 60 km and runs to a depth of 40 meters. As a first attempt to understand the sediment transport outside the 20 meter depth line, about 40 boxes are defined in this area. Along the borders of these boxes, the total transport, thus bed load and suspended load

transports summed up, is integrated. The orientation of the borders of the boxes do not follow specific depth lines, as is normally the case close to the shore, but are parallel to the main tidal flow and the coastline. Then the transport through a section parallel to the coastline is purely cross-shore directed and does not involve longshore transport. It is however not guaranteed that the boxes in Appendix I figure I.2 are exactly defined along the streamlines, thus the values may be biased due to the orientation of the lines. Along the coast, the longshore transport over a width of 60 km is about 2 million m^3/m per year (including the surf zone), being four times the sediment transport close to the shore.

B.4 Sensitivity of transport formula and bed roughness

Using the astronomic tidal forcing with the settings mentioned above, the Moholk model was run to simulate one year of morphological changes. To assess the wave schematization and model performance the longshore sediment transport curve along the Holland coast was extracted from the model results for comparison with previous studies.

B.4.1 Nearshore longshore transport

Figure B.10 shows the longshore sediment transport rates in the surf zone between +3 and -8 NAP from the Moholk model using TRANSPOR 1993 (blue), TRANSPOR 2004 (red) and TRANSPOR 2004 without bed roughness predictor (orange). It can be seen that the yearly sediment transport rates in the surf zone quickly pick up after the Noorderdam at Hoek van Holland to about 200-300 thousand m^3/year and that the Scheveningen harbour moles locally block the sediment transport. Closer to IJmuiden the sediment transport steadily decreases until at IJmuiden harbour the transport is completely blocked. North of IJmuiden, the transport increases to about 100-200 thousand m^3/year , until it further increases between Petten and Den Helder to about 250-400 thousand m^3/year . The transport rates using TRANSPOR 2004 with the bed roughness predictor are about 50% lower than using TRANSPOR 2004 with a constant bed roughness or using TRANSPOR 1993. The transports in figure B.10 differ from the transports given in figure B.7 due to the use of an earlier version of the Moholk model with different parameter settings (In the earlier version Fredsoe 1984 has been used as model for the wave current interaction and in the later version van Rijn, 2007. See also Appendix G.2). The inter comparison between the three sediment transport rates in figure B.10 is still valid.

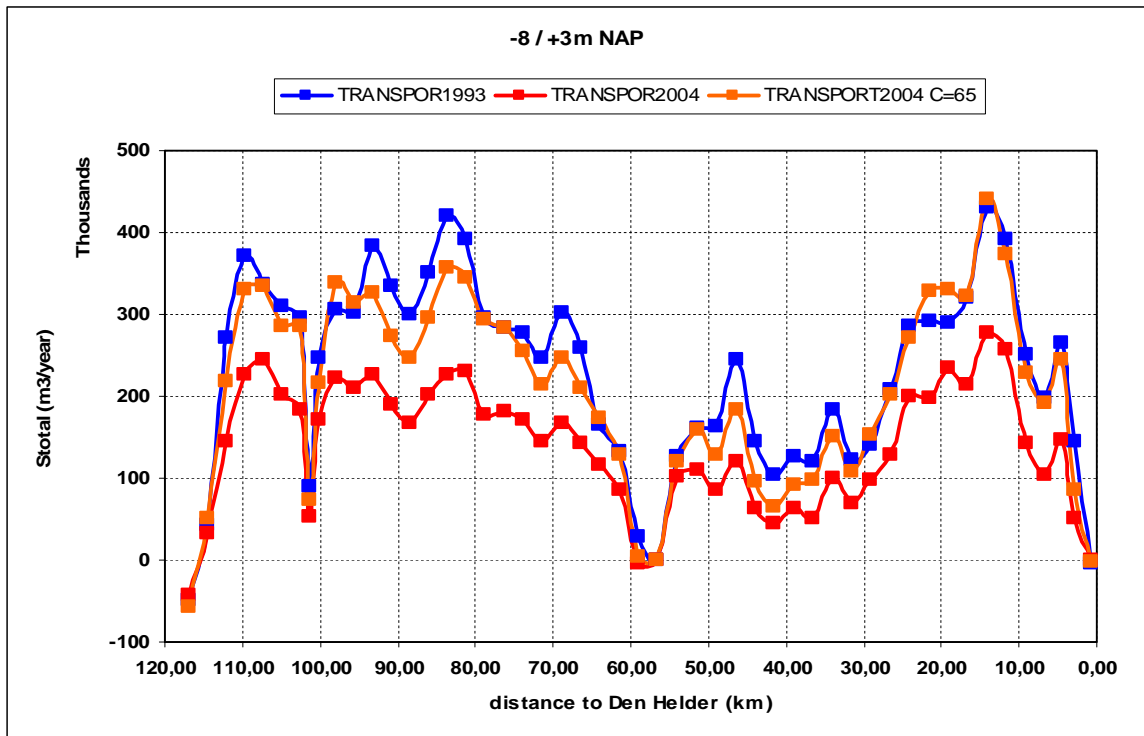


Figure B.10 Long shore sediment transport rates in the surf zone (3 to -8m NAP) from the Moholk model using TRANSPOR 1993 (blue), TRANSPOR 2004 (red) and TRANSPOR 2004 without bed roughness predictor (orange)

B.4.2 Deep water longshore transport

Figure B.11 shows the long shore sediment transport rates in deep water between -8 and -20m NAP from the Moholk model using TRANSPOR 1993 (blue), TRANSPOR 2004 (red) and TRANSPOR 2004 without bed roughness predictor (orange). Transport rates using TRANSPOR 1993 are much higher (5x) than using TRANSPOR 2004 with and without bed roughness predictor.

After a further investigation, it was concluded that TRANSPOR 1993 overestimates the sediment transports in deeper water due to

- An overestimation of the wave effects in deep water by an overestimation of vertical mixing by waves and
- an inaccurate implementation of TRANSPOR 1993 in Delft3D resulting in inaccurate representation of the concentration profile close to the bed. TRANSPOR 2004 was developed using more extensive wave data and thus represents the vertical mixing effect by waves better, moreover, the implementation of TRANSPOR 2004 features a sub grid model to better represent the concentration profile close to the bed.

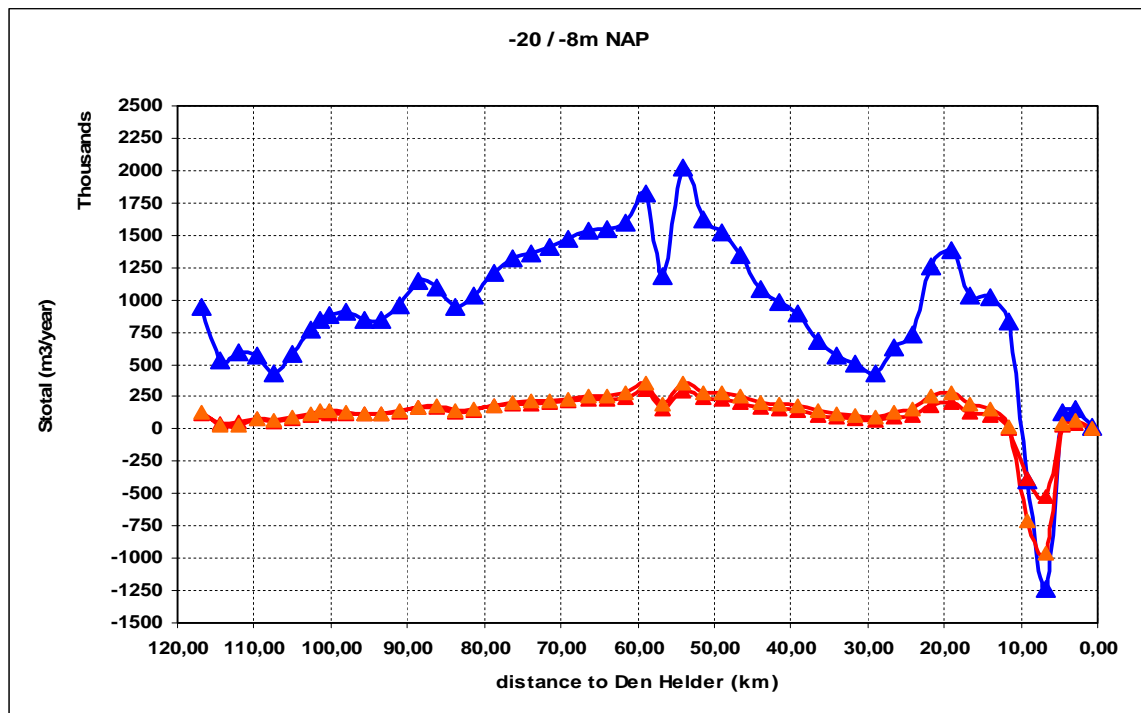


Figure B.11 Long shore sediment transport rates at deep water (-8 to -20m NAP) from the Moholk model using TRANSPOR 1993 (blue), TRANSPOR 2004 (red) and TRANSPOR 2004 without bed roughness predictor (orange)

The analysis of differences in long shore sediment transport rates using the TRANSPOR 1993 and 2004 was carried out by Luo Xiao Feng from the Nanjing Hydraulic Research Institute (NHRI) as part of a collaboration between Deltares and NHRI. The main findings of this analysis were (see also Appendix C):

- Apparent differences in sediment transport rates between Van Rijn (1995) and Van Rijn (1997) are due to the fact that in Van Rijn (1995) sediment transports are used excluding pore volumes while in Van Rijn (1997) sediment transport are presented including pore volumes.
- Van Rijn (1995, 1997) reduces the yearly-averaged sediment transport rates at -20m NAP by about 40% to account for the overestimation of the relatively large velocities of the representative tide and the slightly over estimated wind effect
- The sediment transport is dominated by currents in deeper water, while it is dominated by waves in the surf zone. Inaccuracies between observed sediment transport in either deeper water or surf zone may be related to specific schematization accuracy of either hydrodynamics or waves.
- Analysis of Van Rijn (1997) and the present Moholk model results showed that wind has a significant effect on the sediment transport rates as it may double the yearly sediment transport rates in both deep and shallow water. The wind effect in Van Rijn (1995) may be slightly overestimated and is not represented in detail in the present Moholk model as the long-term average wind speed and direction were applied.
- A pragmatic hydrodynamic assessment of the bed roughness predictor was carried out by comparison of hydrodynamics with results using a constant Chezy roughness of $65 \text{ m}^{1/2}/\text{s}$. It was found that water level amplitudes using the bed

roughness predictor are somewhat smaller, especially closer to land (5km) where differences of about 5-10 cm were observed. Velocity differences up to 10% were observed at a depth of -8m with differences at -20m being smaller.

B.5 Morphodynamics

In the model domain, the morphodynamic active areas are in the surf zone of the closed coastal system (South-Holland and North-Holland), around the harbors of Rotterdam and IJmuiden and on the shoals and gullies of the tidal inlets Marsdiep, Eierland and Vlie (Appendix I Figure I.3). Near the southern boundary some artificial erosion and sedimentation is visible, which is due to minor problems in the boundary conditions.

B.5.1 Surf zone

The surf zone is morphologically very active due to high transports by wave breaking. It is therefore a complex area to model. In the Moholk-model the coastal profile in North Holland is schematized with an average of 10 grid cells across the surf zone. The surf zone is defined in this study as the area between +3 m NAP and -8 m NAP. The gentle sloping surf zone is eroded rapidly during the calculation to a steep beach slope and a gentler sloping foreshore. On this steep profile small waves (~ 1 m) hardly break, but are reflected while high waves (>2 m) break in 1 or 2 grid cells, putting more pressure on the steep surf zone (figure B.12). Small waves do not dissipate on the beach, causing the surf zone transport to decrease to almost zero. This unwanted effect is a result of the coarse grid. It might be counteracted by tuning the parameters α_{Bn} (slope factor), $SusW$ and $BedW$ (factor for onshore/offshore sediment transport), $ThetSD$ (factor for erosion of adjacent dry cells). Other model improvements are to refine the grid more in the surf zone or to develop a beach module which maintains the smoother profile.

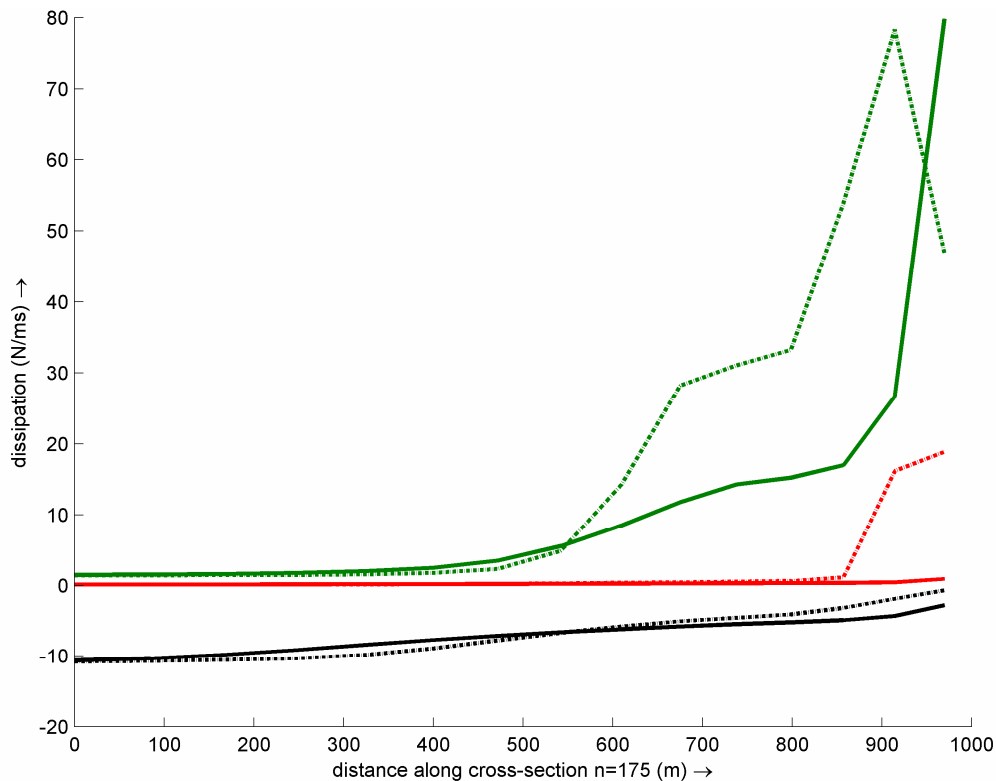


Figure B.12 Wave energy dissipation at start (dashed line) and end (straight line) of simulation for a small wave (red line) and a high wave (green line). The bottom profile (m) is plotted in black.

B.5.2 Marsdiep delta

The western Wadden Sea can be divided in three basins with three corresponding outer deltas, being from west to east the Texel basin, the Eierland basin and the Vlie basin. The 10-year sediment balance of this system is shown in figure B.13. The tidal divide between the Vlie and the adjacent eastern basin forms a boundary of the model. The gross volume exchange of water over the tidal divides is rather high and very sensitive to the hydrodynamic forcing. The eastern model boundary lies very close to the tidal divide between the Marsdiep basin and the Vlie basin and is thereby influencing the cumulative discharge over the tidal divide and through the Marsdiep Inlet. The net exchange of sediment between basins is almost zero. The basins exchange only sediment through the tidal inlets. The Marsdiep basin is filling up at the cost of the its outer delta with 22 Mm^3 in 10 years, while the outer delta also loses 10 Mm^3 more to the Eierland outer delta than comes in from the Holland Coast. The Eierland basin is exporting 2 Mm^3 in 10 years and the Vlie basin and outer delta are both filling up. The sedimentation of the Vlie outer delta is incorrectly modelled due to the close presence of the model boundary. The values in figure B.13 for the Vlie basin are not realistic; from sand balance studies it is known that the outer delta of the Vlie basin is showing erosion rather than sedimentation. Along the eastern boundary of the outer Vlie delta, the residual sediment transport should be in eastern direction.

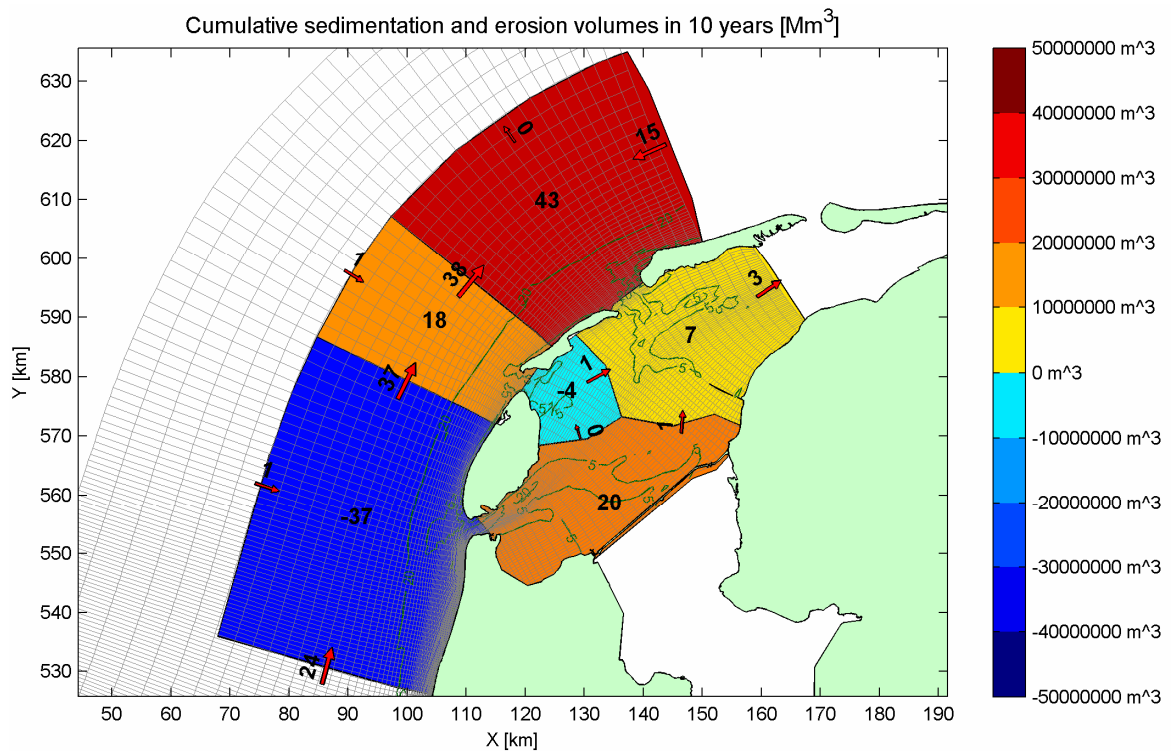


Figure B.13 Mass balance over 10 years for the Western Wadden Sea basins and outer deltas Marsdiep basin, Eierland basin and Vlie basin. Volumes are in Mm^3 and include pore volumes

Focusing on the Marsdiep tidal basin, the sediment import through the Marsdiep is about 2 Mm^3 per year. The outer delta is a complex area with several tidal gullies and shoals (figure B.4). Figure B.14 indicates the residual direction of the sediment transport on the outer delta through several sections. These sections are based upon the sections used in Elias (2006), and defined in such a way that shoals and channels are separated from each other by these sections. Most of the sediment is circulated on the outer delta. Sediment is exported southwards with the ebb-current through the Schulpengat and Nieuwe Schulpengat. Part of the sediment is brought to the Zuiderhaaks and the Noorderhaaks, from which it is transported through the Molengat and the Breewijd into the tidal basin. Along the coast of Noord-Holland a northward directed transport of sediment in the surf zone is seen, which also flows into the tidal basin.

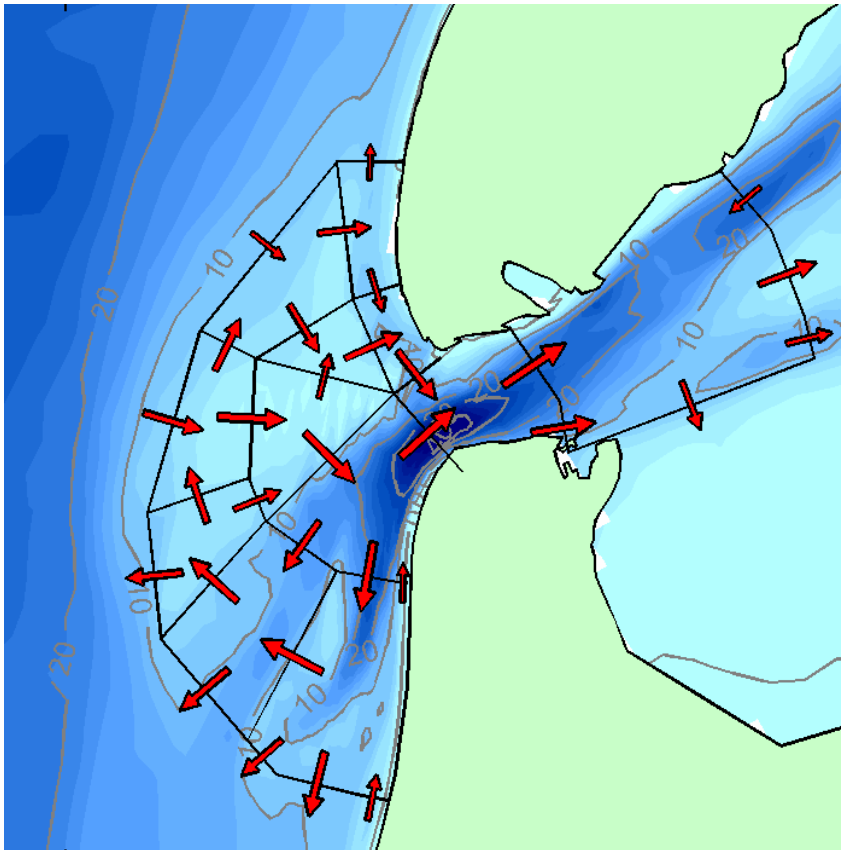


Figure B.14 Sediment transport pattern on outer delta indicated with arrows

With the Moholk model an import of 2 Mm^3 sediment per year through the tidal inlet was derived. In figure B.15, the outer delta is further divided into sections for the adjacent North-Holland coast, the delta and the Texel coast. The border between the delta and the adjacent coastal sections follows the 15 m depth line around the delta. The edge between the outer delta and the basin is drawn along the grid lines in the Marsdiep. The location and orientation of this division line is very sensitive, because the morphological development in the Marsdiep is rather large with erosion reaching the fixed layer (5 m) and with sedimentation values higher than 10 m. The borders facing the open sea are situated at the 20 m water depth line, which is considered to be the edge of the morphologically active zone along a closed coast system. It was already found that large amounts of sediment are transported over the 20 m depth line along the closed coast. For the deltaic area, an import of 10 Mm^3 in 10 years over the 20 m depth line is seen (figure B.15). The adjacent sections import less sediment, respectively 1 and 6 Mm^3 for the North-Holland coast and the Texel coast, being less active sections. The import of 2 Mm^3 sediment through the Marsdiep per year is partly imported from deeper water and mostly eroded from the North-Holland coast and the outer delta. In table B.1 the erosion and sedimentation volumes are further derived into the development in the first 5 years and the last 5 years. It appears that the first 5 years are dominant for the erosion and sedimentation volumes, and the import volume in the Marsdiep tidal basin. In the first year, the channels in the deltaic area are scoured heavily, mostly in the section Marsdiep delta. Deposition of this large scour volume occurs in the Marsdiep basin section. The sediment import generated with this model is merely a local readjustment of the bathymetry in the first year, than a significant import of sediment into the basin.

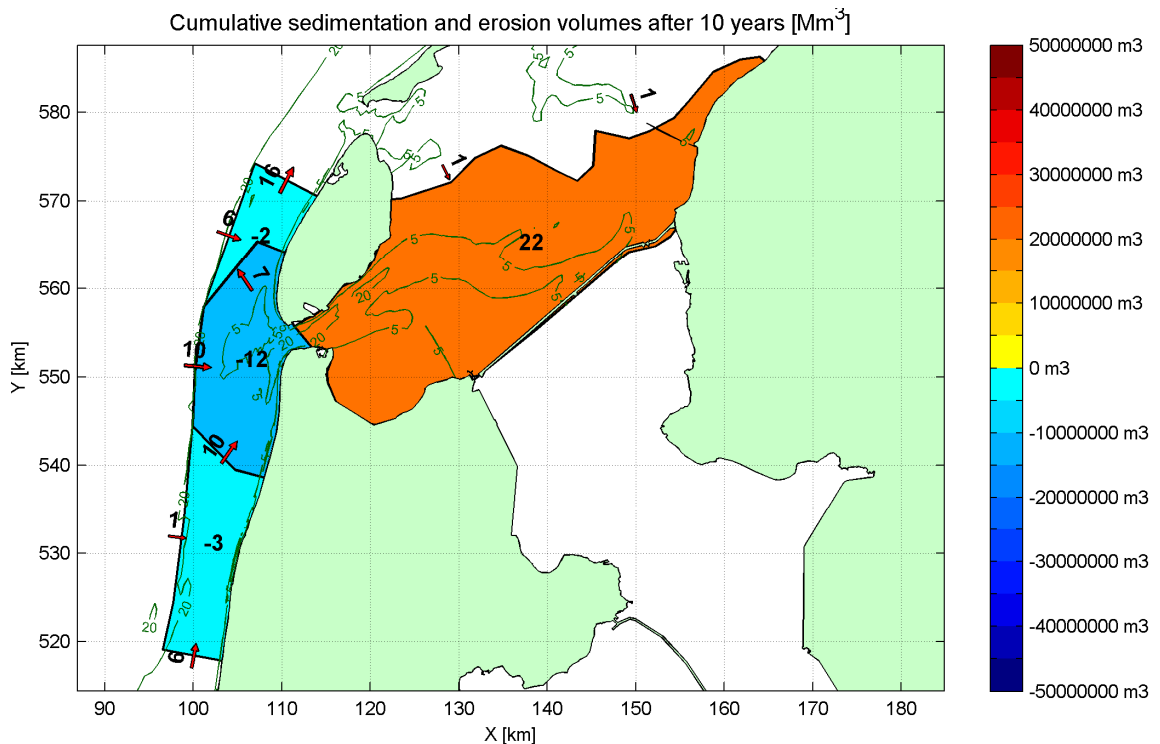


Figure B.15 Sedimentation and erosion in 10 years of morphological simulation in sections; 1) Marsdiep delta 2) Marsdiep basin 3) Texel coast and 4) North-Holland coast, including sediment exchange ($Mm^3/10yr$) in between sections and with the surrounding environment.

	10 years	0 - 5 years	5 – 10 years
1. Marsdiep Delta	-12.0	-11.2	-0.8
2. Marsdiep Basin	+21.9	+18.9	+3.0
3. Texel	-2.5	-1.6	-0.9
4. North-Holland	-3.2	-1.6	-1.6

Table B.7 Sedimentation and erosion volumes in million m^3 in the four sections within three time spans; the full 10 years, the first 5 years and the last 5 years. Areas are shown in figure B.15

On the outer delta, the bathymetry development over 10 years is large. Figure B.16 shows the cumulative sedimentation and erosion per square meter on the outer delta and the most active part of the basin near the inlet. Erosion is up to 5 meters due to the maximum erodable layer of 5 m. Sedimentation is however up to 15 meter (range limited in figure B.16). This figure learns us that the channels Texelstroom, Helsdeur and Breewijd are eroding mainly due to the ebb dominated current. The Schulpengat and the Nieuwe Schulpengat are shifting in seaward direction, but this is largely prevented by the maximum erodable layer. This is most prominent in the Nieuwe Schulpengat channel, because it is the deepest channel in the outer delta and thus erodes more when shifting somewhat. In figure B.17, the bed topography of the shoals (5m depth line) and channels (10m, 20m and 30 m depth lines) is indicated. Focusing on the Nieuwe Schulpengat channel it is seen that the 20 m and 30 m depth lines are fixed after 5 years, due to reaching the fixed layer. This limited flexibility of channel movement is demonstrated in figure B.18, where the Schulpengat channel (the less deepest channel) and the Nieuwe Schulpengat channel after 5 years have moved seawards up to the non-erodable layer. In the following 5 years an extra channel is developing in between. Correctly modelling of the dynamics of the channels and shoals on the long term is still a problem in this model, as the measure for limiting channel deepening (with a fixed layer) is

also limiting the dynamic behaviour. Recently, significant progress is made on this subject by Dastgheib et al. (2008), by including multiple sediment fractions in the model.

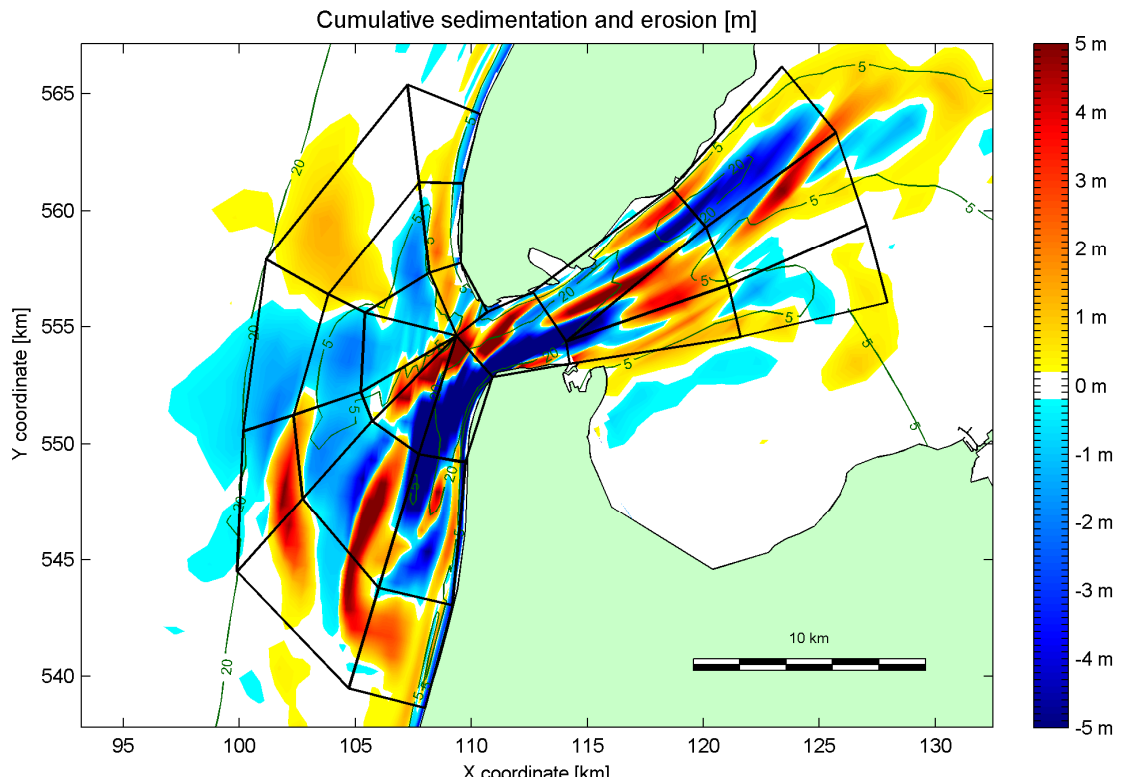


Figure B.16 Cumulative sedimentation and erosion in Texel Inlet in 10 years

While in many cases in numerical models the channels are deepened and the shoals are raised, this is not the case for the Molengat channel along the Texel coast. This channel is not eroding but accreting. The observed trend for the Molengat channel is that the channel is fixed in its position between the landward moving Noorderhaaks and the southern tip of Texel. In the observed trend, close to the Marsdiep throat the channel is deepening and narrowing under the pressure of the eastward movement of Noorderhaaks. The other end of the channel is accreting, as is the spit at the northern side of Noorderhaaks (Elias et al, 2006a).

The sedimentation and erosion trend suggests that Noorderhaaks is eroding. The topography map in figure B.17 with 5 m, 10 m and 20 m depth contour lines for three bed level positions in time, indicates that the shoal is getting smaller, but that it is also moving further landward, thereby narrowing the ebb-dominated channels Breewijd and Marsdiep. The large outer delta sediment circulation probably brings most of the sediment from the Breewijd and the Marsdiep towards the ends of the channel Schulpengat and Nieuwe Schulpengat, where the shoals Zuiderhaaks and Franse Bankje are nourished. Through the residual circulation sediment is passed towards the basin.

A 10-years difference map from measurements (Vaklodingen) shows less extreme bed changes (max 3 m sedimentation and erosion) in the deltaic area than the model. In figure B.19 the same sectional boundaries are plotted in the sedimentation and erosion map. The area of morphological activity is smaller and within the channels the pattern shows the propagation of sand banks over the bed. These differences suggest that the grid is too coarse

for this dynamic area. The measurements show the clear development of a landward movement of Noorderhaaks, the erosion of the channel Nieuwe Schulpengat and the sedimentation of Zuiderhaaks, Franse Bankje and the spit north of the Molengat. These aspects of the development of the outer delta are also correctly represented by the numerical model.

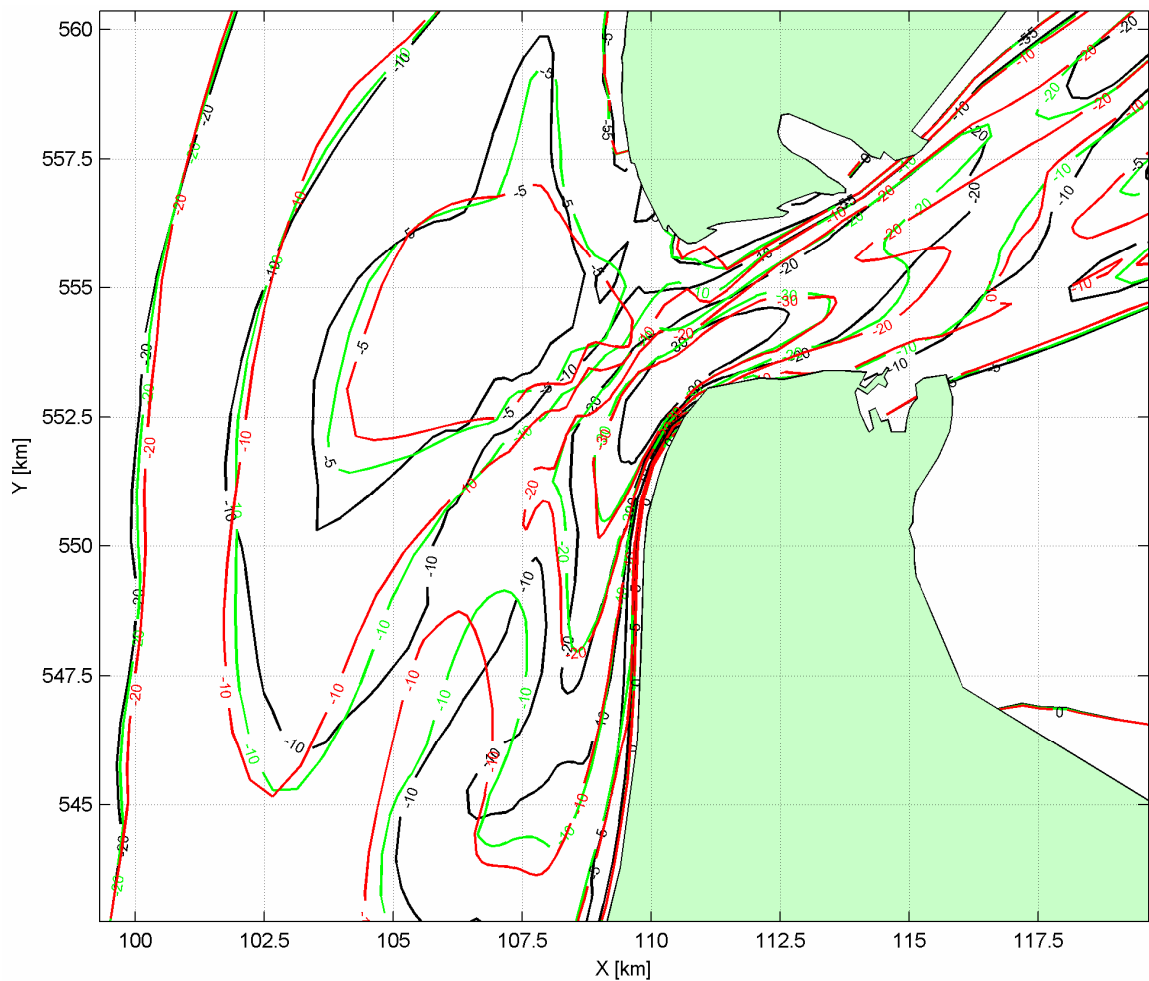


Figure B.17 Modelled bed topography of Marsdiep outer delta at three time frames: $t=0$ (black), $t=5$ years (green) and $t=10$ years (red)

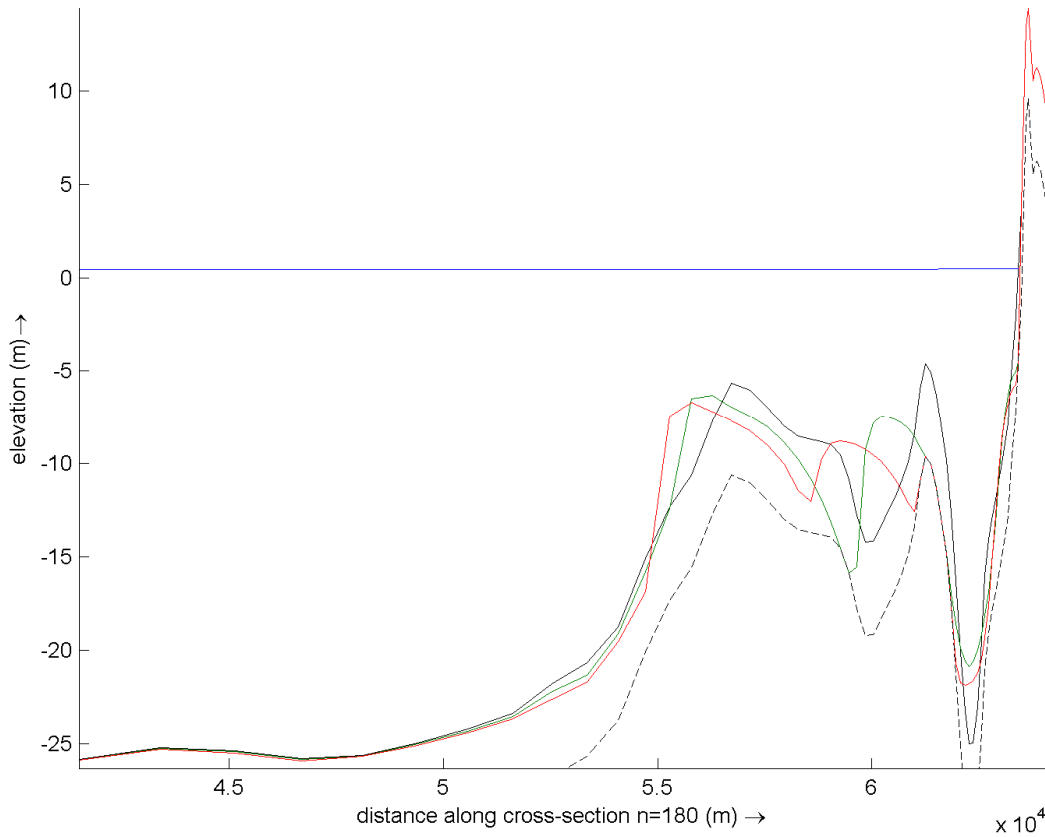


Figure B.18 Cross-section of modelled bed development in ten years over Schulpengat and Nieuwe Schulpengat channels, with initial bottom (straight black line), position of non-erodable layer (dashed black line), bed topography after 5 year (green line) and bed topography after 10 years (red line)

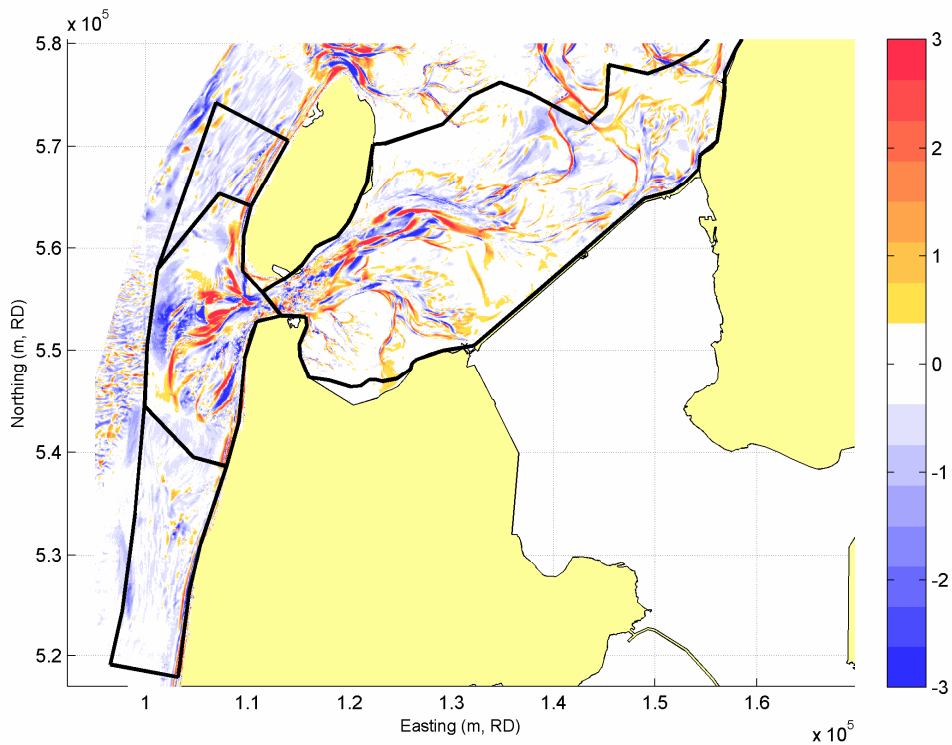


Figure B.19 Measured sedimentation and erosion (Vaklodigen) in Marsdiep delta in 10 years (1995-2006)

B.6 Synthesis

The development of the Moholk-model serves two goals; 1) the development of an accurate and at the same time efficient calculating large-scale sediment transport model for the Dutch coast and 2) to evaluate the effects of mega-nourishments on the North-Holland coast in a time span of up to 10 years. This has resulted in a relative coarse coastal model (highest resolution in the nearshore of 22 m by 260 m) containing the most important driving factors; tidal currents, wave driven currents, sediment transport and accelerated bed updating. The model covers almost the entire coastline, only parts of the southern delta and the eastern Dutch Wadden Sea are not included.

The model performance on hydrodynamic and morphodynamic behaviour has been evaluated in this chapter. The primary currents along the coastline (residual current) and within the Marsdiep Inlet (ebb and flood dominated gullies) are accurately modelled. The residual current along the coastline is in northern direction as a result of tidal forcing, wind and the variance of the A0 tidal component along the coastline. Secondary currents, normally present in the surf zone and in the Marsdiep Inlet, are not represented as these were not defined as a goal. Instead, some parameters are introduced to account for three-dimensional effects on the sediment transport, such as the reduced onshore wave related transport to account for the lack of undertow in the surf zone. In the Marsdiep Inlet, the exclusion of secondary currents in combination with the coarseness of the model results in small order of magnitude differences from the ferry measurements, but the general pattern of flood and ebb currents on the deltaic area is well reproduced.

The tidal currents generating the sand transport patterns are reasonably well modelled in the Moholk model, although the residual current in the Marsdiep is more exporting than the NIOZ ferry measurements indicate. The model boundary along the Vlie basin lies too close to the area of interest and has some influence on the tidal flow in the Marsdiep basin. In the Moholk model the residual sand transport over the tidal divide of Marsdiep and Vlie is almost zero, while according to measurements this could be about 40 to 50 Mm³ per 10 years. Further research on the sediment transport over the tidal divide is necessary..

For the closed coastal system, from Hoek van Holland up to the Hondsbossche Sea Wall, the residual longshore transport shows good agreement with the literature study from Van de Rest, 2004. In the nearshore, defined from the dune foot (+3 m NAP) up to a water depth of 8 m NAP, the average longshore transport is in the order of 100,000 m³/year. Up to a water depth of 20 meters the average longshore transport is 450,000 m³/year and from the beach to 60 km offshore the longshore transport is modelled in the order of 2 million m³. A combination of the grid coarseness and the morphological updating settings results in steeping of the foreshore. This is a local readjustment of the cross-shore profile and does not create model instabilities. It is however not a realistic development and causes inaccuracies in hydrodynamics currents in the foreshore. It is therefore recommended that the parameters α_{Bn} (slope factor), $SusW$ and $BedW$ (factor for onshore/offshore sediment transport) and $ThetSD$ (factor for erosion of adjacent dry cells) are further optimised or that a beach module is implemented to maintain a smooth beach profile in long term morphological model studies.

The morphodynamic variability is largest in the Marsdiep Inlet, where erosion and deposition depths of more than 5 meters occur within a few years due to small channel shifts. This area is subject to morphological spin-up in the first year, as the tidal channels are artificially

deepened up to the non-erodable layer at 5 m below the initial bed level. Due to this spin-up artefact the yearly sediment import averaged over 10 years is 2 – 2.5 Mm³, while if averaged over the last 5 years it is only circa 0.5 Mm³ per year. This sediment import is rather low compared to the most recent sand balance study of the Western Wadden Sea (Elias, 2006) with volume import estimate of 5 – 6 Mm³/year through the Marsdiep Inlet. The problem of artificial channel deepening can be minimised by introducing multiple sand fractions in the model. With multiple sand fractions the variance in grain size in a deep tidal gully is simulated, which is necessary to represent the armouring effect in gullies and channels. This will make the use of a fixed layer redundant. Some promising results have already been made by Dastgheib et al, 2009.

The research done by Elias, 2006 has formed the basis for the analysis of the model performance concerning the Marsdiep Inlet. Elias, 2006, presented a sand transport model for the Texel Inlet (figure B.20). The erosion and deposition areas identified in the Moholk-model compare well with those defined in the sand transport model, as well as the sediment circulation pattern, indicated in figure B.20. The westward movement of the shoal Noorderhaaks is also reproduced in the Moholk-model, which is an important driving process within the Marsdiep tidal inlet.

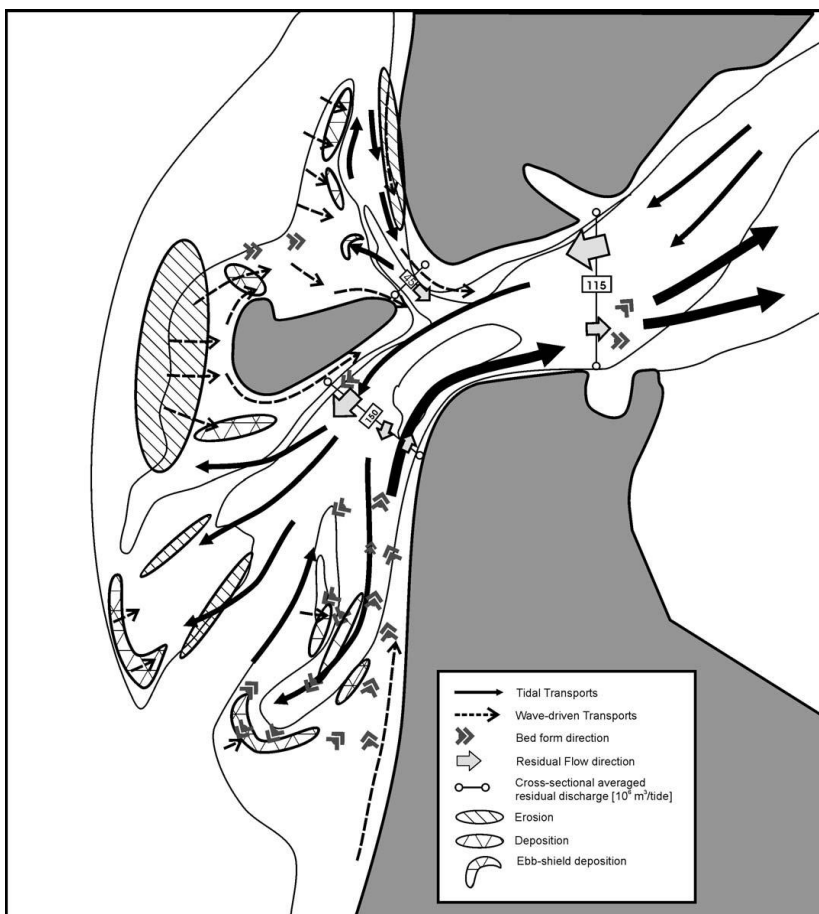


Figure B.20 Observation-based schematic representation of transport patterns on Texel ebb-tidal delta (Elias, 2006)

C Validation of longshore currents, comparison with former studies

The analysis of differences in long shore sediment transport rates using the TRANSPOR 1993 and 2004 was carried out by Luo Xiao Feng from the Nanjing Hydraulic Research Institute (NHRI) as part of a collaboration between Deltares and NHRI.

C.1 Comparison with Van Rijn, 1995, Van Rijn e.a, 1995 and Van Rijn, 1997

In two reports (van Rijn,1995 and Van Rijn e.a.,1995) and the succeeding paper (van Rijn,1997) a study has been reported on the longshore and cross-shore currents along the Dutch coast. The 1997 paper provides a summary of the two 1995 reports. In the first report a sand budget study is given using data of the period 1964-1992. These data were used to derive an estimate of the longshore sand transports (see figure C.8). The second study concerns a sensitivity analysis on 18 items, including wind-induced currents, density currents and wave climate parameters. The results are based on calculations with a so-called point model including the transport formula TR1993 (Transport 1993). The point model study is performed for four cross sections perpendicular to the coast, being;

- Scheveningen at RSP 103.
- Noordwijk at RSP 76.
- Egmond at RSP 40.
- Callantsoog at RSP 14.

In table C.1 the results of the point model are given for the longshore transport in $m^3/m^1/year$ for the base case. In figure C.1 the results for varying transport formulations in a water depth of 8 m are given. The upper graph shows the results for Delft3D with TR1993, the middle one for Delft3D with TR2004 and bed roughness predictor and the lower one for Delft3D with TR2004 with constant bed roughness. The black lines give the bandwidth reported in van Rijn e.a.,1995, while the best estimate is provided in table C.1. The blue dotted line presents the Delft3D results for the run without wind and waves and the red line the Delft3D results for all wind and wave classes combined. The black lines should be compared with the red line, the total transport. The best comparison is found for Delft3D with TR1993, the worst comparison is found for Delft3D with TR2004 with constant bed roughness.

In figure C.2 the results for the water depth of 20 m are given. The upper graph shows the results for Delft3D with TR1993, the middle one for Delft3D with TR2004 and bed roughness predictor and the lower one for Delft3D with TR2004 with constant bed roughness. The black lines give the results reported in van Rijn e.a.,1995 for the upper and lower limit, while in table C.1 the best estimate is given. The blue dotted line shows the Delft3D results for the case without waves and the red line the Delft3D results for all wind classes combined. The black lines should be compared with the red line, total transport. The results for Delft3D with TR1993 are too high and the results for Delft3D with TR2004 are too low compared with the point model (van Rijn e.a. , 1995). The use of the bed roughness predictor does not make any difference at this water depth.

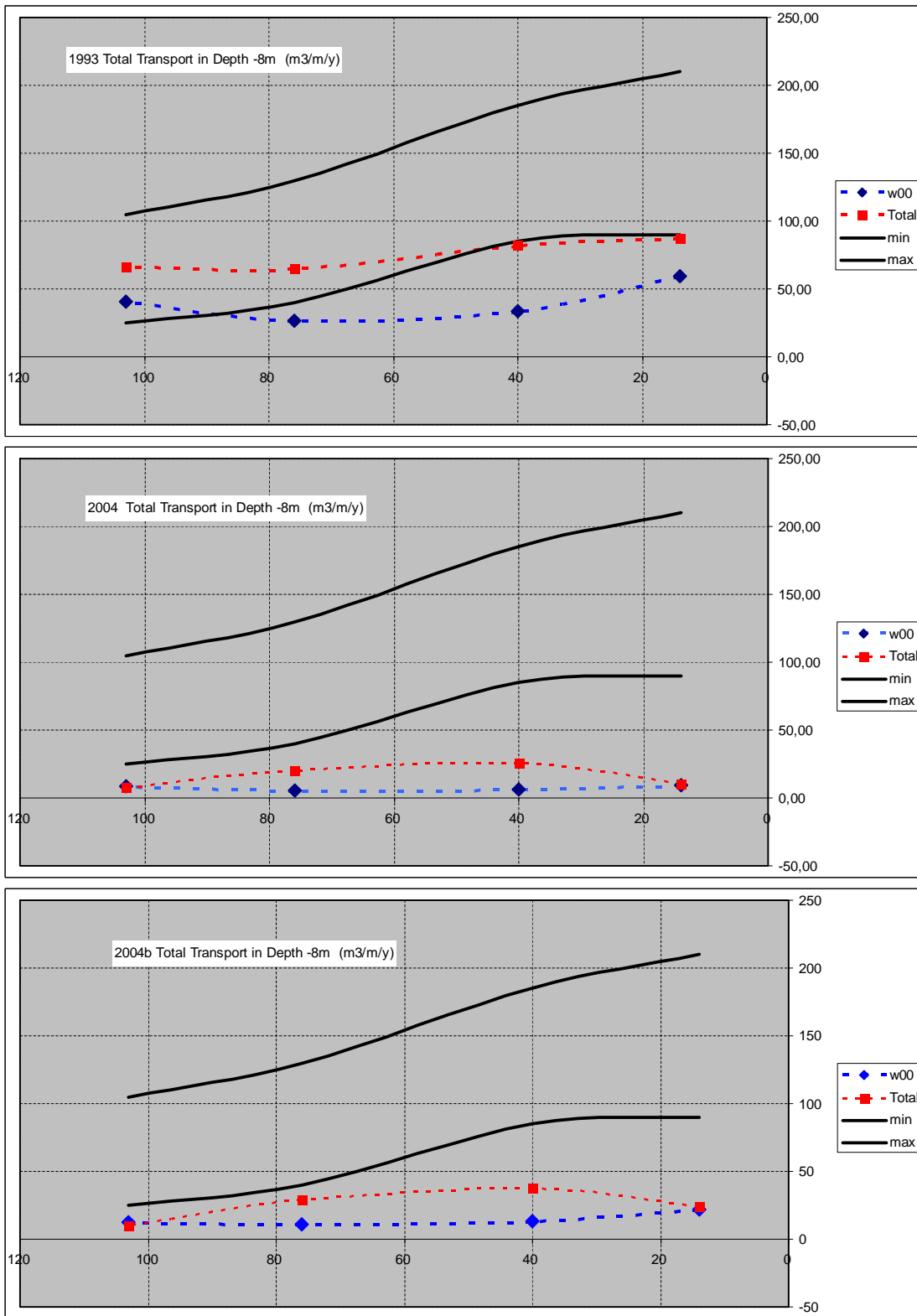


Figure C.1 Results of the longshore transport for a water depth of 8 meter (see text for explanation)

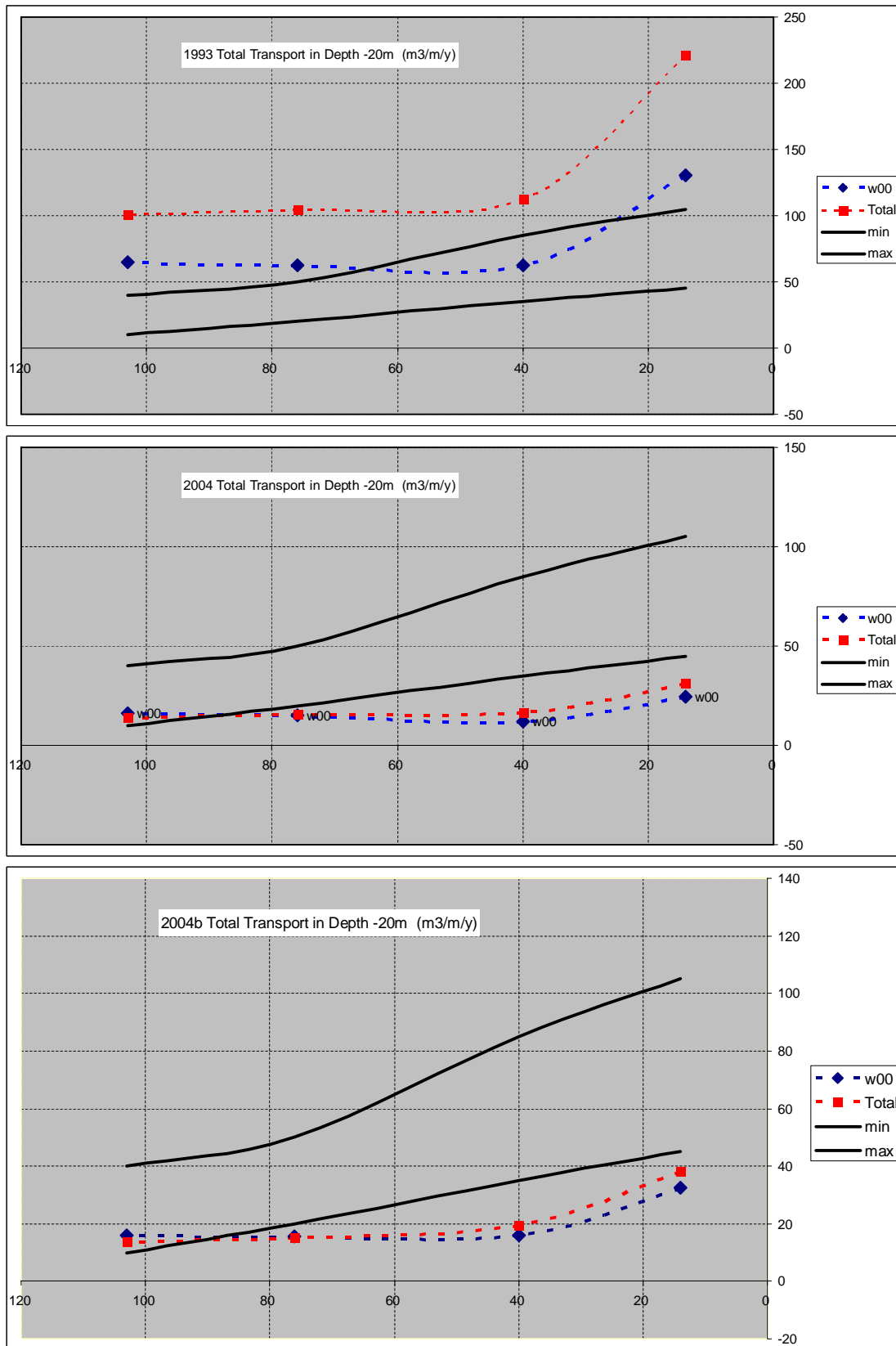


Figure C.2 Results of the longshore transport for a water depth of 8 meter (see text for explanation)

The results of the point model have been modified by Van Rijn due to inaccuracies in the tidal currents used as input for the point model (see table C.1). For the 8 m depth a correction of a factor 2 has been used and for the 20 m depth a factor 0,6. The values of the transport excluding pores have been multiplied with a factor 1,67 (40% pores) to derive the transports including pores. In figure C.3 the final estimates of both studies (point model and budget) are given. In a later study (van Rijn e.a. 2005,) a comparison has been made with the point model including the TR2004 transport formulae for one location, Noordwijk 20 with a water depth of 20 meter. The longshore transports for TR 2004 were about 25% less compared with TR1993. The final results and the ratio between the point model and Delft3D are given in the last three columns of table C.1. In case of the model Delft3D only the results for TR 2004 are shown. As mentioned in Appendix B the results for TR 1993 in Delft3D are highly overestimating the sediment transports in deeper water.

Depth 8 meter		Base Case van Rijn 1995		van Rijn 1995 best guess excl. pores TR1993	van Rijn 1997 incl. pores * 1,67 TR1993	Delft3D Total no roughness pr TR2004	Factor G/H
Longshore transport m ³ /m ¹ /jaar		excl. pores TR1993	Corr with 2				
Callantsoog (14)		59,5	119	90	150	24	6,3
Egmond (40)		82,8	165,6	80	135	37	3,6
Noordwijk (76)		37,5	75	50	85	29	2,9
Scheveningen (103)		35	70	40	65	10	6,5

Depth 20 meter		No Density Gra van Rijn 2005	No Density Gra van Rijn 2005	Base Case van Rijn 1995		van Rijn 1995 best guess excl. pores TR1993	incl. pores * 1,67	Delft3D Total no roughness pr TR2004	Factor G/H
Longshore transport m ³ /m ¹ /jaar		excl. pores TR2004	excl. pores TR1993	excl. pores TR1993	Corr with 2				
Callantsoog (14)				80	48	45	75	31	2,4
Egmond (40)				53,1	31,86	35	60	17	3,5
Noordwijk (76)				28,4	17,04	20	35	15	2,3
Scheveningen (103)				22,6	13,56	15	25	14	1,8
Noordwijk (76)	25,8				15,48		26	15	1,7
Noordwijk (76)			33,1		19,86		33	15	2,2

Table C.1 Comparison of transport rates in Delft3D (TR2004) with the results of van Rijn 1995, 1997 and 2005

The results show lower values for Delft3D compared to the van Rijn study. At a water depth of 20 meter the transport rates in Delft3D are a factor 2 to 3 lower. At a water depth of 8 meter the transport rates in Delft3D are a factor 2 to 6 lower.

The main findings of the study of Luo Xiao Feng are:

- Apparent differences in sediment transport rates between Van Rijn (1995) and Van Rijn (1997) are due to the fact that in Van Rijn (1995) sediment transports are used excluding pore volumes while in Van Rijn (1997) sediment transport are presented including pore volumes.
- Van Rijn (1995, 1997) reduces the yearly-averaged sediment transport rates at -20m NAP by about 40% to account for the overestimation of the relatively large velocities of the representative tide and the slightly over estimated wind effect.
- The sediment transport is dominated by currents in deeper water, while it is dominated by waves in the surf zone. Inaccuracies between observed sediment transport in either deeper water or surf zone may be related to specific schematization accuracy of either hydrodynamics or waves.
- Analysis of Van Rijn (1997) and the present Moholk model results showed that wind has a significant effect on the sediment transport rates as it may double the yearly sediment transport rates in both deep and shallow water. The wind effect in Van Rijn (1995) may be slightly overestimated.

C.2 Comparison of TR2004 and TR1993 within Delft3D

When using Delft3D with TR1993, the vertical grid is set standard to 15 layers, when using TR2004, it is set standard to 50 layers. In case of no wave forcing the results for both transport formulae are more or less the same (figure C.3), but in case of higher wave forcing the results start to differentiate (figure C.4). The velocity profile in that case is still the same for both transport formulae.

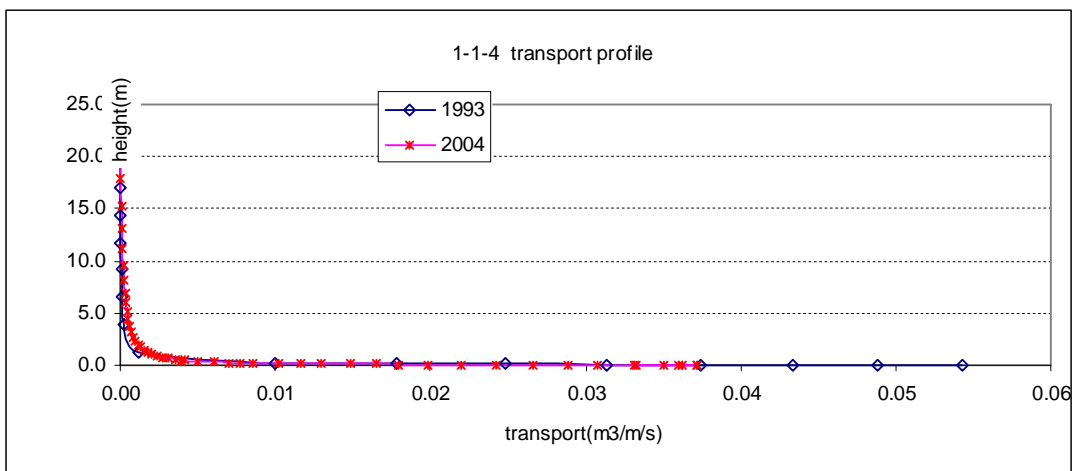


Figure C.3 Transport Profile at profile 76 at depth -20m (no waves)

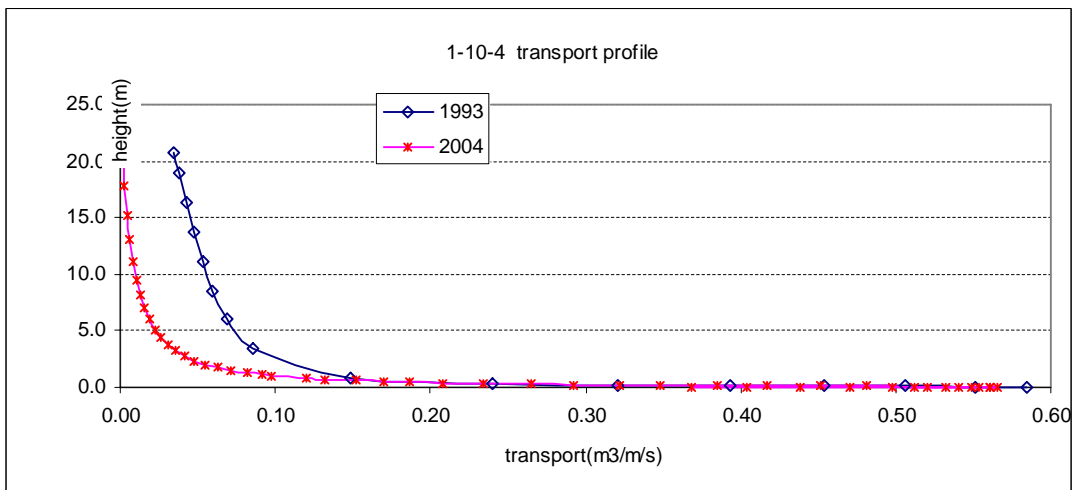


Figure C.4 Transport Profile at profile 76 at depth -20m (wave height 4.25m, angle 195)

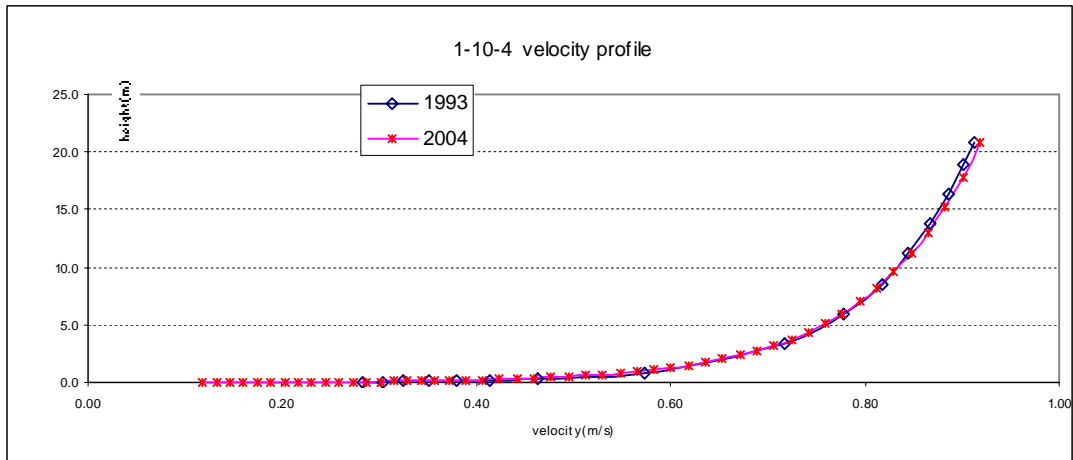


Figure C.5 Vertical velocity distribution at profile 76 at depth -20m (wave height 4.25m, angle 195)

When comparing the results over a cross section perpendicular to the coast the differences are even more pronounced. Figure C.6 shows the differences in cross section Noordwijk (76) for a small wave condition W02 (wave height 1.2 m, wind direction 240 degrees). The left graph shows the velocities and the right graph the transports.

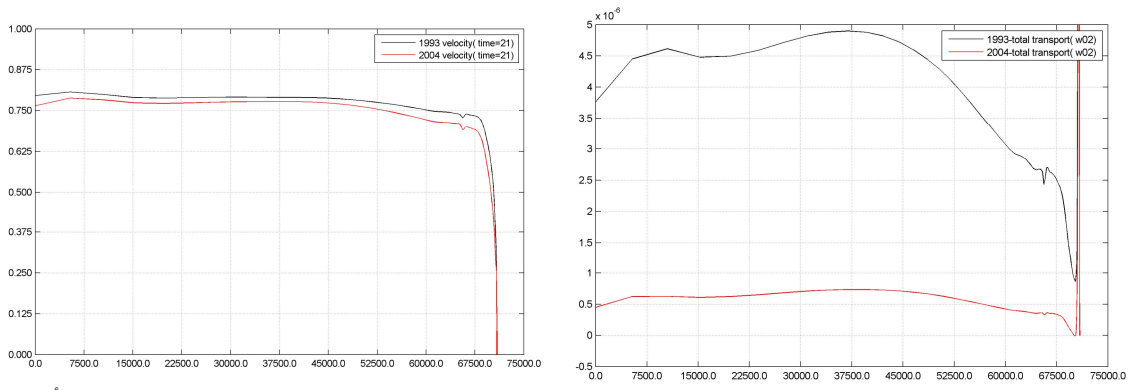


Figure C.6 Comparison of the total longshore transport between the dune foot and the 8 meter depth contour for TR 1993 and TR 2004 in the Delft3D model.

In Van Rijn, 1995 and Van Rijn, 1997 also the total longshore transports between the dune foot and the 8 m water depth contour are given. Compared to the results of van Rijn (see table C.2) the Delft3D results are a factor 2-4 too high. The paper by Van Rijn, 1997 mentions that taking into account the effects of the breaker bars can increase the results by another 10 to 50%.

Longshore transport dune foot - 8m water depth m3/year	Base Case van Rijn 1995 incl. pores TR1993	Delft3D TR2004	Factor
Callantsoog (14)	570000	150000	3,8
Egmond (40)	300000	50000	6,0
Noordwijk (76)	250000	170000	1,5
Scheveningen (103)	600000	170000	3,5

Table C.2 Comparison longshore transports Van Rijn, 1995 and Delft3D

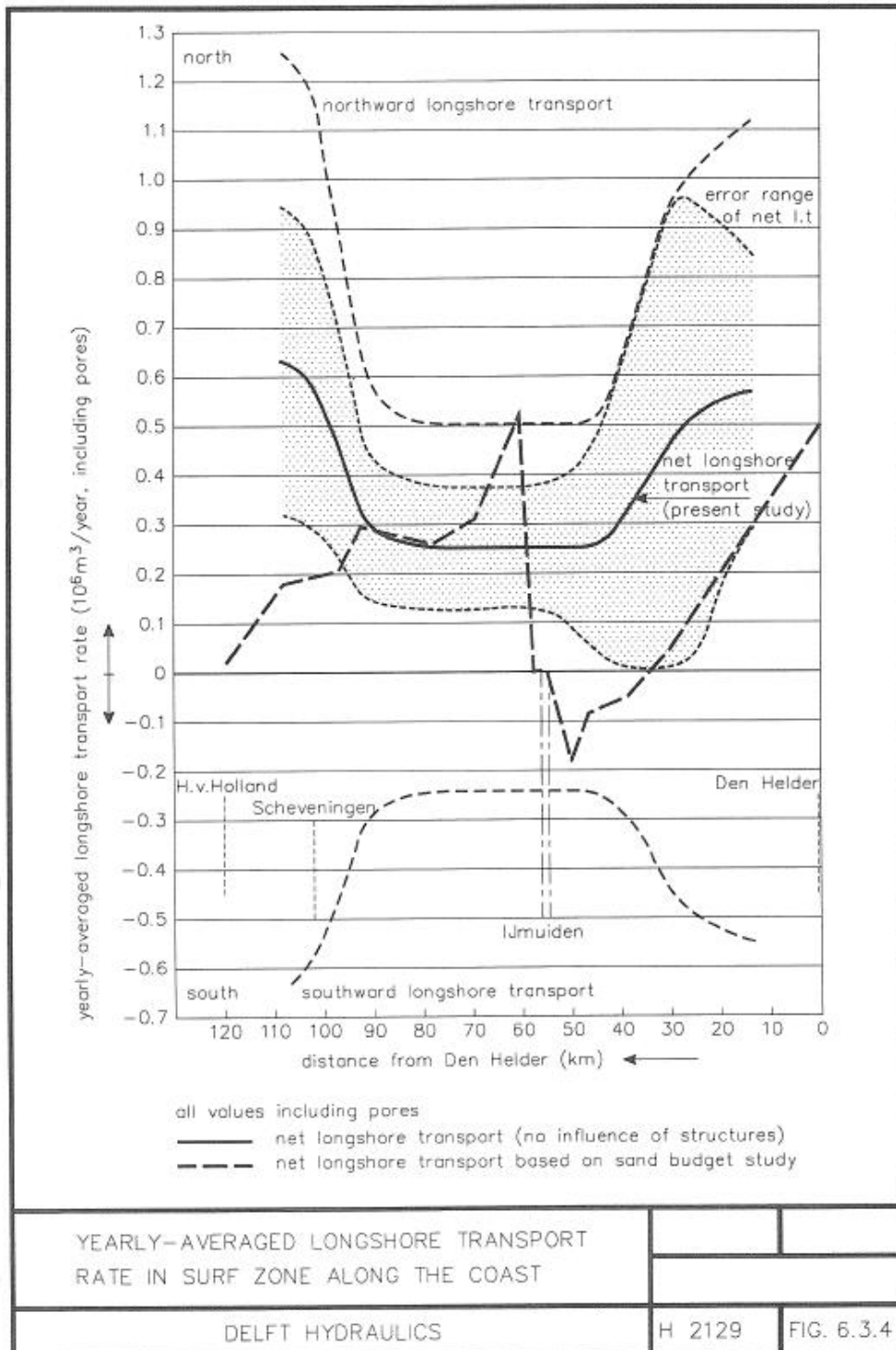


Figure C.7 Estimates of longshore transport by a sand balance study and by a model study (Van Rijn, 1995)

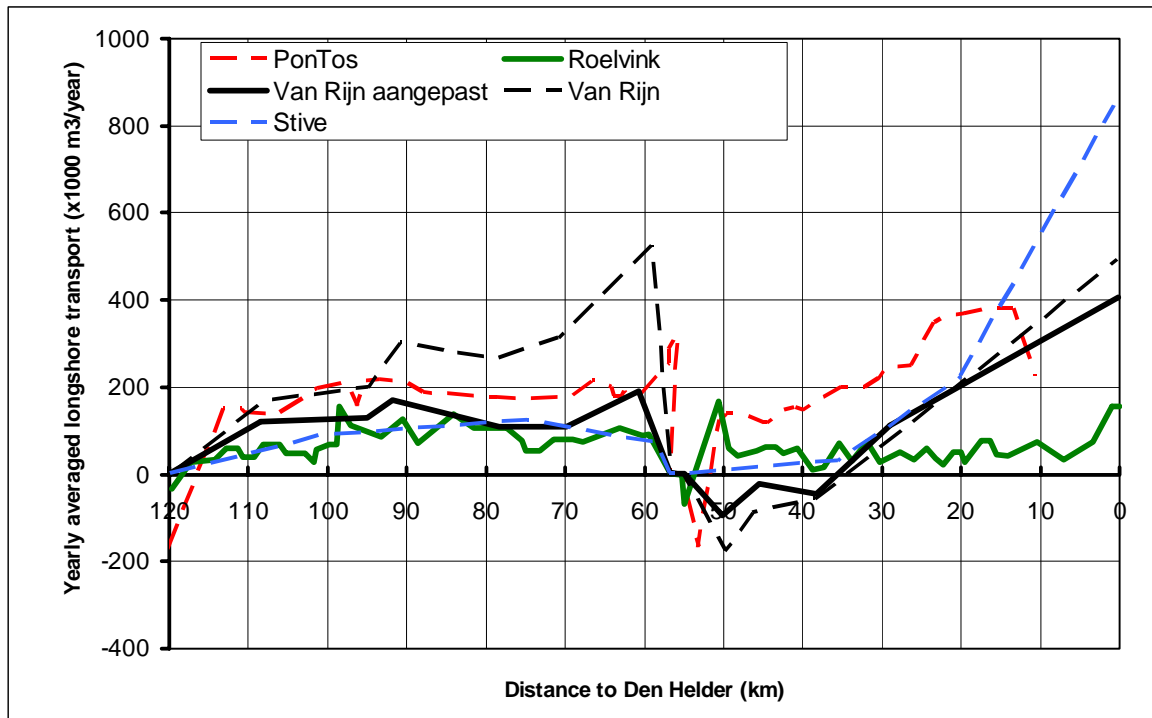


Figure C.8 Estimates of longshore transports by different studies (Van de Rest, 2004)

C.3 Comparison of MOHOLK results with the measurements of the “ Dammetje van Wiersma”

North of the “Eurogeul”, the shipping gully to the port of Rotterdam, about 3.5 Mm^3 of sand has been deposited during the period between September 1982 and December 1986. With this material a small dam has been made to reduce the back flow of dumped harbour silt. With depth measurements and volume calculations an increase of longshore transport has been derived of about $20 \text{ m}^3/\text{m}/\text{year}$ in a water depth between 15 to 23 meter. A relation of this increase with water depth could not be derived (Van Rijn and Walstra, 2004).

In a later study (Tonnon, 2005) an area has been defined in the shallow coastal zone with a length of 1600 meter parallel to the coast and a width of 700 meter. The water depth is between 16 and 18 meter. On the sand dam a loss of 7 to $13 \text{ m}^3/\text{m}/\text{year}$ caused by migration has been found. On the other side of the dam accretion of 5 to $8 \text{ m}^3/\text{m}/\text{year}$ occurred. A longshore transport on top of the sand dam can be derived with a maximum of $10 \text{ m}^3/\text{m}/\text{year}$. The “natural” sand transport in the case without the sand dam will be (a lot) smaller. Model results calibrated with the above mentioned values support a total transport of $65 \text{ m}^3/\text{m}/\text{year}$ at a water depth of 15 meter and $50 \text{ m}^3/\text{m}/\text{year}$ at a water depth of 19 meter (Van Rijn and Walstra, 2004). These values match with figure G09 (without bottom update) from Tonnon, 1995. All other values in this report are lower and have a value of 10 to $20 \text{ m}^3/\text{m}/\text{year}$. This can be compared with the Scheveningen result from the MOHOLK model ($14 \text{ m}^3/\text{m}/\text{year}$).

It can be concluded that the longshore currents in the MOHOLK model compare relatively well with former model studies, which are calibrated on the measurements of the “Dammetje van Wiersma”.

C.4 Final comparison

In many studies it has been tried to estimate the longshore transports along the Dutch coast. The results are summarized in figure C.8 (van de Rest, 2004). In this figure two studies by Van Rijn are given, the original one and a corrected one. Van de Rest used the data over the period 1965-1997 (Stam, 1999) to correct the sand budget of van Rijn.

The results of the point model (van Rijn e.a. ,1995) (Table C.1 and figure C.7) are not shown in figure C.8, in general they are a lot higher than the budget results. Between IJmuiden (km 55) and Petten (km 20) the budget results are negative (to the south) while the point model results are to the north and bigger in magnitude.

Hoek van Holland - IJmuiden

On average the Delft3D longshore transports are about 175.000 m³/year with smaller values at Hoek van Holland, Scheveningen and IJmuiden due to the harbour breakwaters. The Pontos model results are a little bit higher and the other results are somewhat lower. The Scheveningen breakwaters are only accounted for in the Delft3D model, that is why the lower values at kilometre 103 only appear in these results.

In general the Delft3D results compare well with the results of the other studies. The point model results (figure C.1) are very high compared to the other studies.

IJmuiden – Den Helder

On average, the Delft3D longshore transports are about 125.000 m³/year with smaller values at IJmuiden and Den Helder. The Pontos model results are higher and the other results are a lot lower. Near IJmuiden all results are negative except for Delft3D, in which the results are zero. Between IJmuiden and Den Helder all results differ from each other.

In general the Delft3D results are in the same range with the results of the other studies. Uncertainties remain high. The point model results (figure C.3) are very high compared to the other studies.

Taking all studies into account, the results of the MOHOLK model compare well. It is clear from all studies that the uncertainties involved are still very high. The uncertainty can be estimated to be about a factor two.

D Wave climate, contribution different conditions

The combination of weighted wave conditions generate a yearly averaged sediment transport. In this appendix the individual contributions of the wave conditions is discussed. The wave climate is constructed from one small and one large wave condition for 6 wave bins and an additional zero wave condition (w00) for the remaining time of year with insignificant wave height. The weight factors are shown in table D.1. The high waves (W07-w12) have a much lower weight factor, as the presence of high waves is much lower during a year. The zero wave condition is most frequently present on the Dutch coast.

	H_s (m)	T_p (s)	Dir (deg)	Weight factor
W00	0	0	0	0.210
W01	1.3	5.5	210	0.100
W02	1.2	5.7	240	0.119
W03	1.2	5.8	270	0.075
W04	1.2	6.1	300	0.079
W05	1.2	6.5	330	0.127
W06	1.1	6.3	360	0.121
W07	2.7	7.2	210	0.030
W08	2.9	7.2	240	0.047
W09	3.1	7.8	270	0.027
W10	3.1	8.0	300	0.025
W11	3.1	8.4	330	0.031
W12	2.8	7.8	360	0.010

Table D.1 Weight factor per wave condition

As expected, the 6 high waves generate the largest transport if not weighted (Figure D.1), both in southern as in northern direction. The weighted and summed average longshore transport is 100,000 m³/m/year (Chapter 3). The individual storm conditions are exceeding this yearly transport and the small wave conditions do not seem to produce a longshore transport. When weighted according to occurrence in a year, the high waves are scaled down and the small waves are scaled up (Figure D.2). From figure D.2 it follows that the average yearly longshore transport is the result of five large wave conditions. The low waves do not contribute to the longshore transport.

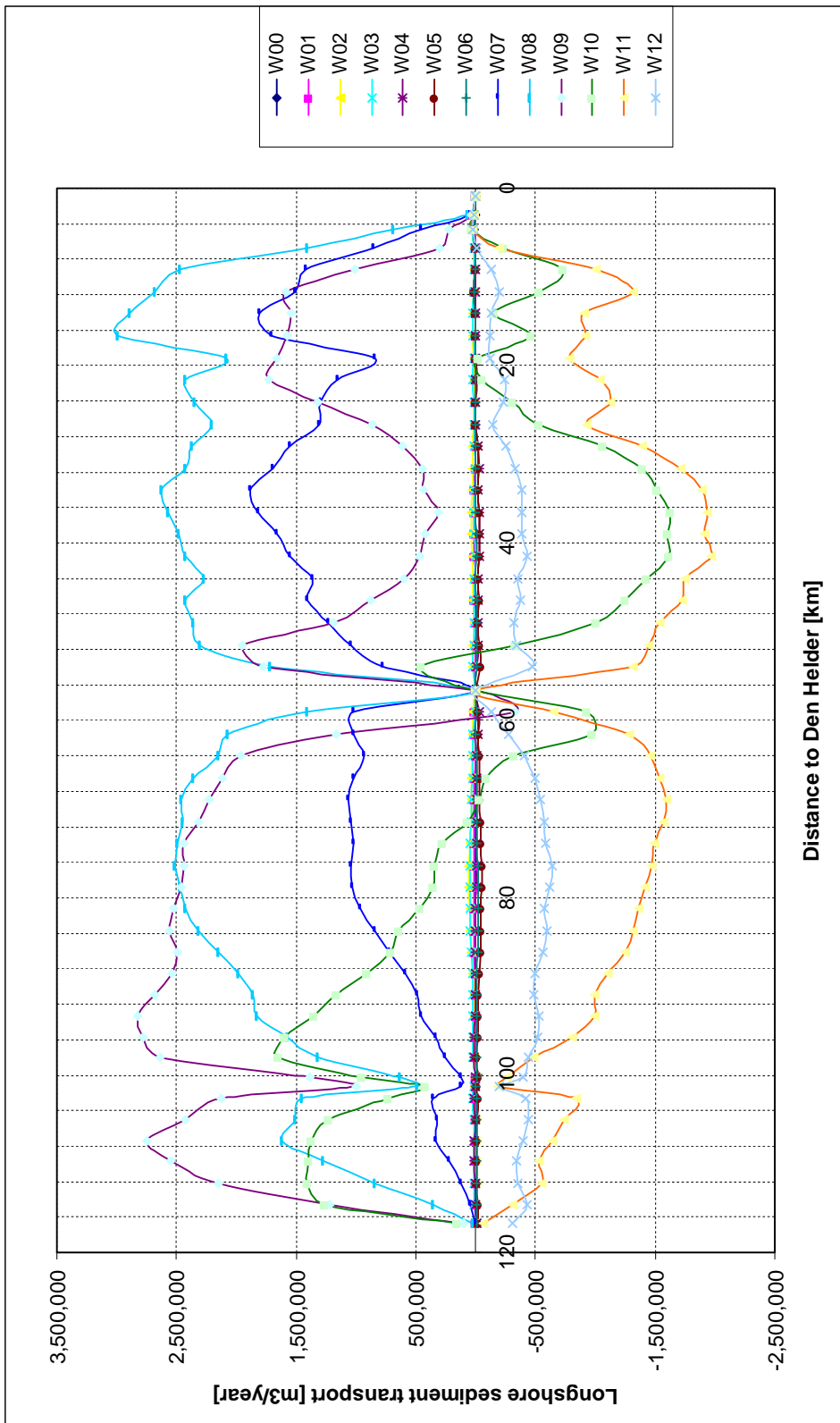


Figure D.1 Separated sediment transport per wave condition without weight factors

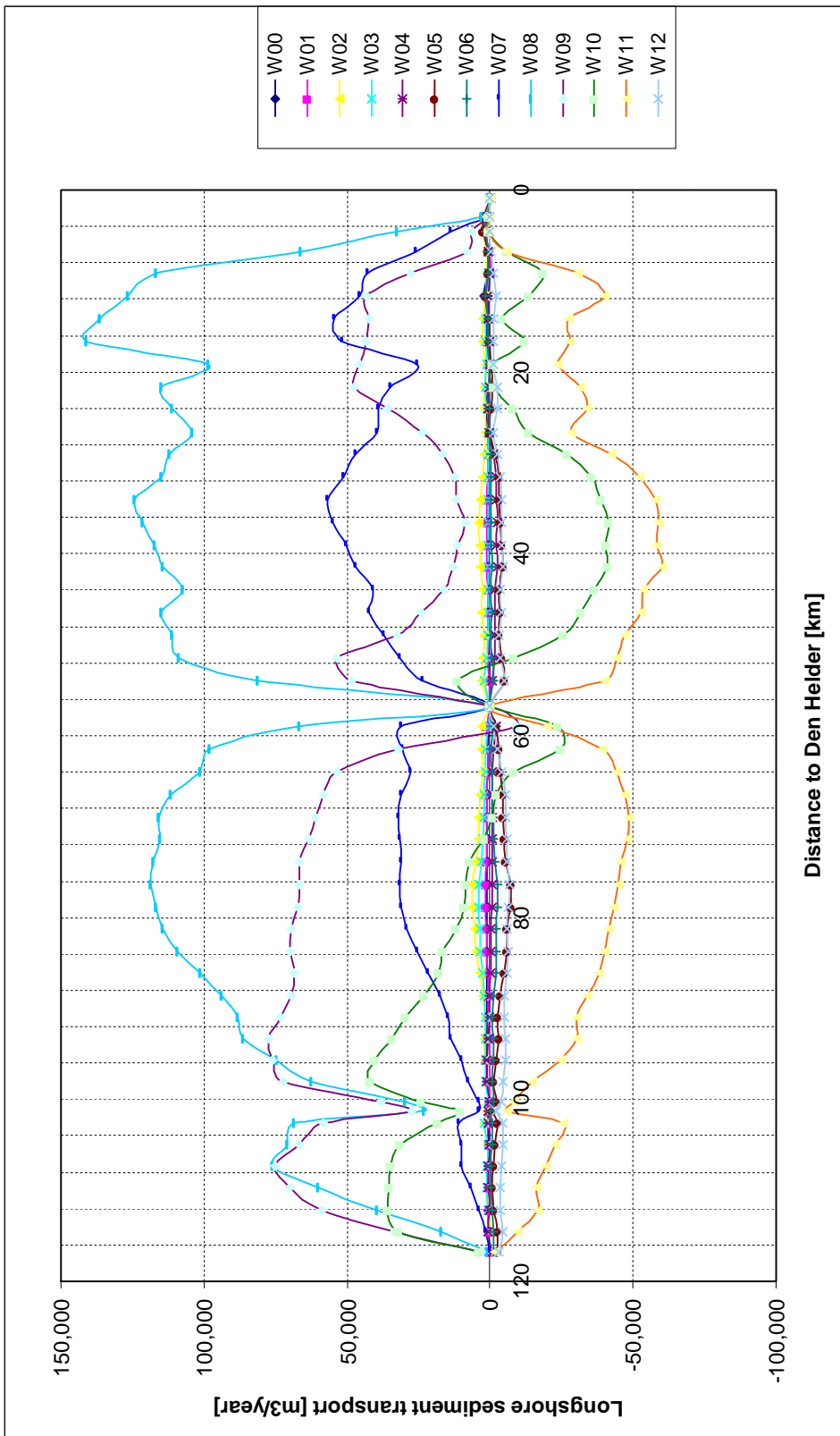


Figure D.2 Separated sediment transport per wave condition with weight factors

E Sensitivity of tidal forcing

The Moholk model is forced by a double spring neap tide of 30 days. A disadvantage of the usage of a neap spring cycle is a lower possible morphological factor for morphological updating, because it is limited by the high velocities and thus the largest bed level changes during spring tide, while during neap tide the morphological development is much smaller. With a morphological tide of 1490 minutes, which represents the mean sediment transports, a higher morphological factor may be applied. This can reduce the necessary computation times. However, for morphological simulations of 10 to 20 years still a multiple of the morphological tide is necessary, so the reduction in calculation time can only be achieved by an increased morphological factor.

E.1 Description of tidal schematizations

For the Moholk Model the two tidal representations have been derived in previous studies. For simplicity these are used in this sensitivity study instead of deriving a new set of the boundary conditions, which is more time consuming. The two cycles have the following characteristics:

- Double neap spring cycle defined with 39 astronomical components, derived in the study for Maasvlakte 2. The time span runs from 23-04-1999 13:00 to 23-05-1999 13:00, which is 43200 min or 30 days.
- Simplified semi-diurnal tide consisting of 6 even components and A0 representing water level set-up. The diurnal inequality has been removed from the tide. This tide has been derived for the Flyland study. The time span runs from 04-08-1988 11:36 tot 05-08-1988 12:26, which is 1490 min. This period has been derived to represent the tide driven time-averaged longshore sediment transport in 18 points in the Haringvliet.

Besides, a comparison is made between a single 15 days cycle and a 30 days cycle for 300 days morphological time. On the 15 days run a morphological scale factor of 20 is applied and on the 30 days run a morphological scale factor of 10 is applied to reach the 300 days morphological simulation time.

E.2 Time averaged residual longshore transports

The total transports, calculated by Delft3D for each flow/wave simulation, are afterwards (after the run has been finished) weighted and summed with matlab and excel, to get to the numbers and figures in this paragraph.

E.2.1 Nearshore

The nearshore is defined in this analysis as the area enclosed by the depth lines of -8 m NAP and +3 m NAP, which is dominated by the complex hydrodynamic and transport patterns of the surf zone. In this area wave action is the dominant factor in generating currents and sediment transport, and thus in the residual sediment transport in longshore direction. Figure E.1 shows the yearly residual longshore sediment transports along the Holland Coast, from Hoek van Holland at km 120 until Den Helder at km 0, and 20 km along the Texel North Sea

coastline. In this graph the residual longshore transports are compared for the three tidal schematizations. The graphs overlap each other, meaning that the residual transport is almost the same for each tidal schematization. However, between km 10 and km 25 a discrepancy is seen for the morphological tide.

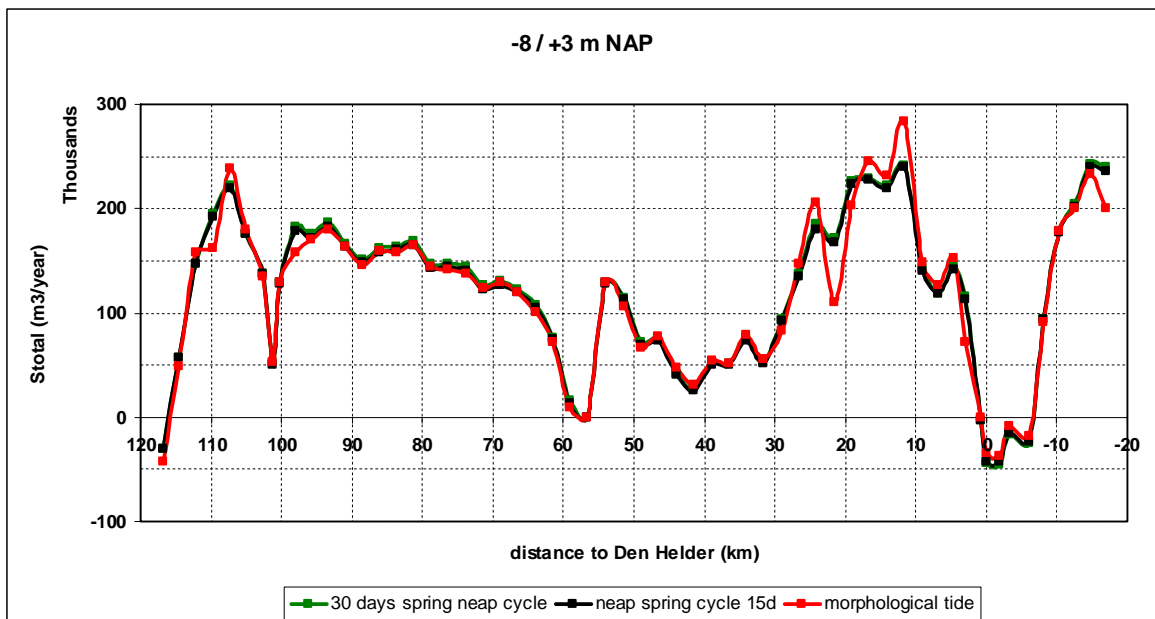


Figure E.1 Longshore sediment transports through coastal sections defined between the water depth of -3 meters (dune foot) and the water depth of 8 meters. Positive transport is transport in northward direction

E.2.2 Offshore

The offshore is defined in this analysis as the area enclosed by the depth lines of -20 m NAP and -8 m NAP. The water depth line of -20 m is known as the outer boundary of the morphologically active zone, or Dutch coastal zone. In this area the tidal current is the dominant factor in generating currents and the residual sediment transports along the Dutch coastline. Figure E.2 shows the yearly residual longshore sediment transports along the Holland Coast for the three tidal schematizations. Each of the three tidal schematizations generates a different magnitude of longshore sediment transport, which indicates that the type of tidal schematization has an important influence on the residual sediment transport. The two spring-neap tidal cycles vary a factor two in magnitude along the entire coastline. The second 15 days of the spring neap cycle generates higher current velocities, which increases the sediment transport capacity by a factor 3. This results in residual sediment transports being twice as large. The morphological tide is producing residual sediment transports of a factor 2.5 lower than the 30 days spring neap cycle, which is a large underestimation of the longshore sediment transport.

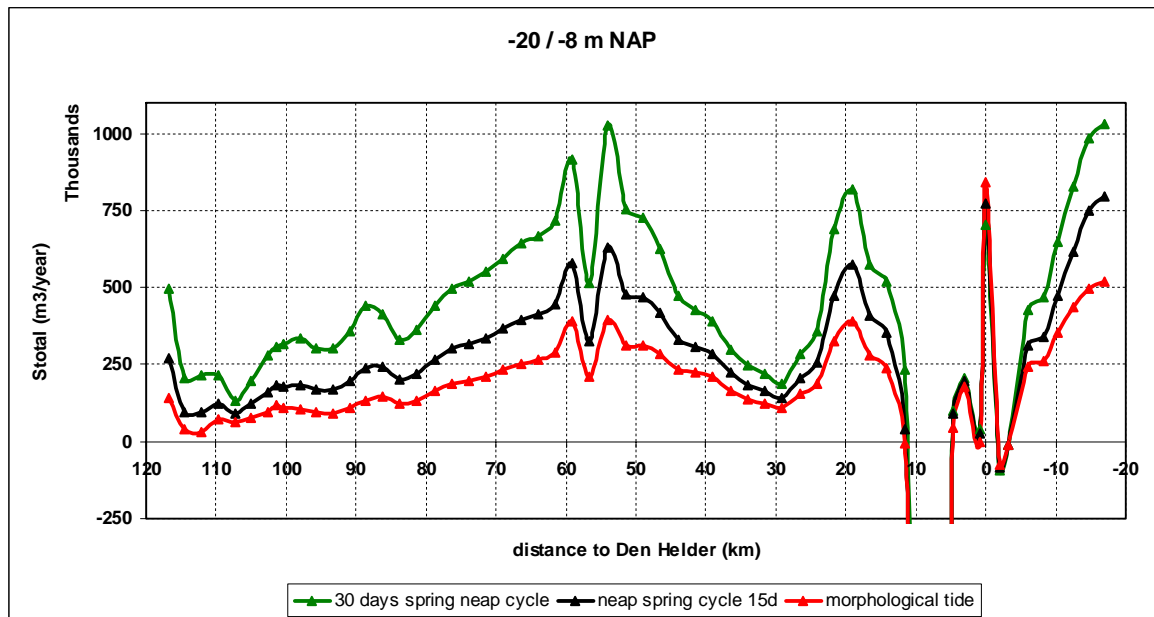


Figure E.2 Longshore sediment transports through coastal sections defined between the water depth of 8 meters (dune foot) and the water depth of 20 meters. Positive transport is transport in northward direction

E.2.3 Marsdiep

A closer look at the morphological development of the Marsdiep tidal inlet shows that the large volume of sediment import through the inlet is the result of scouring of the gully and filling up of the area directly at the eastern side of the defined transect. When the Marsdiep gully is eroded for the maximum value of 5 m, also the sediment import into the Wadden Sea decreases to zero (figure E.3). Averaged over simulation length this results for the two spring neap cycles in the same order of magnitude of 'sediment import' into the Wadden Sea.

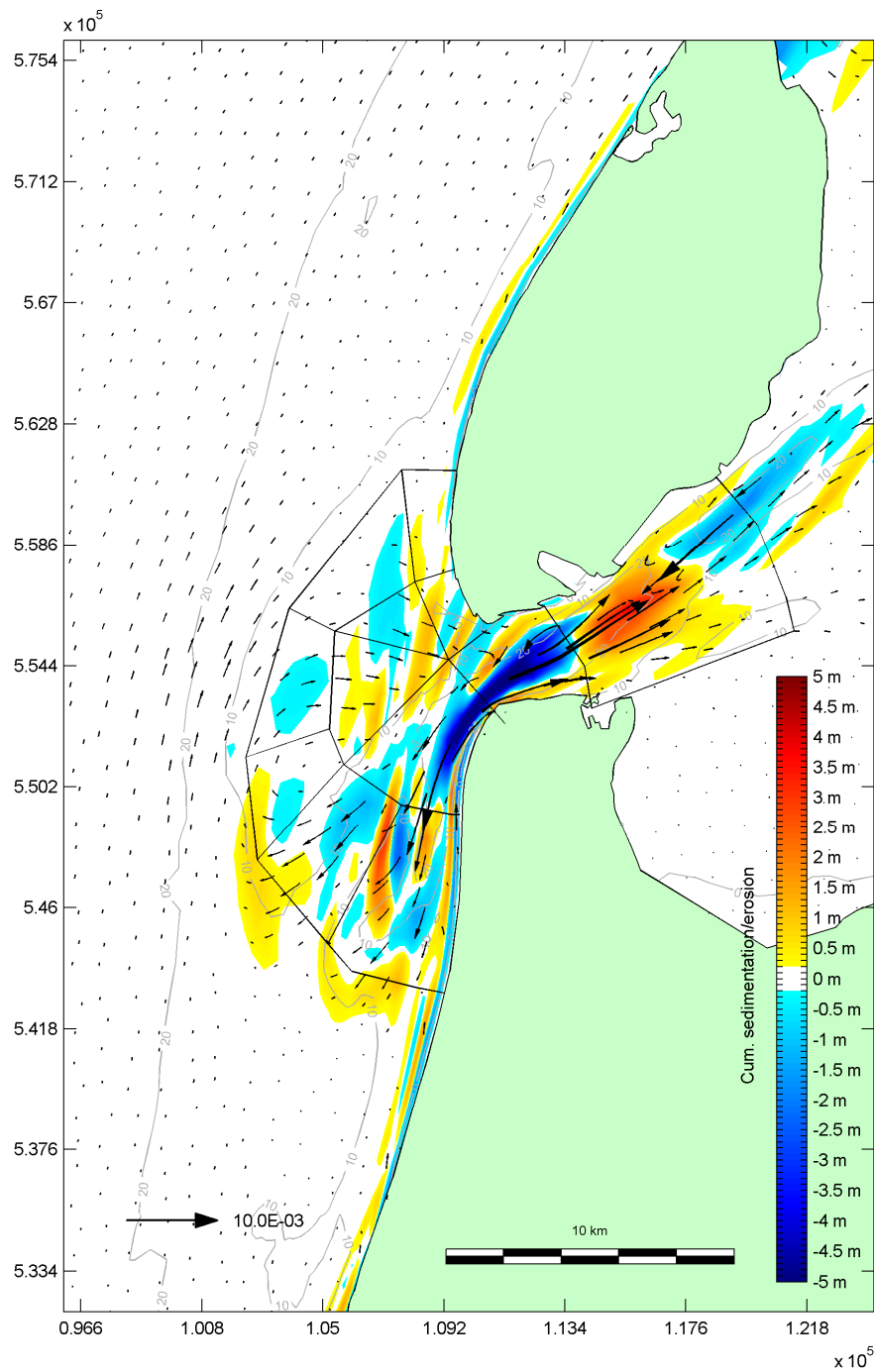


Figure E.3 Cumulative sedimentation and erosion in the Marsdiep delta for a 15 days spring neap cycle. In colours is shown the cumulative sedimentation and erosion after one morphological year, the arrows indicate the direction and magnitude of the yearly averaged total sediment transport

E.3 Neumann boundaries

In this analysis a simple derivation of Neumann boundaries for the lateral sea boundaries is applied to represent the tidal flow. However, this proved not to produce correct velocity fields, especially at the boundaries. It is recommended for such a large model (with lateral boundaries of 60 kilometres) to derive the Neumann boundaries by nesting with multiple sections on the lateral boundaries and not by derivation from existing transformed boundary conditions. In study, this cumbersome procedure is not executed. Nevertheless, an overview of existing formulae for deriving Neumann boundaries is presented here.

During the research on implementing Neumann boundaries, it was found that at the eastern sea boundary with the water level boundaries also incorrect circulation patterns occurred in the nearshore. This causes large sediment transports and erosion in the model at that boundary. However, the influence of that boundary is far off the area of interest.

E.3.1 Formulae for deriving Neumann boundaries

The Neumann type of boundary is used to impose the alongshore water level gradient. Neumann boundaries can only be applied on cross-shore boundaries in combination with a water level boundary at the seaward boundary, which is needed to make the solution of the mathematical boundary value problem well-posed. The water level gradient is formulated as follows:

$$\eta(x, t) = \sum_{j=1}^N \hat{\eta}_j \cos(\omega_j t - k_j x - \varphi_j)$$

All wave components j are independent of each other, thus in the following the summation and the subscript j are left out.

E.3.2 Computer program INTCOM

This program can be used to derive Neumann boundaries for very small coastal models in the Dutch coastal zone. The values for the Neumann boundaries and the offshore water level boundary are derived from calculated water levels (TRIANA) of stations in the North Sea. For both lateral boundaries the calculated amplitudes have the same value, but the phase is different for each boundary. The amplitude and phase of the boundary conditions are then calculated with:

$$\frac{\partial \eta}{\partial x}(x, t) = k \hat{\eta} \sin(\omega t - kx - \varphi) = k \hat{\eta} \cos(\omega t - kx - \varphi - \frac{\pi}{2})$$

$$\hat{\eta}_{north} = \hat{\eta}_{south} = k \hat{\eta}, \varphi_{north} = \varphi_2 + \frac{\pi}{2}, \varphi_{south} = \varphi_1 + \frac{\pi}{2}$$

This method is described in Roelvink and Walstra (2004), "Keeping it simple by using complex models". The manual derivation following this method is described in the Delft3D FLOW manual.

E.3.3 HVM – model

For the Haringvlietmondong model a derivation of the Neumann boundaries is applied which takes into account the varying water levels along the offshore boundary. Therefore this method can be applied on larger models than the previous method INTCOM. The boundary sections of the offshore boundary adjacent to the lateral boundaries are used for the derivation. The start and end values of these boundary sections are used as input in the following formulas for the northern lateral boundary;

$$\hat{\eta}_{north} = \frac{\sqrt{(\hat{\eta}_{end} \cos \varphi_{end} - \hat{\eta}_{start} \cos \varphi_{start})^2 - (\hat{\eta}_{end} \sin \varphi_{end} - \hat{\eta}_{start} \sin \varphi_{start})^2}}{\Delta x},$$

$$\varphi_{north} = \text{Arctan} \frac{\hat{\eta}_{end} \sin \varphi_{end} - \hat{\eta}_{start} \sin \varphi_{start}}{\hat{\eta}_{end} \cos \varphi_{end} - \hat{\eta}_{start} \cos \varphi_{start}}$$

, which is derived from;

$$\frac{\partial \eta}{\partial x}(x, t) = \frac{\hat{\eta}_{end} \cos(\omega t - kx - \varphi_{end}) - \hat{\eta}_{start} \cos(\omega t - kx - \varphi_{start})}{\Delta x} = \frac{\hat{\eta}_{north} \cos(\omega t - kx - \varphi_{north})}{\Delta x}$$

This derivation is described in more detail in the report of De Vries (2007), Morphological modelling of the Haringvlietmondong using Delft3D.

E.3.4 Mathematical derivation

A mathematical derivation of the following formula;

$$\frac{\partial \eta}{\partial x}(x, t) = \frac{\partial \hat{\eta}}{\partial x} \cos(\omega t - kx - \varphi) + k \hat{\eta} \sin(\omega t - kx - \varphi) = \hat{\eta}_{north} \cos(\omega t - kx - \varphi - \varphi_2)$$

with the trigonometry formulas;

$$D \cos(x - \varphi) = D \cos \varphi \cos x + D \sin \varphi \sin x$$

$$D \cos(x - \varphi) = A \cos x + B \sin x$$

$$A = D \cos \varphi, B = D \sin \varphi$$

Gives

$$D = \sqrt{A^2 + B^2}, \varphi = \text{Arc tan}(B/A)$$

This results in the formulas for the amplitudes and phases of the Neumann boundary conditions;

$$\hat{\eta}_N = \sqrt{\left(\frac{\partial \hat{\eta}}{\partial x}\right)^2 + (k\hat{\eta})^2}, \quad \varphi_N = \text{Arc tan} \left(\frac{k\hat{\eta}}{\frac{\partial \hat{\eta}}{\partial x}} \right) + \varphi$$

$$\text{met } k = \frac{\Delta \varphi}{\Delta x} \text{ en } \frac{\partial \hat{\eta}}{\partial x} = \frac{\hat{\eta}_{eind} - \hat{\eta}_{begin}}{\Delta x}$$

This derivation does not take into account the influence of Coriolis on the tidal motion. The Coriolis force is defined with:

$$\hat{\eta}_{cor}(x) = \hat{\eta}_0 e^{\frac{f}{c}x} \text{ with } f = 2\Omega \sin(\varphi) = 2 \frac{2\pi}{24 \cdot 3600} \sin(51^\circ) \text{ and } c = \text{wave celerity}$$

E.3.5 Conclusion on methods

The first method is only applicable on small coastal models with a uniform profile, where the tidal wave does not deform between the two lateral boundaries. It appeared that the second and third method produce nearly the same boundary conditions. Therefore applying one above the other is not recommended herein.

For larger models, with lateral boundaries larger than 10 km it is recommended to divide the lateral boundary in multiple segments for which separate values for the amplitudes and phases need to be derived.

E.3.6 Lateral boundary in Wadden Sea

A small analysis on the definition of the lateral boundary in the Wadden Sea, though with incorrect Neumann sea boundaries, has shown that the definition of that boundary has a very small influence on the hydrodynamics around the Texel Inlet. The cumulative discharge through the inlet Marsdiep and the shallow area between Terschelling and Friesland are plotted in time for three types of boundaries, being water levels (blue), Neumann = 0 (oranje) and closed boundary (green) in figure E.4. Closing the Wadden Sea boundary or imposing a horizontal water level has almost the same effect on the hydrodynamics in the Wadden Sea. It causes a smaller flux of water into the basin over the Wadden Sea boundary and it causes a slightly smaller outgoing flux through the Marsdiep.

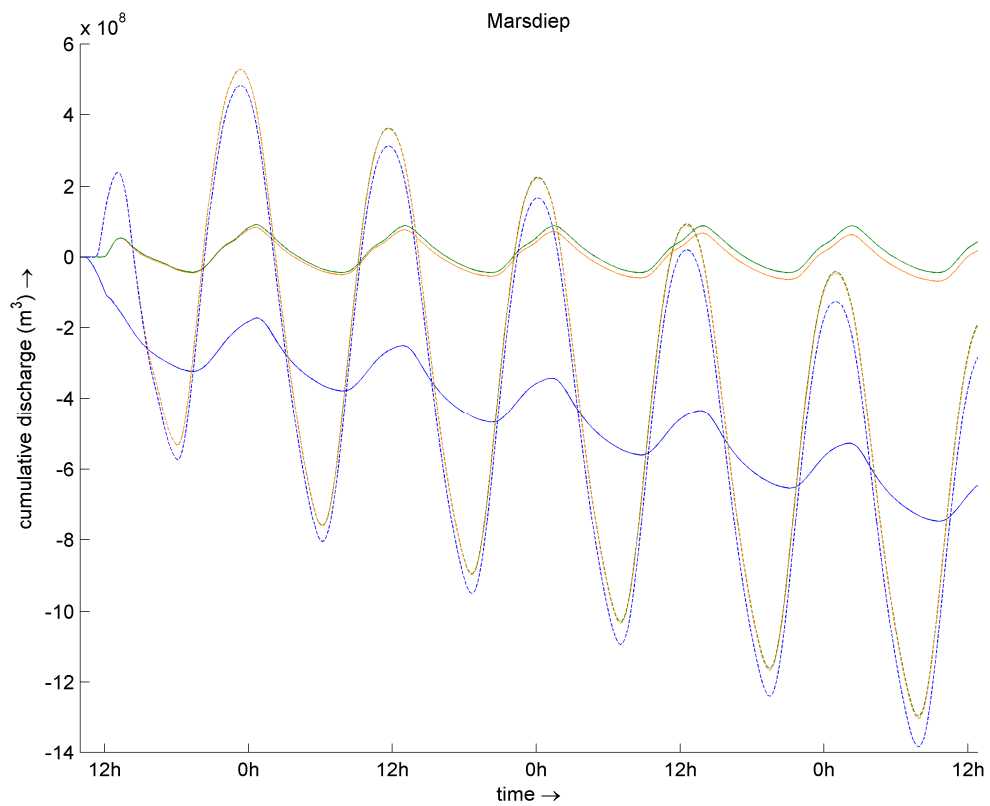


Figure E.4 Comparison of cumulative discharge through two sections in the Wadden Sea. The graphs with a small amplitude are for a cross-section between the island of Terschelling and the mainland in Friesland. The graphs with a large oscillation are for the Marsdiep Inlet. Discharges are compared for the model boundaries at the Wadden Sea boundary with water level (blue), Neumann=0 (orange) and a closed boundary (green)

F Update van Rijn 2004

Within this study, two different Delft3D FLOW versions have been used, being:

FLOW version 3.57.02.2585, with trisim.exe as flow executable

FLOW version 3.60.00.5472, with delftflow.exe as flow executable

Finally, the second version has been applied to evaluate the nourishment alternatives.

In the second version the VanRijn2004 sediment transport formula is updated, which causes significant differences in sediment transport magnitudes and direction. In figures F.1 and F.2 the longshore transport along the Holland Coast for the two versions is plotted. In the surf zone a difference is hardly distinguished, but offshore a large reduction of the longshore sediment transports is seen of up to a factor 2. The effect of the transport formula update lies mostly in the suspended transport.

For the Texel Inlet the import of sediment is doubled over 10 years, all at the cost of the outer delta. The cross-shore transport from the sea into the sections is smaller for the second Delft3D version.

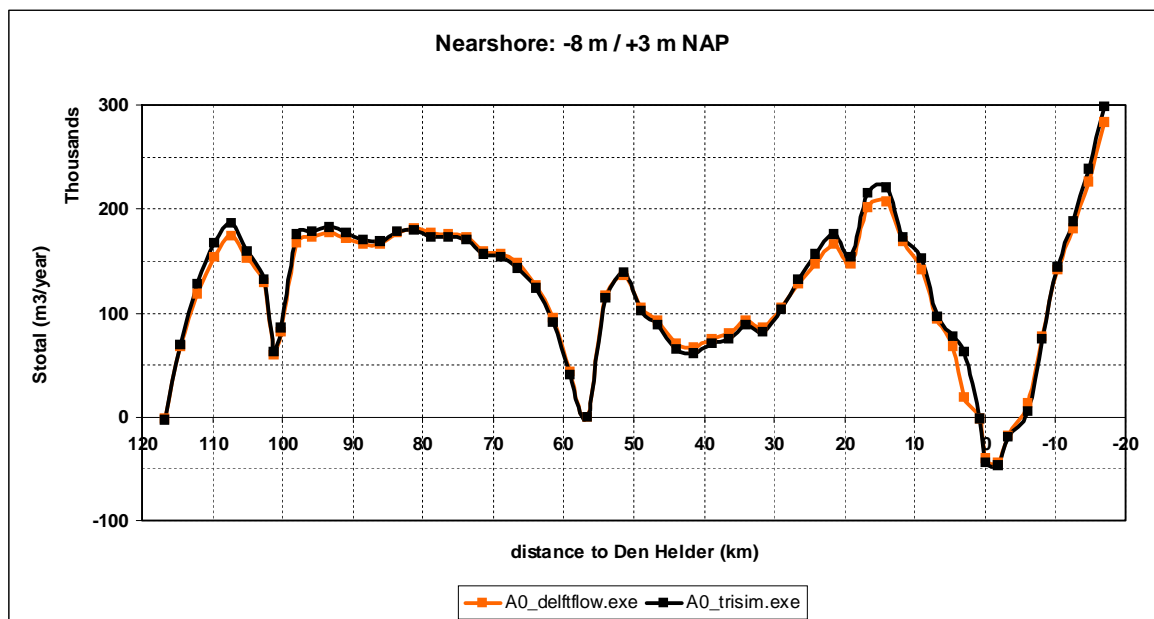


Figure F.1 Longshore residual yearly transports (excl. pores) in the nearshore, defined between water depths -8 m and +3 m NAP

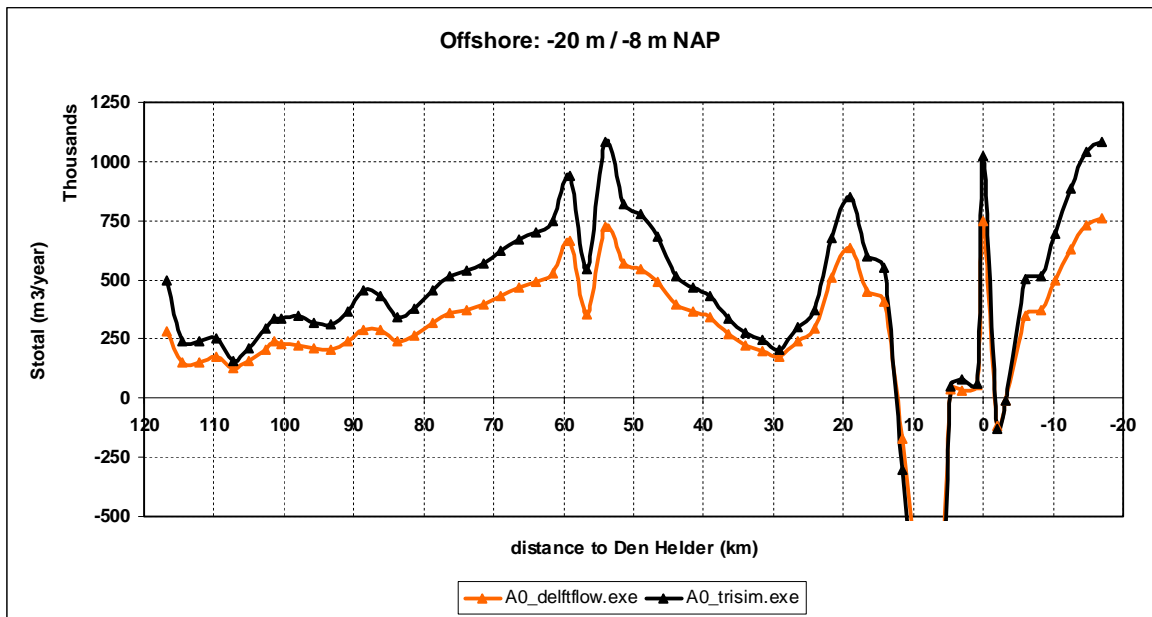


Figure F.2 Longshore residual yearly transports (excl. pores) in the offshore, defined between water depths -20 m and -8 m NAP

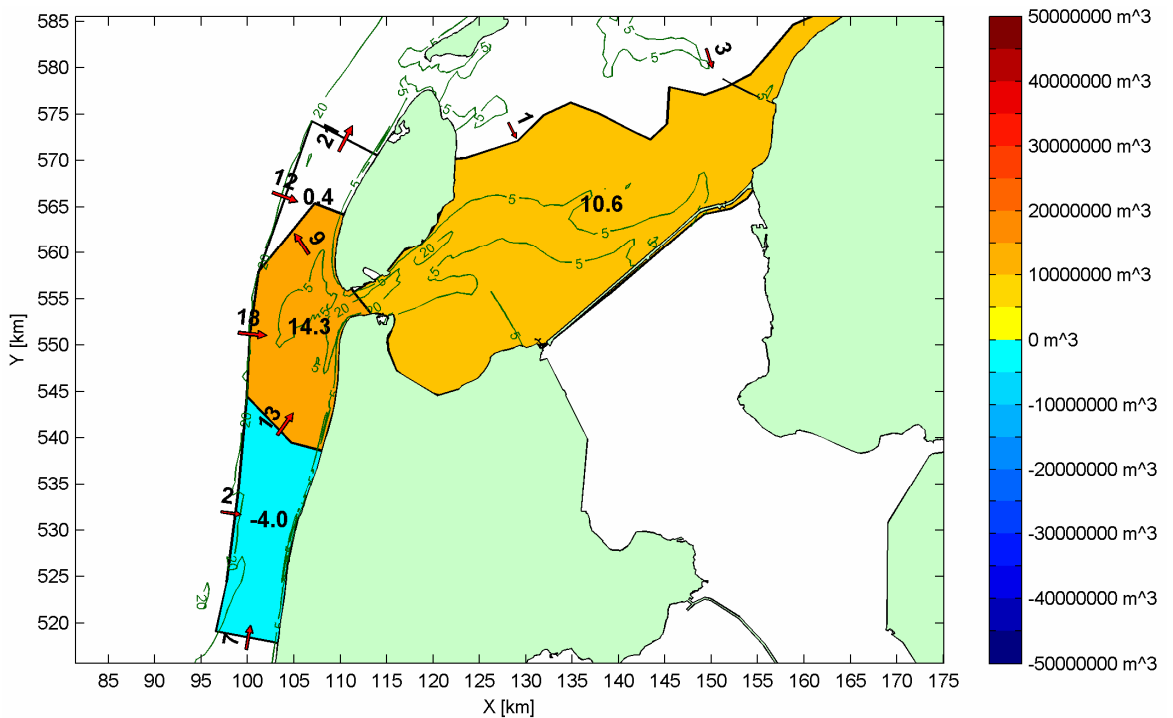


Figure F.3 Cumulative sedimentation and erosion in 10 years morphological simulation in sections for trisim.exe

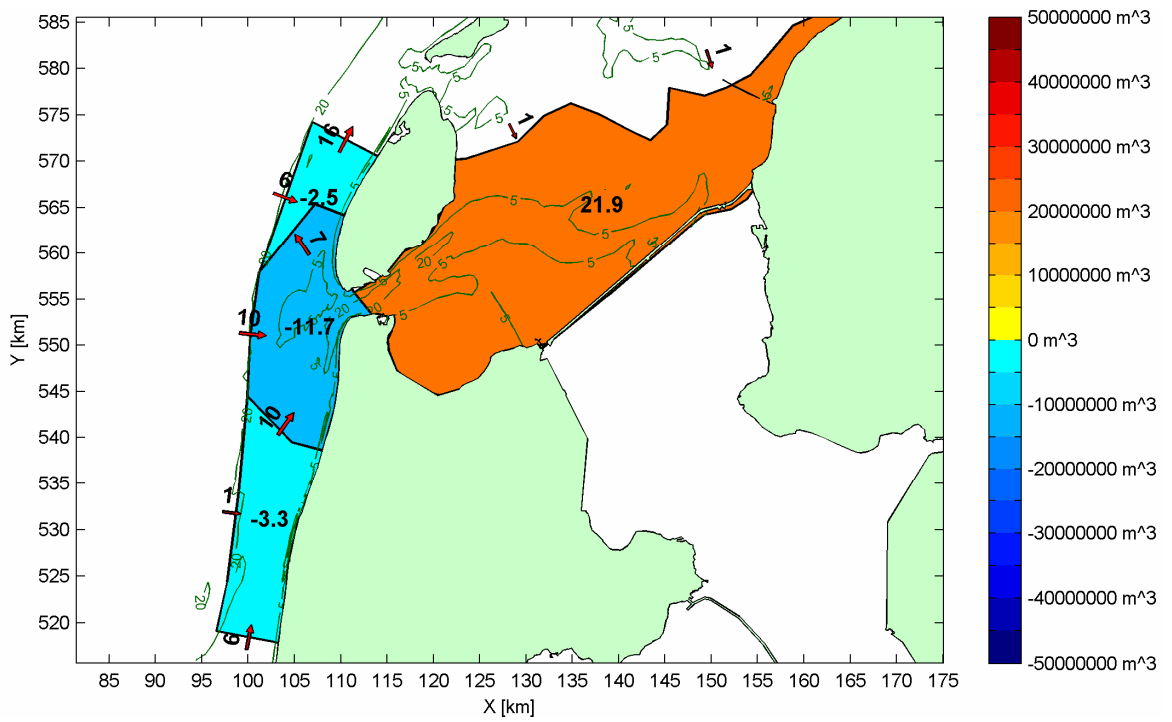


Figure F.4 Cumulative sedimentation and erosion in 10 years morphological simulation in sections for delftflow.exe

G Sensitivity of proposed parameters

The sensitivity of some parameters is investigated to assess the relative influence on longshore sediment transport rates. Table G.1 presents the investigated parameters on how they are defined in the final model of 2008 and proposed for the model of 2009.

	Model 2008	Model 2009
Wind field	Morphological wind Wind speed 7 m/s, Dir = 240°	Varying wind on the flow field, corresponding to the wind in the wave conditions
Rouwav	Fredsoe 84	Van Rijn 2004
Calculation of wave forces	Energy dissipation	Radiation stresses
Communication interval	60 minutes maximum no iterations = 5	30 minutes maximum no iterations = 2

Table G.1 Model parameters

G.1 General sensitivity analysis

In table G.2 the total sediment transport is compared for three different areas, being the surf zone, deep water and through the Marsdiep tidal inlet. The longshore sediment transport is calculated along the Holland Coast and along the Texel coastline in the nearshore (cross-shore distance between -8m and +3m NAP) and in deep water (cross-shore distance between -20m and -8m NAP), which is shown in respectively figure G.1 and figure G.2.

The results of the sensitivity analysis indicate that the manner in which the wave-current interaction is calculated is an important parameter in the calculation of the sediment transport, both in the surf zone (wave driven sediment transport) and more importantly in deep water. The formulation of Van Rijn 2004 enlarges the Wadden Sea sediment import through the Marsdiep by a factor 3 and the longshore transport in deep water by a factor 2.

The calculation of wave forces with energy dissipation generates higher sediment transport in the surf zone, than wave forces calculated with radiation stresses.

The other parameters; wind field and communication interval, are of less importance on the sediment transport. The reduction of the communication interval in combination with less iterations reduces the simulation time with 10%.

	Longshore transport in the surf zone	Longshore transport in the deep water	Marsdiep (Mm ³) Base case = 12.6 Mm ³
Wind field variation	~ even	~ even	12.3
Rouwav FR84	25% more northward transport	50% less northward transport	4.3
Calculation of wave forces with energy dissipation	25% more northward transport	~ even	13.1
Communication interval on 60 minutes	even	even	12.6

Table G.2 Comparison of sediment transports for different parameter settings

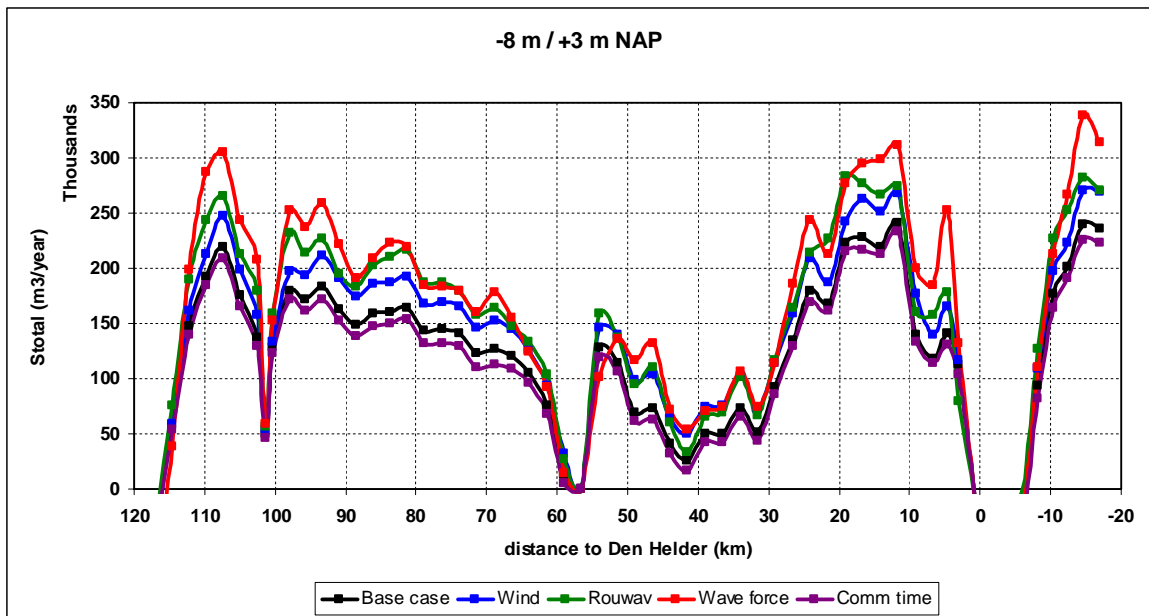


Figure G.1 Yearly averaged longshore transports integrated for the cross-shore distance between water depth -8 m and +3 m (dune foot) NAP. Influence of several parameters on the residual sediment transport

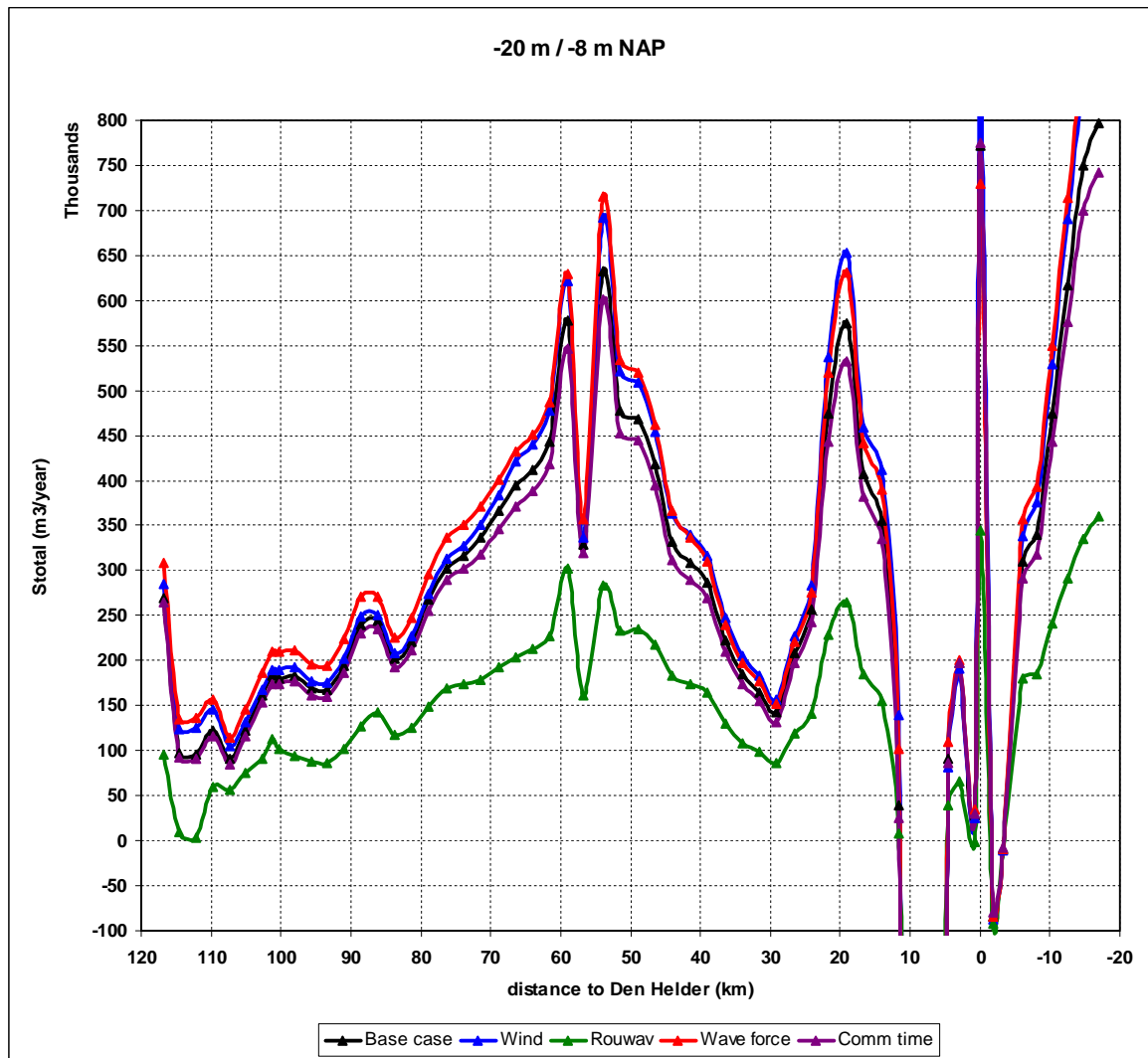


Figure G.2 Yearly averaged longshore transports integrated for the cross-shore distance between water depth -20 m and -8 m NAP. Influence of several parameters on the residual sediment transport

G.2 Wave-current interaction

The sensitivity analysis has led to the conclusion that the formulation of the wave-current interaction causes large differences in sediment transports. This is a large difference to ascribe to one formulation only. Therefore a further analysis is made in which the integrated sediment transport is split up in suspended transport and bed load transport, a bucket model is applied to assess the dependency of the sediment transport on the angle between waves and current and lastly time series for one location are examined to find differences in bruto values.

G.2.1 Bucket model

For a better understanding of the influence of the wave angle in the wave-current interaction on the sediment transport, small test are done with a “bucket” model. This is a simple small scale model (1 km by 20 m, water depth of 5 m) where a uniform flow of 0.5 m/s and a uniform wave height of $H_s = 1.5$ m are imposed in the flow module. Both wave-current interaction formulas are tested for different angles between waves and current. This shows the dependency in both formulas of the bed roughness and the sediment transport on the angle between wave and current, in figures G.3 and G.4. However, a difference is found between Fredsoe and Van Rijn, where the maximum values are out of phase.

Van Rijn proposed a higher apparent roughness for waves and current under an angle of 90 degrees than for coinciding directions, as the current is blocked by the orbital motions of the waves. This causes the velocity profile to bend more forward, thus lower velocities near the bottom and higher velocities near the water surface, while the depth averaged velocity remains equal. This reduces the bed load transport and increases the suspended load transport (figure G.4).

When applying the wave current interaction formula of Van Rijn also the bed roughness predictor is used for the calculation of the sediment transport, although it is not applied for calculation of the hydrodynamics. The difference in usage of the bed roughness predictor in the bucket-model is visible in figures G.3 and G.4, where a Chezy bottom roughness of 65 is compared with the bed roughness predictor, indicated by trt (which stands for trachytopen). The bed roughness predictor does show an increase of the bed roughness, but the effect on the sediment transport is however very small.

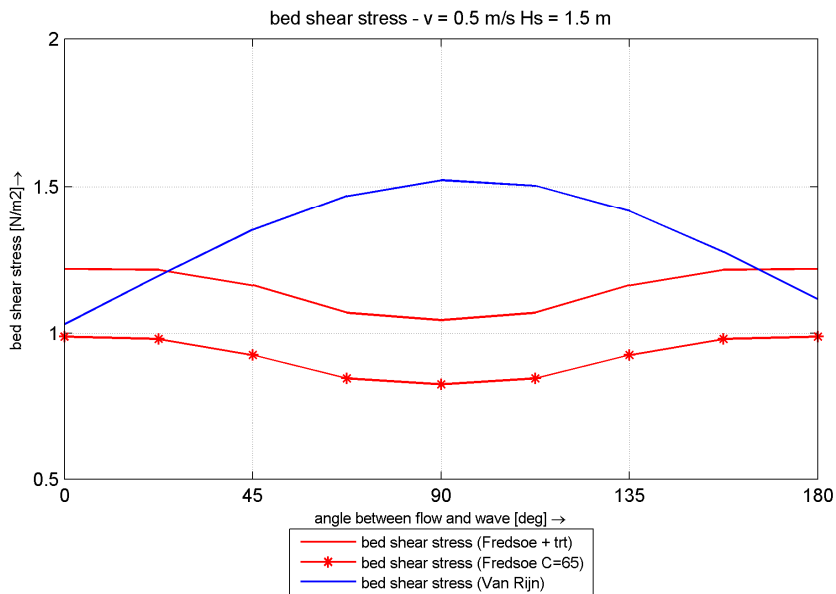


Figure G.3 Dependency of bed shear stress on the angle between current and waves, with an imposed current velocity of 0.5 m/s and a significant wave height of 1.5 m

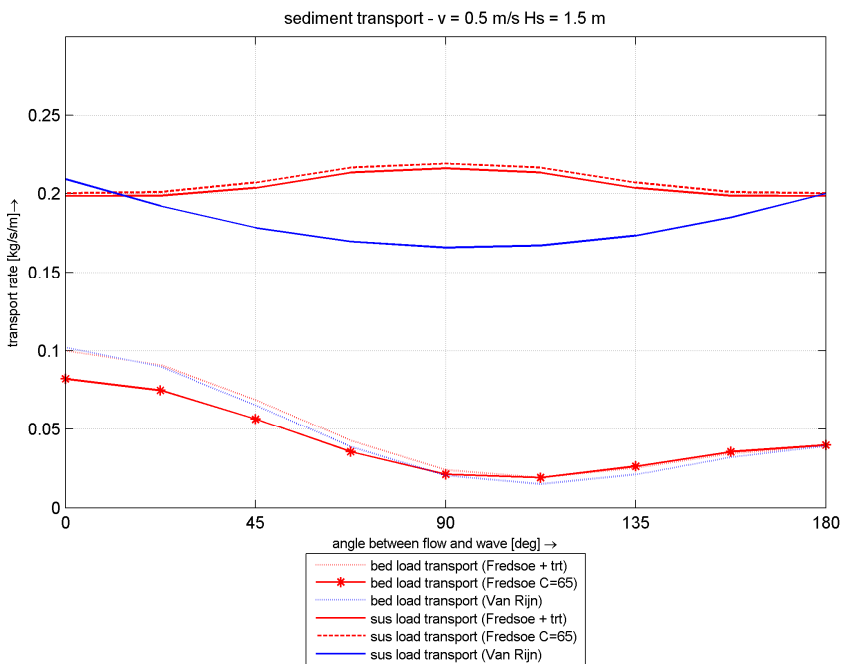


Figure G.4 Dependency of magnitude of the suspended sediment transport and the bed load transport on the angle between current and waves, with an imposed current velocity of 0.5 m/s and a significant wave height of 1.5 m

G.2.2 Moholk Model time series

Only one wave condition (W03) and one location (Noordwijk 60 km) are selected to analyze differences in hydrodynamic and morphological parameters due to wave current interaction definition. This measurement point is located near the seaward edge of the model in a water depth of 28 meters. The wave condition considered here is characterized by a significant wave height of 1.2 m with direction 270° .

The depth averaged velocity is similar for both formulas (Figure G.5), but the bed shear stress (Figure G.6) is lower for Van Rijn. This results in higher sediment concentrations (Figure G.7) and thus higher bed load and suspended load transports (Figures G.8 and G.9).

The time series figures G.8 and G.9 indicate an overall increase in sediment transport for the wave current interaction of Van Rijn, which generates the increase in the residual transport.

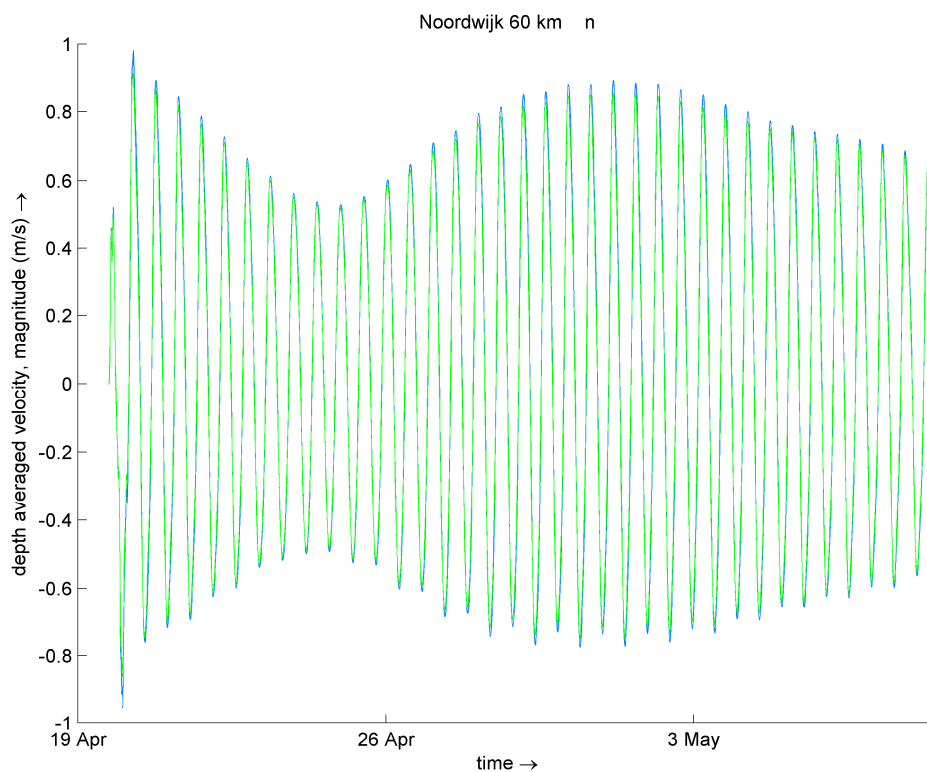


Figure G.5 Timeseries of depth averaged velocities for wci Fredsoe (green) and Van Rijn (blue)

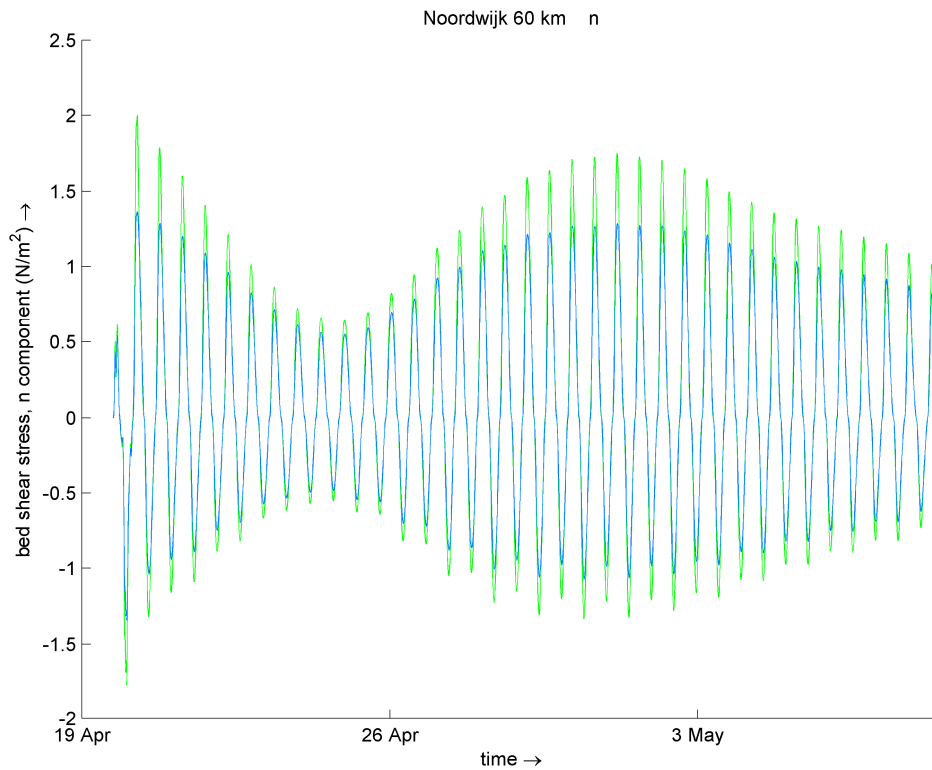


Figure G.6 Time series of the bed shear stress for wci Fredsoe (green) and Van Rijn (blue)

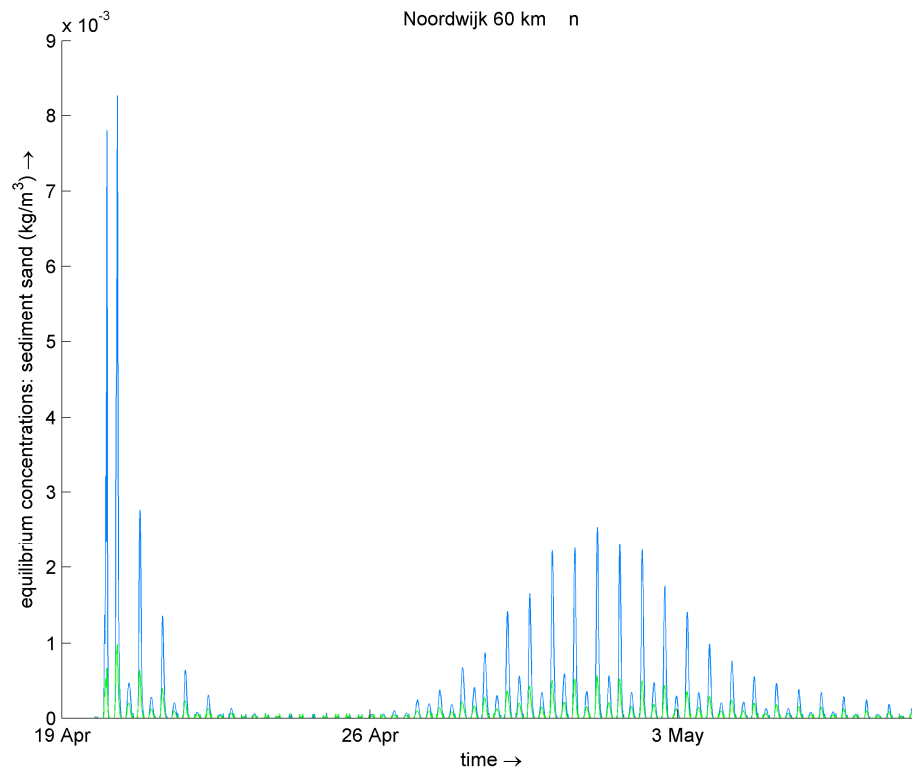


Figure G.7 Calculated equilibrium concentrations of sand in time for wci Fredsoe (green) and Van Rijn (blue)

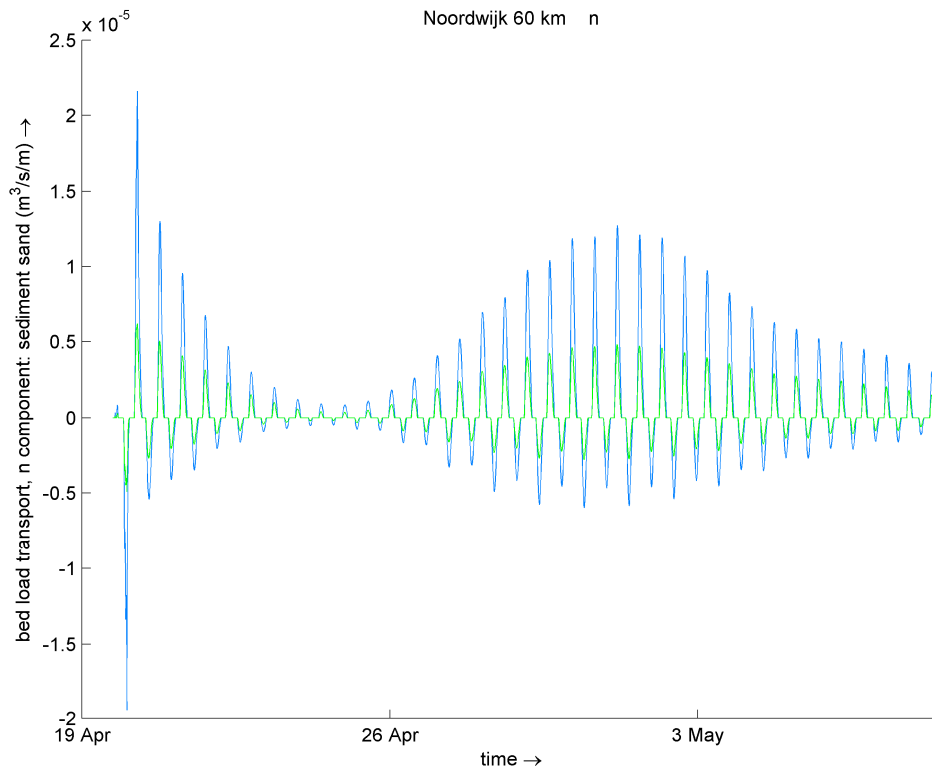


Figure G.8 *Bed load transport in time for wci Fredsoe (green) and Van Rijn (blue). Positive transports are in northward direction along the coast*

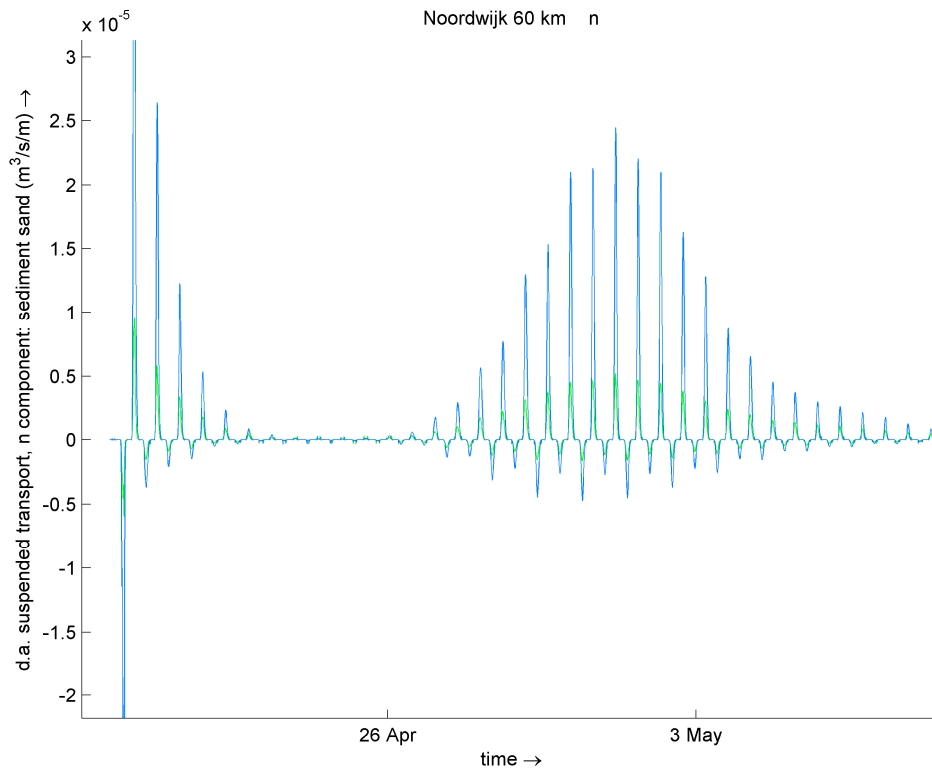


Figure G.9 *Suspended load transport in time for wci Fredsoe (green) and Van Rijn (blue). Positive transports are in northward direction along the coast*

G.2.3 Conclusion

The combined results of the bucket model and the Moholk model do not directly lead to the understanding of the processes governing the wave current interaction and the corresponding influences on the sediment transport. The bucket model seems not to be designed to thoroughly investigate the wave current interaction, while the Moholk model incorporates too much processes which may be affected by the formulation. The wave current interaction definition affects the residual sediment transport by the magnitude of the sediment concentration and not by a distortion of the sediment transport in one direction.

Further fundamental research is needed to understand the effects of the recently implemented wave current interaction and the bed roughness predictor of Van Rijn on the sediment transport and the hydrodynamics in a test environment designed for these formulations.

H Wind influence on residual current

For three wind conditions the effect on the residual current is plotted in figures H.1, H.2 and H.3. The wave conditions are:

- W12 with wind speed 9.1 m/s, direction 10 degrees north.
- W07 with wind speed 13.3 m/s, direction 200 degrees north.
- W00 with wind speed 13.3 m/s, direction 200 degrees north.

The residual current due to tide and morphological wind (7 m/s, 240 degrees north) gives inaccuracies at the boundaries, especially at the eastern boundary. This is shown in figure B.7. Any other wind direction than the morphological wind (7 m/s, 240 degrees north) increases the error in tidal boundary conditions at the eastern and the western open boundaries. For the northern wind the direction of the residual current is in southward direction (figure H.1). The large southwest current at the eastern boundaries imports large amounts of sediment through the boundary close to the coast. For the southwestern wind the residual current field and sediment pattern are more gradual (figure H.2). However, the increase in residual current in northern direction is not natural for a southwestern wind. Without wind, figure H.3, the magnitude of the residual current and the sediment transport is much lower. But still large errors are seen at the boundaries.

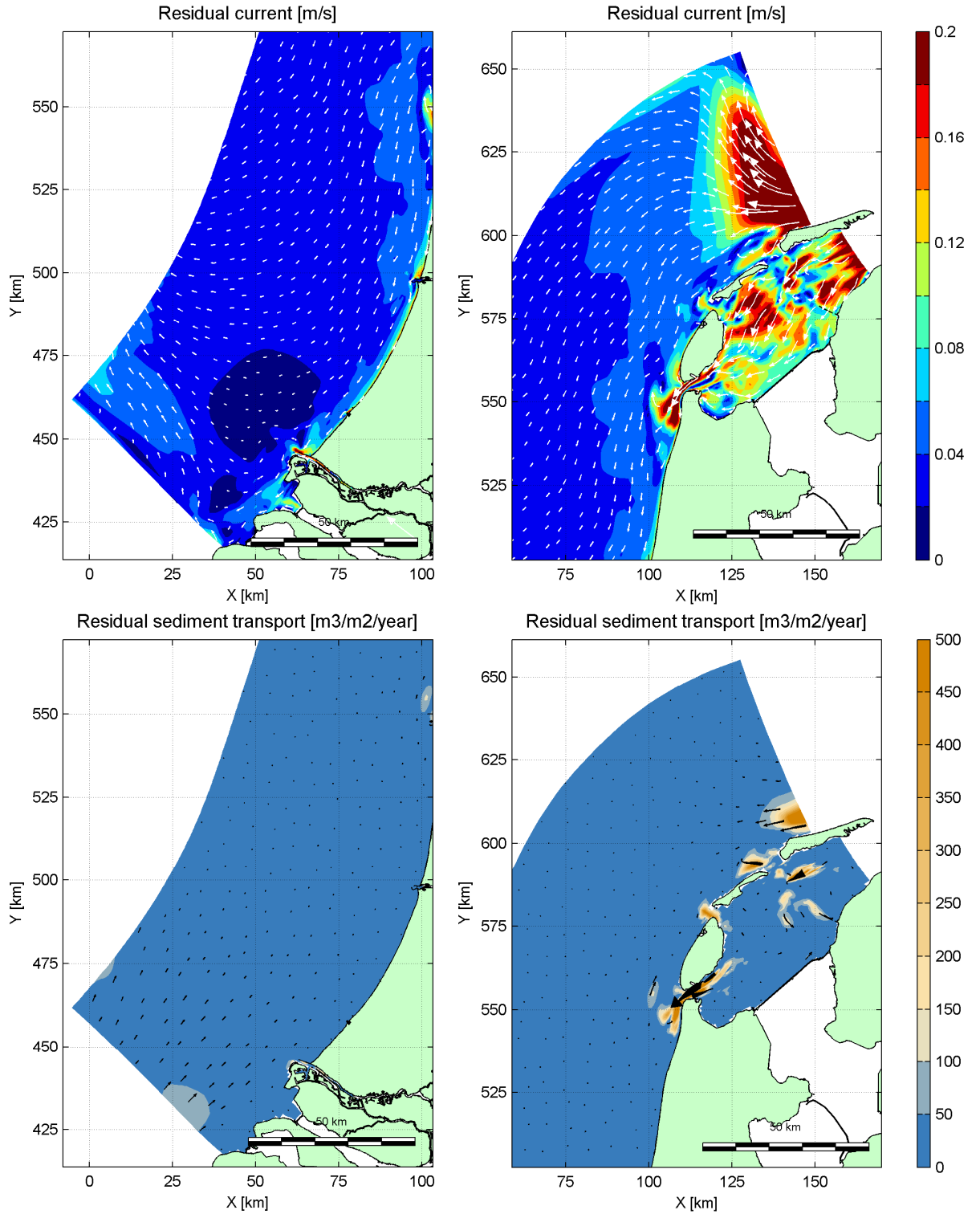


Figure H.1 Residual current and sediment transport for boundary conditions tide and wind w12 (9.1 m/s, 10 degrees north)

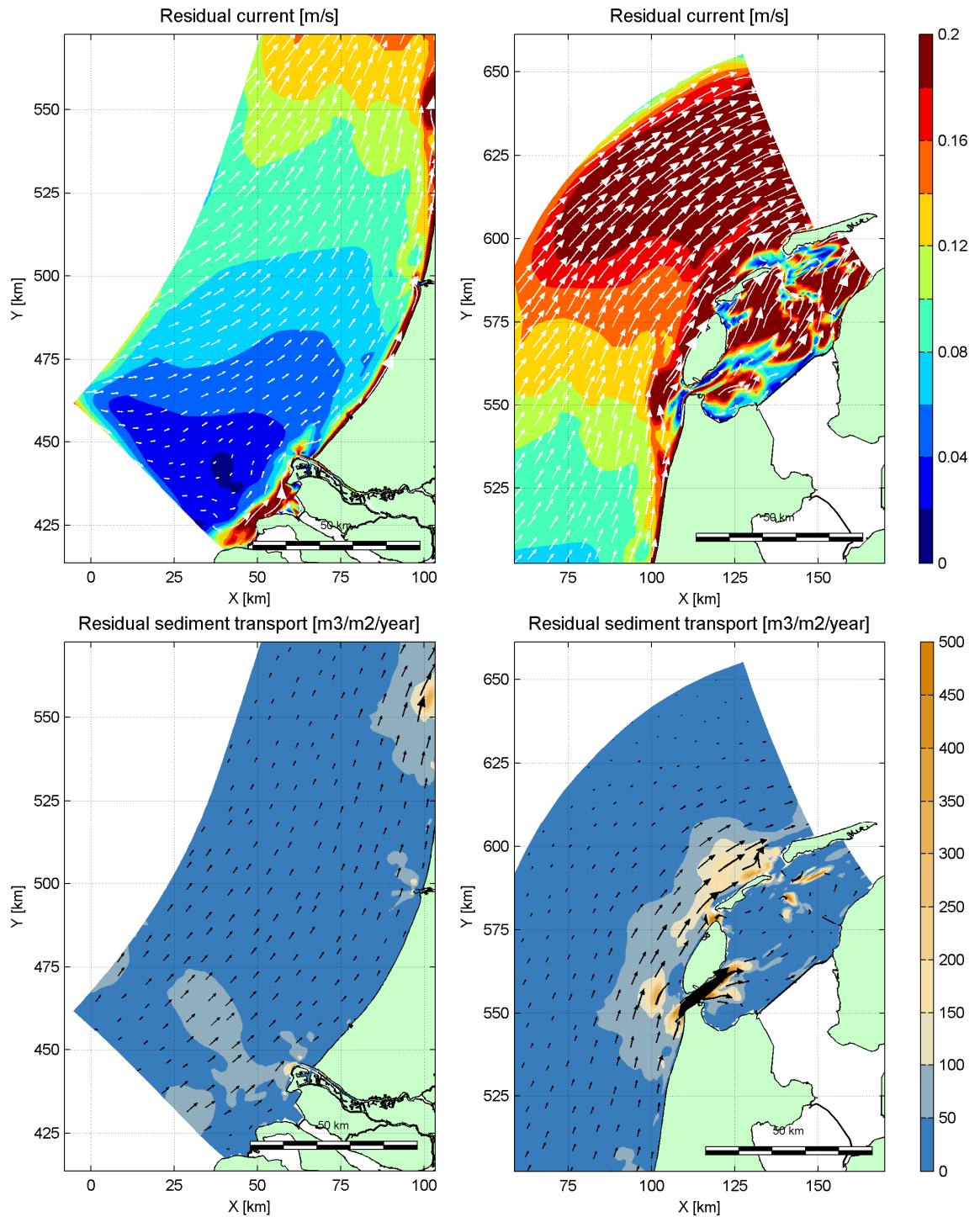


Figure H.2 Residual current and sediment transport for boundary conditions tide and wind w07 (13.3 m/s, 200 degrees north)

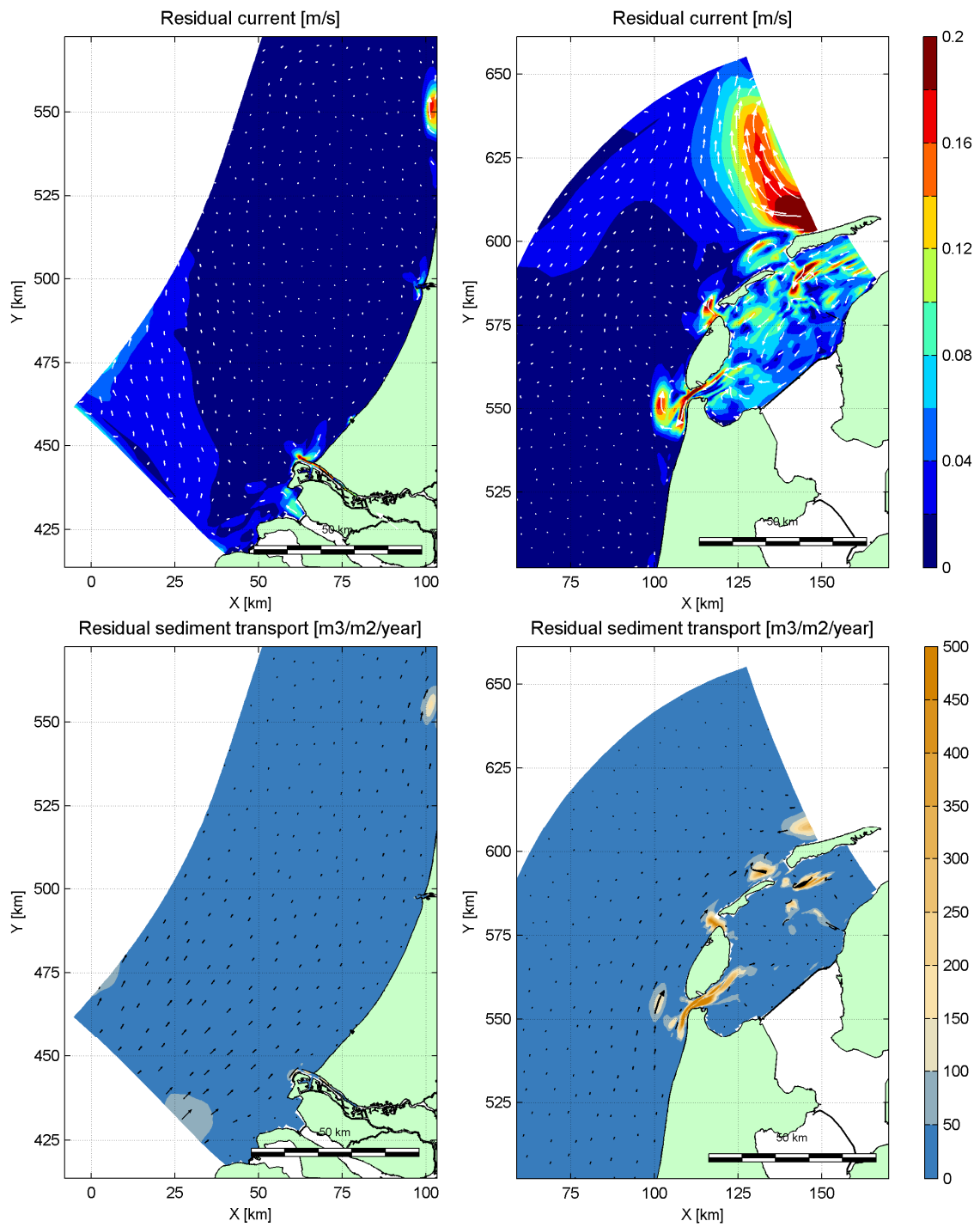
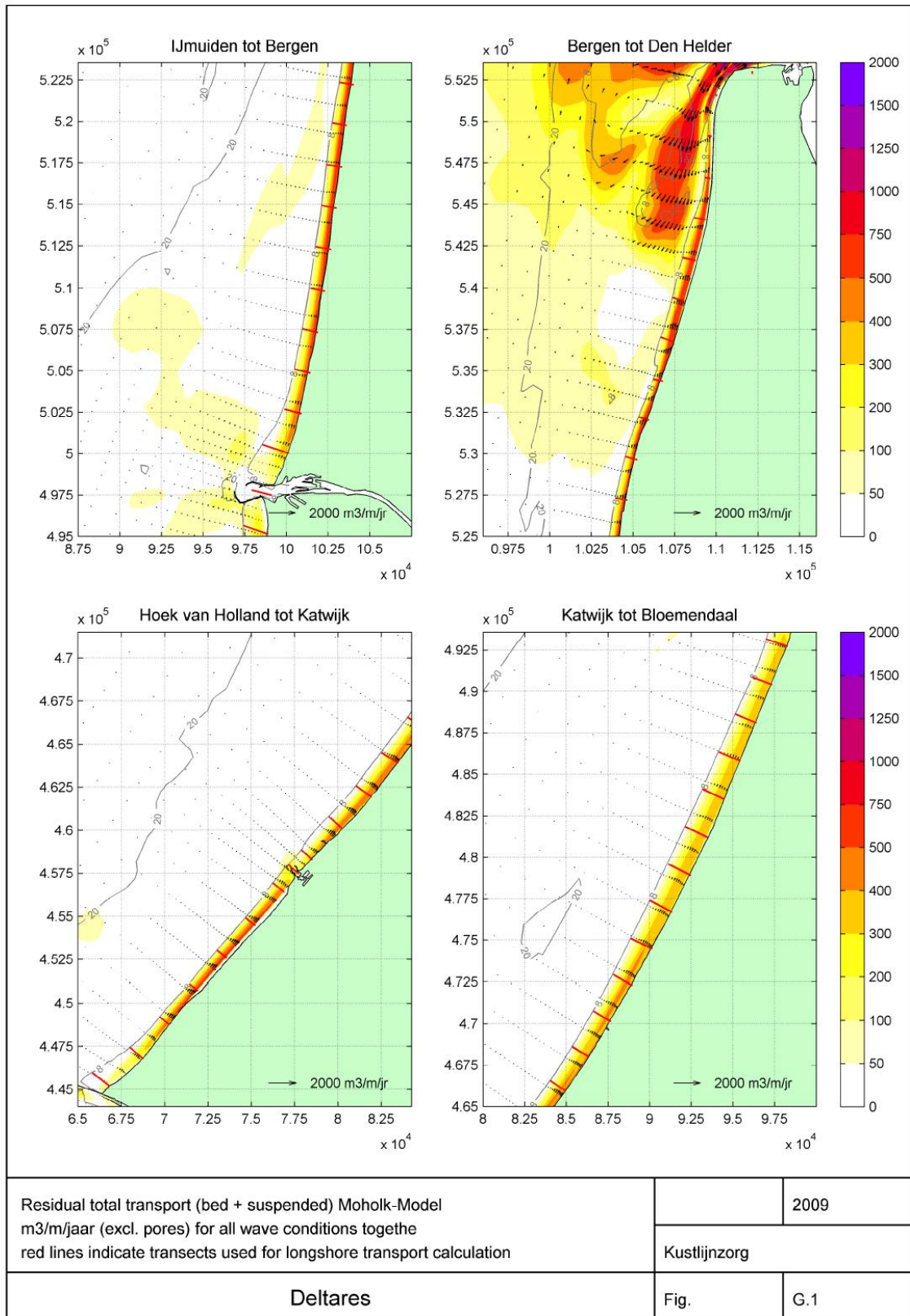


Figure H.3 Residual current and sediment transport for boundary conditions tide and wind w00 (0.1 m/s, 270 degrees north)



Figuur I 1

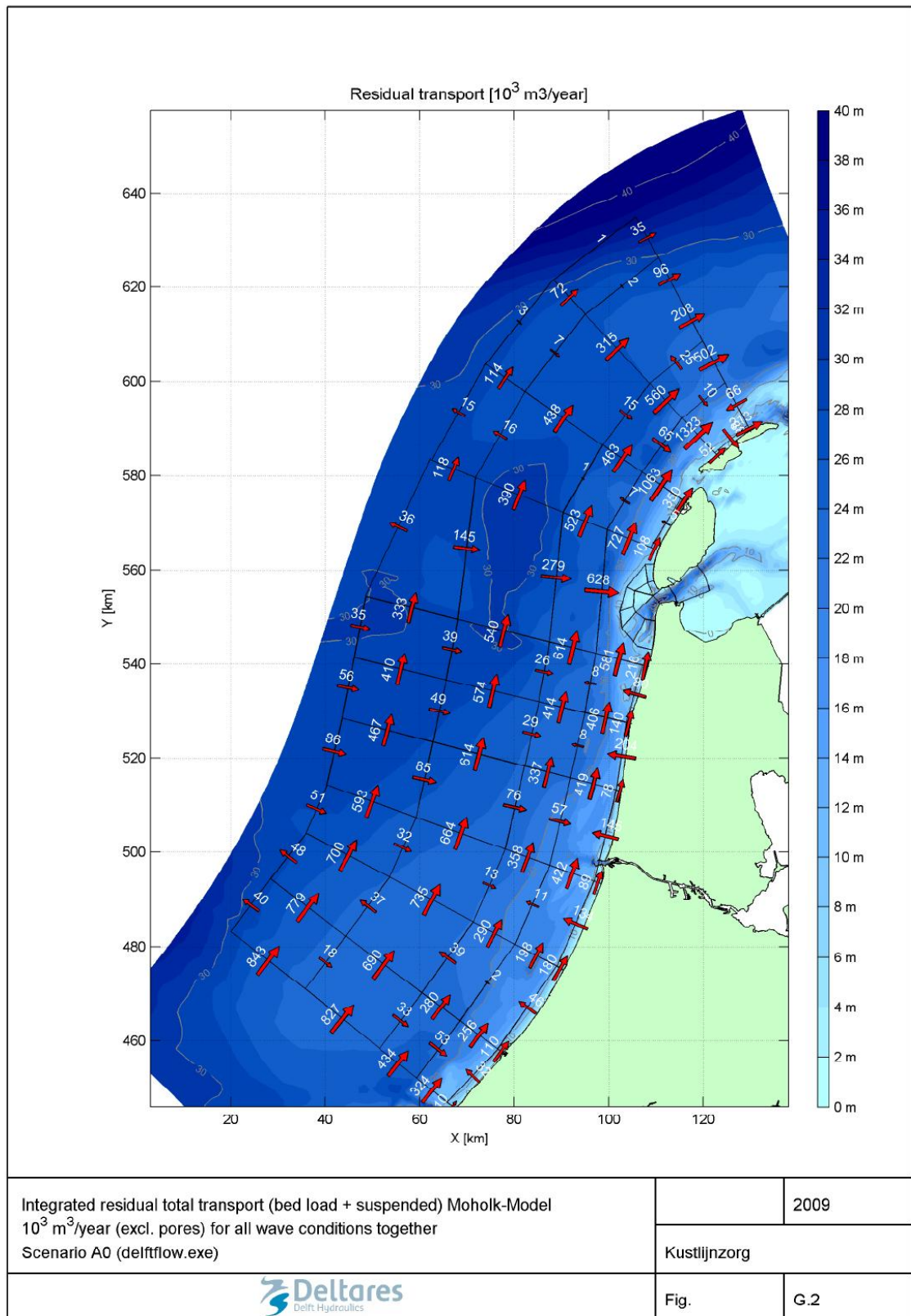


Figure I 2

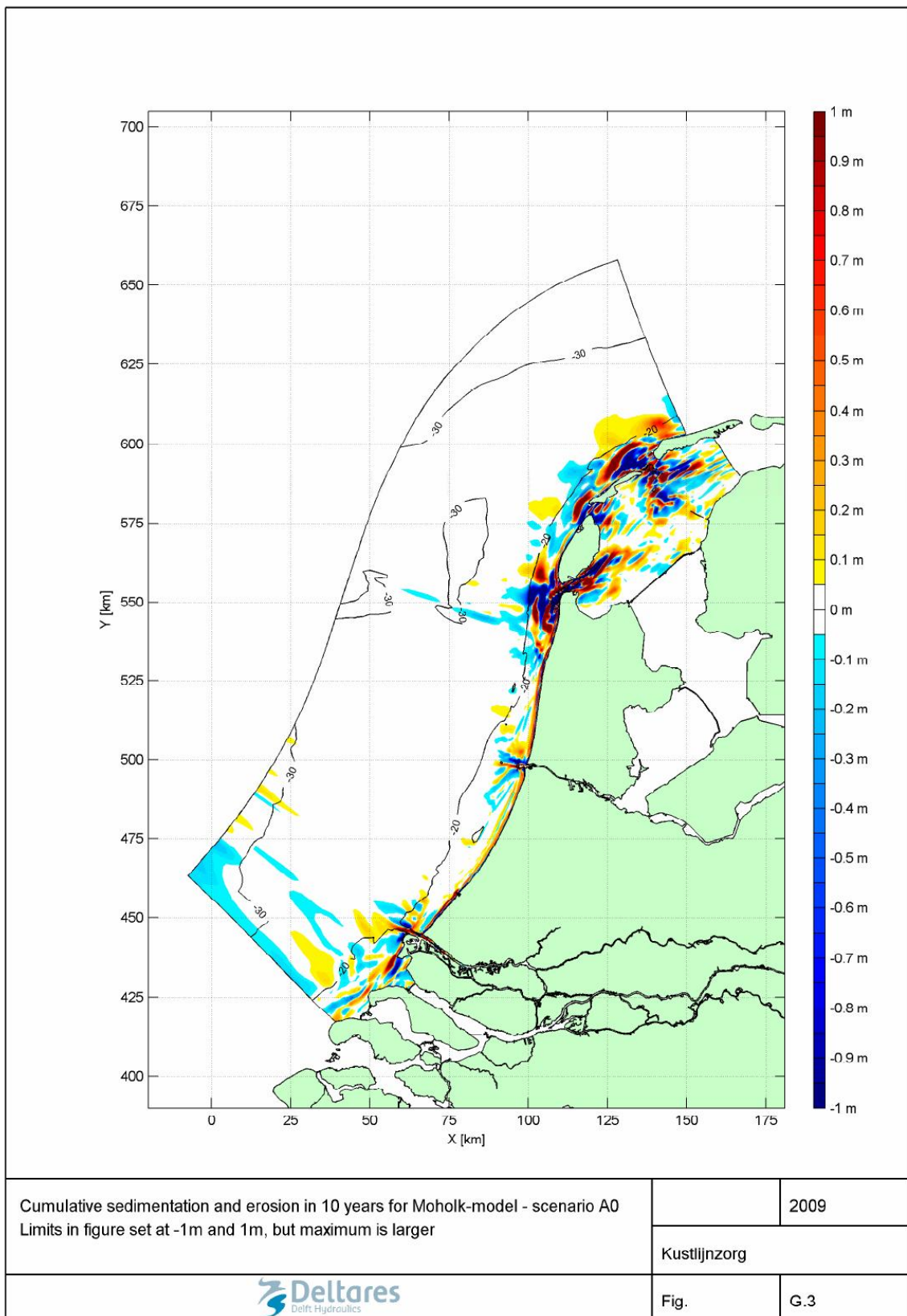
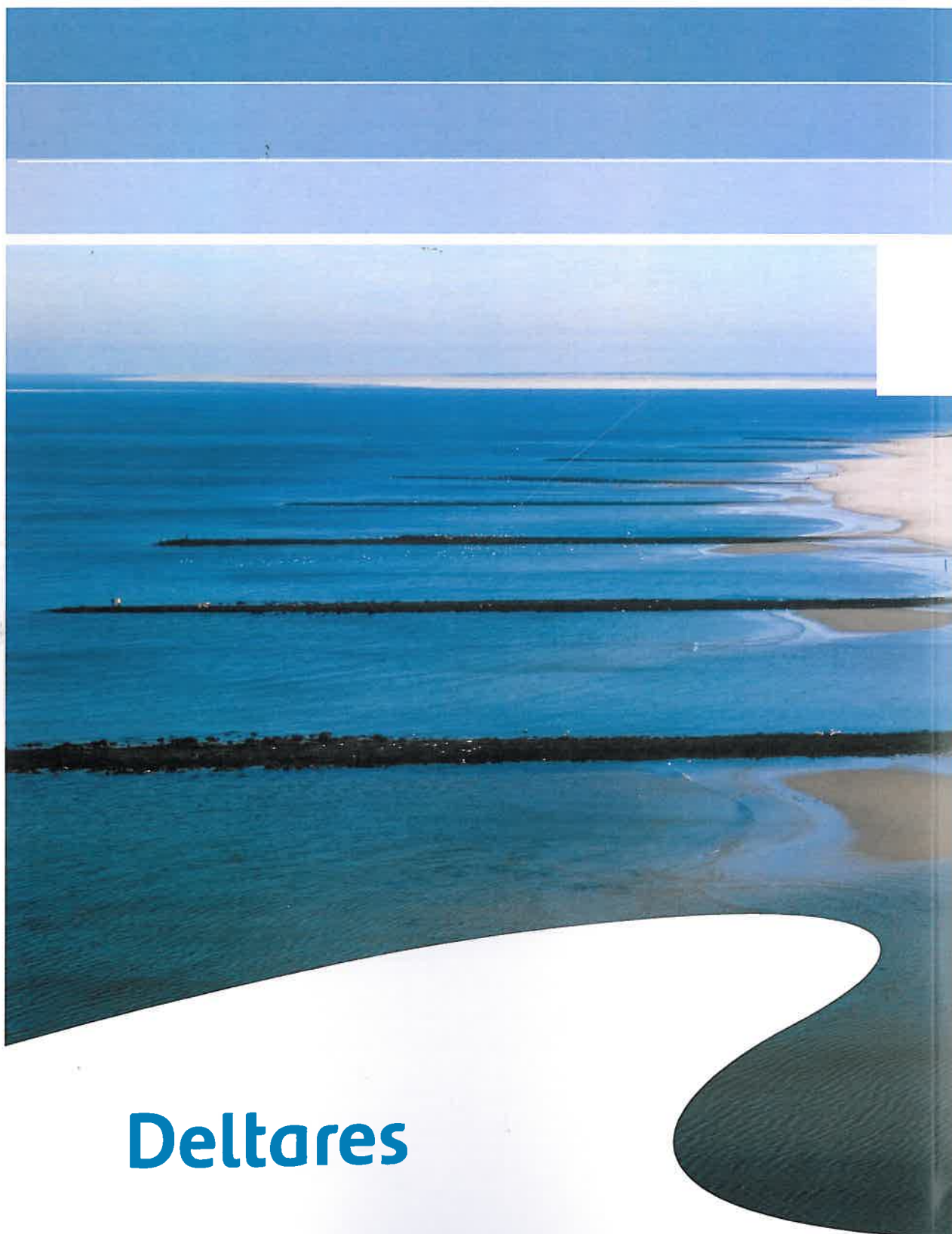


Figure I 3

www.deltares.nl



Deltares